

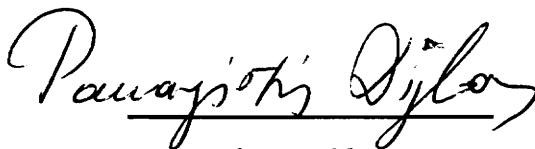
**Settling Characteristics of Particles in a Suspension of Medium to
High Solids Concentration.**

by

Athanasios N. Papanicolaou

Thesis submitted to the Faculty of the
Virginia Polytechnic Institute and State University
in partial fulfillment of the requirements for the degree of
Masters of Science
in
Civil Engineering

APPROVED:



P. Diplas, Chairman



D. F. Kibler



T. Younos

DECEMBER, 1992

C.2

LD
5655
V855
1992
P372
C.2

BATCH SEDIMENTATION

By Athanasios Papanicolaou

Panayiotis Diplas, Chairman

Civil Engineering

(ABSTRACT)

During the thickening process of sludges with intermediate to high solid concentrations three settling regimes are typically encountered, namely, zone, transition, and compression regimes. Recent studies have indicated that the validity of Kynch's formulation, which is the most widely used for sizing settling basins, is limited to the zone settling regime. His formulation is based on the solids mass balance equation and does not consider the role of the rising sediment at the bottom of the settling basin. This limitation is rectified in this study by using a dynamic equation, a second order non - linear partial differential equation for the effective pressure of the solid particles. The equation is solved by using the finite element method. The so obtained effective pressure is used with an appropriate constitutive relation for the volume fraction of solids, to determine the variation of the solids content within the deposited material, and the height of the falling mudline.

Acknowledgements

I wish to express my gratitude to my advisor Dr. Panayiotis Diplas, for his support, guidance, and valuable help that he provided to me over the course of this thesis.

I would like to thank Dr. D.F. Kibler and Dr. T. Younos for their participation in my committee. I would also like to express my appreciation for their help to: Dr. F. Tiller, Professor of Chemical Eng. Dept. at University of Texas, Dr. M. Gunzberger, Professor of Math Dept. at Virginia Tech, Dr. J.N. Reddy, Professor of Mechanical Eng. Dept. at Texas A&M University, and Y.S. Reddy Research Associate of E.S.M. Dept. at Virginia Tech.

I wish to thank the Educational Dept. of N.A.T.O in Greece and the Civil Engineering Dept. at Virginia Tech for the fellowship and financial aid, respectively, that was provided to me during this program. The current research was partially supported by the National Science Foundation grant CTS-8909984, which is gratefully acknowledged.

Special thanks goes to my family for their love and support over the course of my study.

Table of Contents

Abstract.....ii
Acknowledgments.....iii
Table of Contents.....iv
List of Figures.....vii
List of Symbols.....ix

Chapter 1:

Introduction.....1
 1.1 Gravity Thickening Operation and Definitions.....1
 1.2 Classification of the Sedimentation Process in aThickening
 pond.....3
 1.3 Continuous and Batch Type of Gravity Thickening.....5

Chapter 2:

Batch Thickening Theories - Critical Review14

Chapter 3:

Theorems in Batch Sedimentation.....28

Chapter 4:

Objectives of the present work33

Chapter 5:

Theoretical Model in Batch Thickening.....35

- 5.1 Assumptions considered in batch sedimentation.....35
- 5.2 The physical process in batch sedimentation.....36
- 5.3 Consolidation process.....37
 - 5.3.1 Model for the consolidation process.....37
 - 5.3.2 Calculation of the height decrease in a solids bed due to consolidation process.....44
- 5.4 Alternative model for the consolidation process.....48
- 5.5 Model for the suspension process.....51
- 5.6 Methodology to obtain the variation of the variation of the consolidation-suspension interface with time.....54
- 5.7 Construction of the supernatant liquid-mudline interface.....60
- 5.8 Steps to construct the L and batch curves for an under investigation slurry.....62

Chapter 6:

Numerical Solution of the Consolidation Equation by using the Finite Element Method.....64

- 6.1 Finite Element Formulation.....64
- 6.2 Description of the computer code.....76

Chapter 7:

Required experimental data for the numerical scheme.....79

- 7.1 Experimental data.....79

7.2 Calculation of the parameters included in the constitutive equations.....82

7.3 Measurement of the solidosity in the compression zone.....85

Chapter 8:

Conclusions.....86

References.....88

Appendix: Computer code.....93

List of Figures

Figure 1: Clarification and sedimentation processes in a thickening pond.....2

Figure 2: Classification of settling processes.....4

Figure 3: A typical gravity thickener.....6

Figure 4: Batch (H vs. t) and rising sediment (L vs. t) curves from a typical settling test.....9

Figure 5: Typical batch curve for a slurry of low initial concentration.... 11

Figure 6: A typical batch curve for a slurry with intermediate initial concentration..... 12

Figure 7: A typical batch curve for a slurry with high initial concentration..... 13

Figure 8: Material balance in a layer..... 17

Figure 9: A typical flux curve..... 18

Figure 10: Kynch's characteristics.....20

Figure 11: Tiller's characteristic line.....23

Figure 12: Generalized Kynch- type construction (after Fitch, 1983).....24

Figure 13: Upward propagation velocity of a sediment discontinuity.....29

Figure 14: Downward propagation velocity of a sediment discontinuity.....30

Figure 15: Stable (AB) and unstable (BC) discontinuity, and second order of discontinuities.....31

Figure 16: Consolidation - suspension problem.....36

Figure 17: Stresses in a sediment layer.....38

Figure 18: Consolidation of a layer at time $t+\Delta t$45

Figure 19: Use of the flux curve to compute the volume fraction of solids of the falling material at the top of the sediment-suspension interface.....53

Figure 20: Multiple batch tests to construct the L-curve.....55

Figure 21: Steps in the consolidation - suspension process.....57

Figure 22: Steps in the consolidation - suspension process.....60

Figure 23: Estimation of the mudline height.....61

Figure 24: Finite element discretization of the domain: (a) Physical problem, (b) Mathematical idealization, and (c) Finite element discretization.....65

Figure 25: The (H vs. t) and (L vs. t) curves for attapulgite.....80

Figure 26: Solids velocity, u_s , vs. volume fraction of solids Φ_s 81

Figure 27: Flux curve for the attapulgite.82

▲

List of Symbols

- a Compressibility coefficient.
- b_0 A constant parameter in Eq. (5.34).
- b_1 A constant parameter in Eq. (5.34).
- b_2 A constant parameter in Eq. (5.34).
- B_0 A constant parameter in Eq. (2.9).
- B_1 A constant parameter in Eq. (2.9).
- B_2 A constant parameter in Eq. (2.9).
- B_3 A constant parameter in Eq. (2.9).
- C The consolidation curve.
- C_t The height of the compacted layer at time t, (m).
- d_i The diameter of solids in a sublayer i, (m).
- $(d_i)_{t+\Delta t}$ The decrease of the height of a sublayer i due to consolidation process at time t+ Δt , (m).
- $dL_{t+\Delta t}$ The total decrease of a layers' height at time t+ Δt due to consolidation process during a time period Δt , (m).
- D_c Diameter of the settling column, (m).
- e The void ratio, $e = \frac{V_e}{V_s}$.
- F_t The height of the falling material at time t, (m).
- g Acceleration of gravity, 9.807 (m/sec²).
- G Solids handling capacity, (m/sec).
- H_0 Initial height of a suspension in batch sedimentation, (m).

- H_{12} Intercept height between parallel line to the vertical axis that passes through (t_1, L_1) and tangent to curve $H_2 = f(t_2)$, (m).
- H_t Height determined by construction on plot of (H vs. t) for batch settling, (m).
- H_j Height determined by construction on plot of (L vs. t) for batch settling, (m).
- I The intensity of a radiation beam, (photons/m²-sec).
- I_0 The incident intensity of a radiation beam, (photons/m²-sec).
- K Intrinsic permeability, (m²).
- K_0 Permeability of unstressed bed, (m²).
- k Hydraulic conductivity, $k = \frac{K \rho g}{\mu}$, (m/sec).
- $(l_i)_t$ The height of a sublayer i at time t , (m).
- L The sediment - suspension curve.
- L_t The height of the rising sediment layer at the bottom of a batch cylinder, (m).
- m_{vi} The coefficient of compressibility of a sublayer i , (m²/N).
- P_t Total hydraulic pressure, (Pa).
- P_s Solid effective pressure, (Pa).
- S Solids volumetric flux, $S = u_s \Phi_s$, (m/sec).
- t Time, (sec).
- u Propagation velocity of a discontinuity, $u = \frac{\Delta S}{\Delta F_s}$, (m/sec).
- u_t Liquid settling velocity, (m/sec).
- u_s Solids settling velocity, (m/sec).
- v Characteristic velocity, $v = -\frac{dS}{dF_s}$, (m/sec).
- $(V_{si})_t$ The volume of solids of a sublayer i at time t .
- x Distance from cylinders bottom, (m).

Greek letters.

- α_0 Local specific flow resistance on the top of the sediment, (m^2).
- β Compressibility coefficient.
- δ Compressibility coefficient.
- ϵ Porosity, $\epsilon = \frac{V_e}{V_t} = \frac{V_e}{V_e + V_s}$.
- ϵ_s Volume fraction of solids in sediment layer or solidosity, $\epsilon_s = \frac{V_s}{V_t} = \frac{V_s}{V_e + V_s}$.
- ϵ_{s0} The null stress solidosity.
- λ Linear radiation attenuation coefficient.
- μ Dynamic viscosity, (Pa-sec).
- ρ Density of liquid, (Kg/m^3).
- ρ_s Density of solids, (Kg/m^3).
- Φ_s Volume fraction of solids in suspension, $\Phi_s = \frac{V_s}{V_t}$
- Φ_{s0} Initial concentration of solids in slurry, volume fraction .

CHAPTER 1

INTRODUCTION

1.1 Gravity thickening operation and definitions

Thickening is defined as the process of solids separation from a suspension, resulting in a solid-rich slurry and relatively clear supernatant fluid. Other terms used to describe a particular aspect, and sometimes the whole process, of thickening include: clarification, sedimentation, dewatering. It is a process that is widely used in several engineering disciplines. Knowledge of the mechanics of sedimentation is important to the environmental engineer because it could lead to more efficient and economical design of waste treatment facilities. For the coastal engineer such knowledge plays a significant role in the design of harbors and associated dredging operations. Chemical, material, mineral, and geotechnical engineers are also concerned with the sedimentation properties of various mixtures and their respective applications.

The procedures commonly employed by the industry for obtaining a slurry of desirable solids concentration use either gravity, filtration, or centrifugation as means of separating the solids from the liquid. The focus of the present work will be on gravitational

thickening, which, among other areas, is widely used in waste treatment facilities. This method of settling requires relatively low cost for mechanical equipment and maintenance and therefore, it usually constitutes the most economical method. However, it tends to be slower than the other methods and requires a settling pond with large surface area.

The Sedimentation process constitutes the dominant factor in the solid-liquid separation and it consists of: a) Suspension of the particles and b) Consolidation of the deposited particles (Kos 1977, and Fitch 1979). Figure 1 illustrates these processes in a settling pond. The rate at which the liquid moves upward when consolidation occurs in the deposited solids indicates the required detention time to obtain desirable concentrations at the bottom of the under design settling tank.

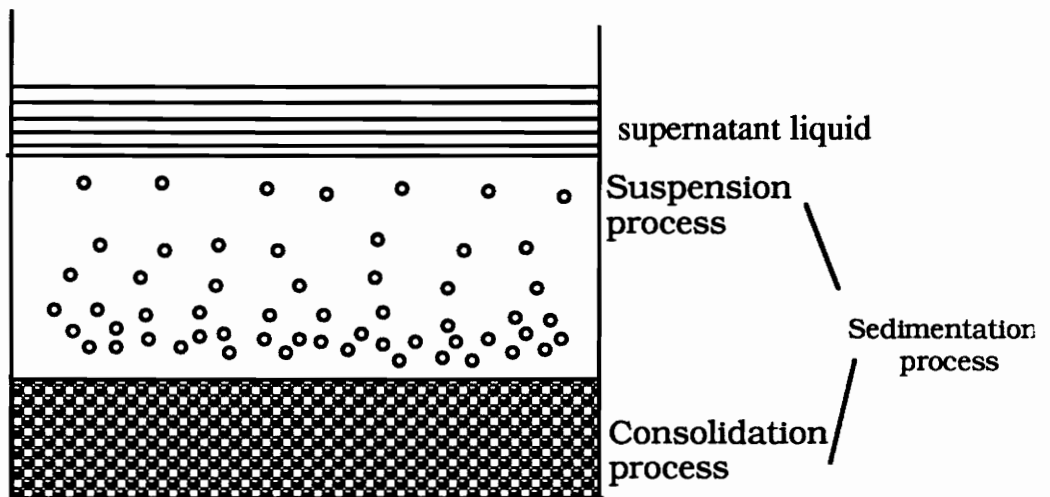


Figure 1: Clarification and sedimentation processes in a thickening pond.

1.2 Classification of the sedimentation process in a thickening pond.

Based on the concentration values of the suspended solids and the degree of interaction among them (multiple particle sedimentation) the following modes of sedimentation can be defined (Pearse 1977, Fitch 1979, and Cullum 1988):

1) Discrete particles settling: Discrete particles fall with a constant terminal velocity in a dilute suspension with no interaction among them.

2) Flocculation: In this case the solid particles collide and agglomerate. This depends on the type of particles that we have; coarser particles will never flocculate. A rough criterion to obtain flocculation is the concentration by volume to be less or equal to 1% .

3) Zone settling: In general, during the zone settling the solid particles settle with constant rate. This mode of sedimentation usually occurs when the solids concentration by volume is in the interval of 1+10 percent. In zone settling, because of the hindering hydrodynamic forces that act among them, individual particles lose their identity and the material is falling "en mass" having uniform concentration.

4) Compression or consolidation mode: For solids concentration higher than about 10 percent by volume, particle bridging is typically observed. In this regime, called compression, further settling is due to the solids own weight while the hydrodynamic forces do no longer influence the phenomenon. In

most of the cases there is a region between the compression and zone regimes which is known as the transition (Kearsey 1963). In this regime, both hydrodynamic forces and particle bridging affect the settling of particles and therefore the laws of zone settling do not adequately describe the suspension process (Fitch 1979, Tiller 1981).

Figure 2, which is known as the "Fitch's paragenesis" (Kos 1977), illustrates the above multiparticle settling classification.

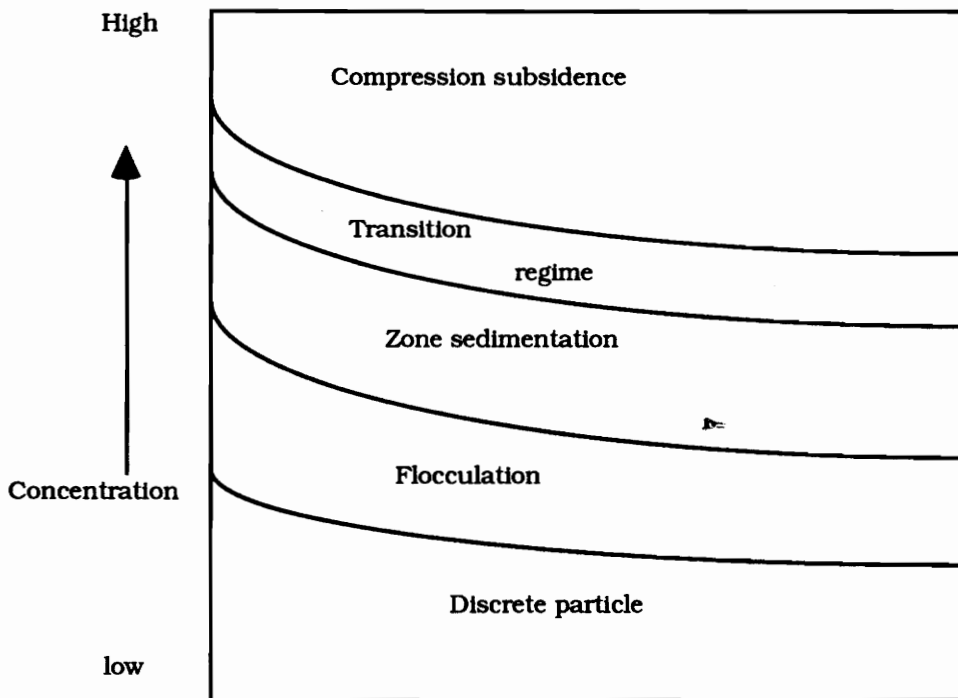


Figure 2: Classification of settling process

The above criteria, which are set for the occurrence of each mode of sedimentation should be considered as very rough, since to a

great extent they depend on the material properties of the solids present in the slurry.

1.3 Continuous and batch type of gravity thickening

Two types of gravity thickeners exist: i) Continuous and ii) Batch gravity thickeners. The continuous thickeners are used for industrial applications (Javaheri 1971). They are usually cylindrical, having a feed inlet, an underflow outlet, and a topflow or overflow outlet (Osborne 1986). The desirable underflow concentration is used to determine the basin area. In most of the continuous thickeners steady operational conditions are preferred. This can be feasible when slurry of the same initial concentration is uniformly fed into the pond. Figure 3 shows a simplified diagram of a typical gravity thickener. The cylindrical feedwell is located at the central point of the tank in order to uniformly distribute the slurry that is subjected to clarification and sedimentation processes.

Thickening devices can also be designed to operate as batch units (Javaheri 1971). In batch thickeners the sedimentation process takes place mechanically or manually. This makes the batch thickening more expensive and less practical than the continuous, for most of the applications.

Although the batch type of thickening operation is not preferred for industrial applications, it is utilized in the laboratory as a preliminary step for sizing continuous thickeners (Javaheri 1971, Kos 1977). It was observed that the lower sections of a batch cylinder

represent the sedimentation process in a continuous thickener (Tarrer 1977).

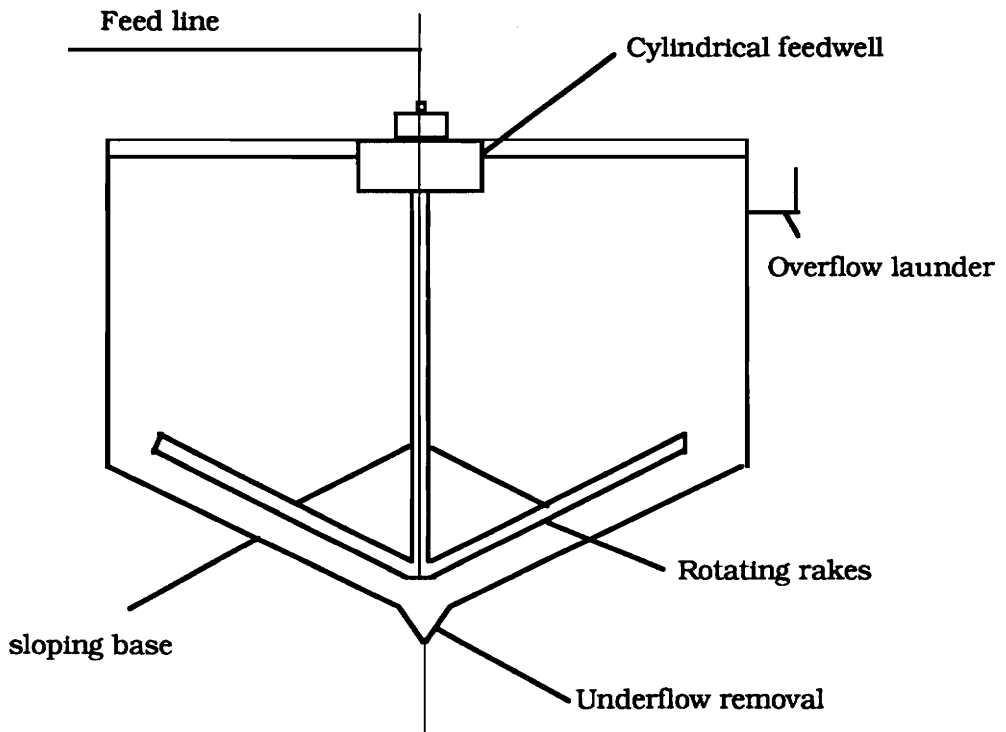


Figure 3: A typical gravity thickener (after Osborne 1986).

Graduated cylinders with total heights up to 200 cm, and different diameters are used for a series of experiments, known as batch tests. During a batch test of a slurry with specific initial height and solids content, a line of demarcation between the supernatant liquid and the suspended solids is visualized, known as mudline interface. A plot of

the mudline height variation with time is called batch settling curve, or normal curve. A typical batch curve (H vs. t) is illustrated in figure 4. The determination of a batch curve constitutes a significant step in the gravity thickening process, since useful information can be deduced from its slope and its shape. The slope of a batch curve indicates the rate at which the solids move downwards to the bottom of a cylinder. A batch curve, generally, consists of three regimes, sections, or phases: (i) The first phase is represented by a straight line and is known as constant rate phase or regime. In the constant regime the solids' settling rate is constant (because the slope of the curve in this section is constant) and is equal to the initial settling rate. By considering the material balance in this section the concentration of the suspended solids in a layer should be equal to its initial value. In this regime, we consider that the particles move downwards as a zone. (ii) The second regime is called transition regime or first falling rate section. In the transition regime the settling process of particles is delayed by the upward movement of the liquid, that comes out from the consolidating solids at the bottom of the cylinder, to the top of the cylinder. (iii) The last regime is known as the compression, consolidation, or second falling rate regime. As the particles accumulate at the bottom of the cylinder, they start gradually to get compacted due to their own weight. This process continues up to a point which is known as the critical consolidation point (point d in figure 4). Beyond this point the height of the sediment remains constant.

During a batch test a second interface can be constructed. It is called sediment - suspension interface, or L-curve, or sometimes rising sediment curve (figure 4) and indicates the rate that the sediment rises from the bottom of the cylinder. This interface most of the times is not visible and to be detected the aid of the x-rays radiation is necessary.

Many researchers (Gaudin et al 1959, Javaheri 1971, Bhargava and Rajagopal 1990) ascertained the role of some basic variables in gravity thickening by doing a series of batch tests. They found that for a given material of known size distribution, the following variables play a dominant role: 1) Initial concentration of the solids in the slurry, 2) Initial height of the slurry in the cylinder, and 3) Liquid viscosity.

Depending on the initial concentration of the slurry, various shapes of batch curves can be obtained. Some typical batch curves describing the settling process are shown in figures 5, 6, and 7 (Gaudin et al 1959, Kos 1985). When flocculants are used in the batch process there is often an induction time that indicates the trend of the solid particles to agglomerate (figure 5). The mudline interface obtained for intermediate values of the initial slurry concentration consists of the constant, transition, and the compression regimes (figure 6).

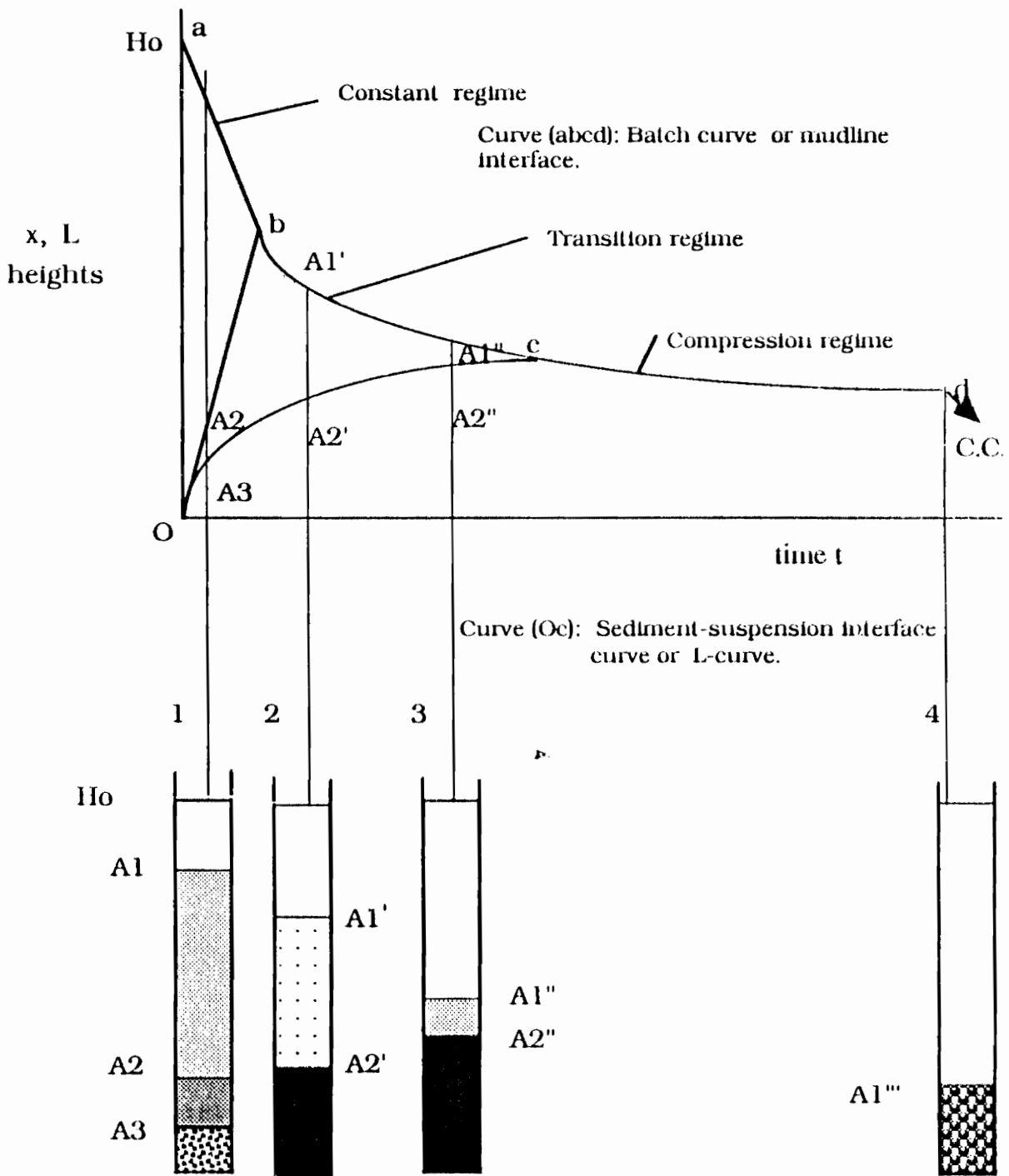


Figure 4: Batch (H vs. t) and rising sediment (L vs. t) curves from a typical settling test.

For high values of the initial slurry concentration only the consolidation regime is experienced (figure 7).

For a slurry of the same solids content, an increase in the initial height causes the delay of the settling process (Diplas et al 1988). The properties of the liquid in the suspension play also an important role to the settling process. An increase in the liquid viscosity leads to the reduction of the solids settling velocity. Solid-liquid separation also can be affected from such factors as, stirring, shape of cylinder bottom, sidewalls and others. Slow stirring can beneficially change the sedimentation process in a cylinder and also a conic shape of the cylinder's bottom can facilitate the thickening process (Javaheri 1971). Settling can also be influenced by the presence of sidewalls. The degree of the alteration depends on the suspension considered. Wall effects can be considered negligible when the diameter of the settling column, D_c satisfies the following inequality (Cullum 1988):

$$D_c > 100 d_i$$

where, d_i denotes the diameter of solids in a sublayer i .

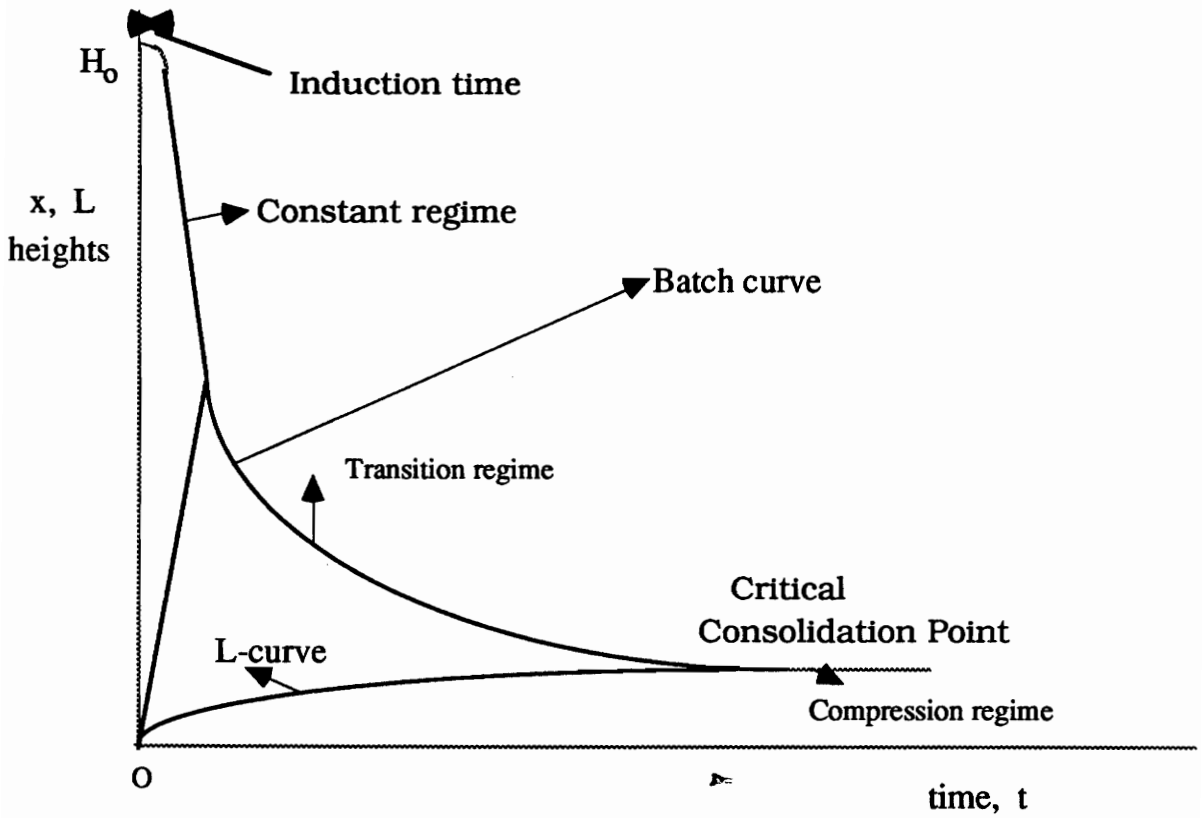


Figure 5: A typical batch curve for a slurry of low initial concentration

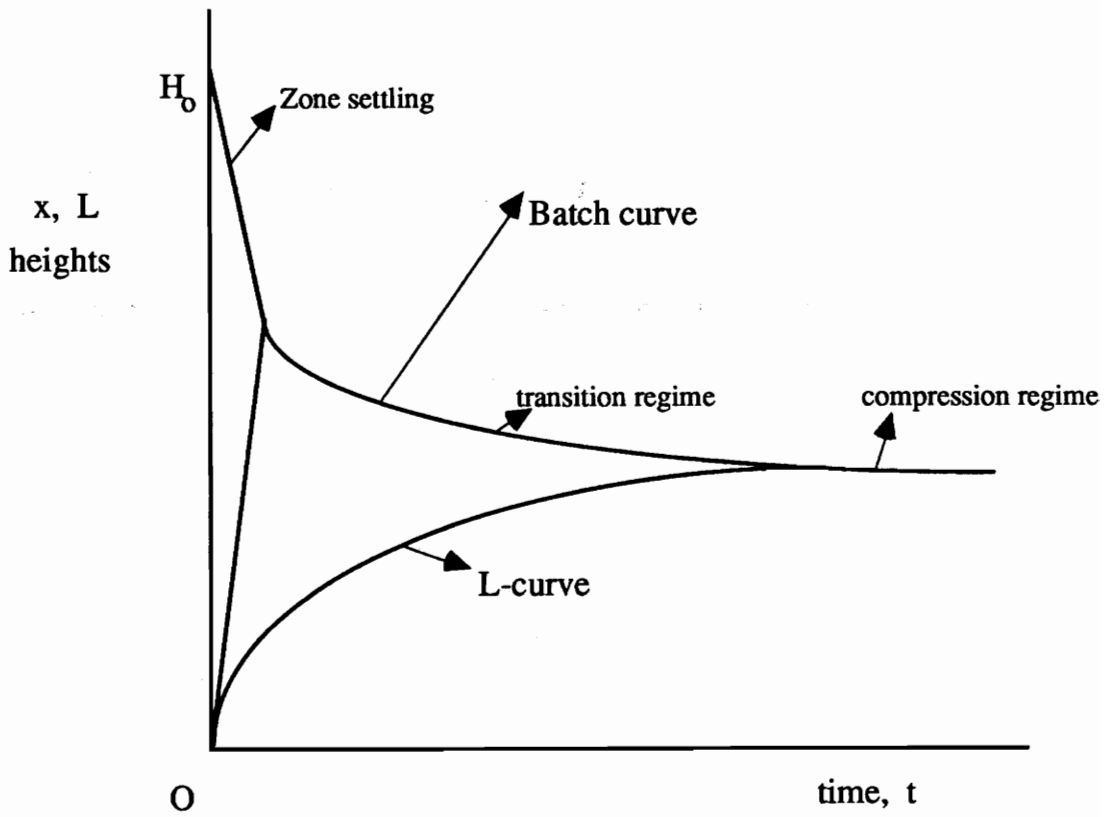


Figure 6: A typical batch curve for a slurry with intermediate initial concentration.

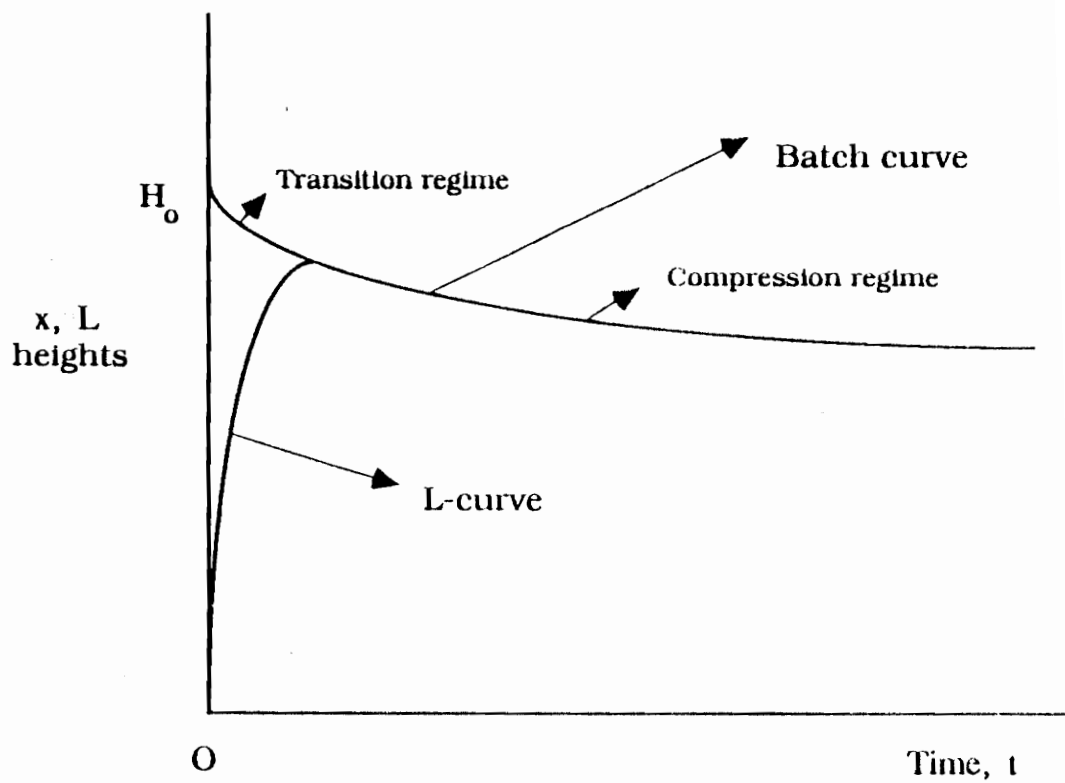


Figure 7: A typical batch curve for a slurry with high initial concentration.

CHAPTER 2

BATCH THICKENING THEORIES-CRITICAL REVIEW

This chapter presents a critical review of the most widely used batch thickening theories. In chronological order they include the Coe and Clevenger's method (1916), Kynch's method (1952), Talmage and Fitch's method (1955), Tarrer's method (1974), Tiller's method (1981), Fitch's method (1983), and Font's method (1988).

Coe and Clevenger's method (1916): Coe and Clevenger did the pioneering work in the sedimentation field. The innovative point of their theory is the proposition that any layer of a suspension has a certain capacity to discharge its solids. This capacity is known as solids handling capacity, G , and is defined by the following equation:

$$G = \frac{u_s}{\frac{1}{\Phi_s} - \frac{1}{\Phi_{su}}} \quad (2.1),$$

where, Φ_s is the volume fraction of solids in a layer and is defined as:

$$\Phi_s = \frac{V_s}{V_t}$$

where V_s is the volume of solids in the suspension and V_t is the total volume in the suspension, Φ_{su} denotes the underflow volume fraction

of solids, and u_s is the settling velocity of solids in a layer. The settling velocity of solids is given by,

$$u_s = \frac{dH}{dt}$$

where, H is the height of the mudline interface at time t .

This technique usually overestimates thickener's capacity and underdesigns the facility in terms of unit area (Pearse 1977, Diplas et al 1988). However, the method yields satisfactory results if it is used in conjunction with empirical safety factors. The method has the following limitations as have been discussed by Pearse (1977):

- it relies on the assumption that the solids settling velocity, u_s , in a layer is only a function of the volume fraction of solids, Φ_s , in this layer,
- it applies to ideal slurries. Ideal slurries are the slurries prepared of incompressible particles of spherical shape and equal size having densities more than the surrounding liquid,
- it is experimentally inconvenient because it requires multiple batch settling tests to determine the area of the required thickener.

Kynch's method (1952): Kynch's theory constitutes the first step in the theoretical analysis of batch experimental data. The theory is based on the following assumptions:

- the particles concentration is uniform across any horizontal layer,
- the initial concentration increases moving downwards through the batch column,

- consideration of a dispersion with similar particles i.e., similar particles, are the particles with the same size and shape,
- the settling velocity, u_s , depends only on the local volume fraction of solids, Φ_s ,
- wall effects can be ignored.

Kynch (1952) was the first to introduce the term solids flux, S , to his mathematical analysis. The solids flux, S , is defined as the product of the solids settling velocity, u_s , with the volume fraction of solids, Φ_s , in the suspension:

$$S = u_s \Phi_s$$

By considering the material balance in a layer with thickness dx in a batch column (figure 8), the accumulation of particles within this layer over a time period dt is the difference between the inflow of particles, $S(x+dx)$, through the upper boundary and the outflow, $S(x)$ from the lower boundary of the layer. By carrying out the solids mass balance the following equation is obtained:

$$\frac{\partial}{\partial t} (\Phi_s dx) dt = S(x+dx) dt - S(x) dt$$

or,

$$\frac{\partial \Phi_s}{\partial t} = \frac{\partial S}{\partial x} \quad (2.2),$$

where, Φ_s denotes the volume fraction of solids, S the solids flux and x is the vertical distance from the bottom of the cylinder.

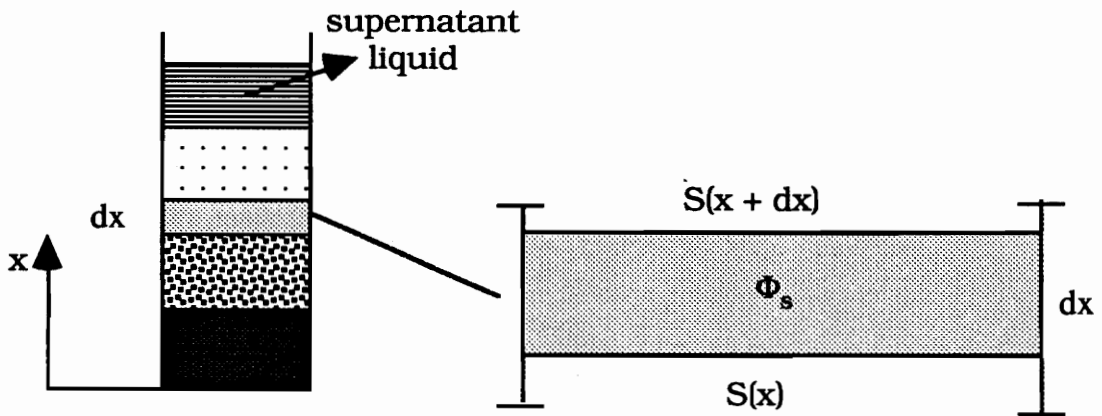


Figure 8: Material balance in a layer.

Equation (2.2) is known as the Kynch's continuity equation (Kynch 1952). By applying the definition of the volumetric solids flux and since $u_s = f(\Phi_s)$ (Kynch's assumption) equation (2.2) can be written as:

$$\frac{\partial \Phi_s}{\partial t} = \frac{dS}{d\Phi_s} \frac{\partial \Phi_s}{\partial x} \quad \text{or,}$$

$$\frac{\partial \Phi_s}{\partial t} + \left[- \frac{dS}{d\Phi_s} \right] \frac{\partial \Phi_s}{\partial x} = 0 \quad (2.3)$$

The term $-\frac{dS}{d\Phi_s}$ is the slope of the flux curve, (S vs. Φ_s). A typical flux curve is illustrated in figure 9.

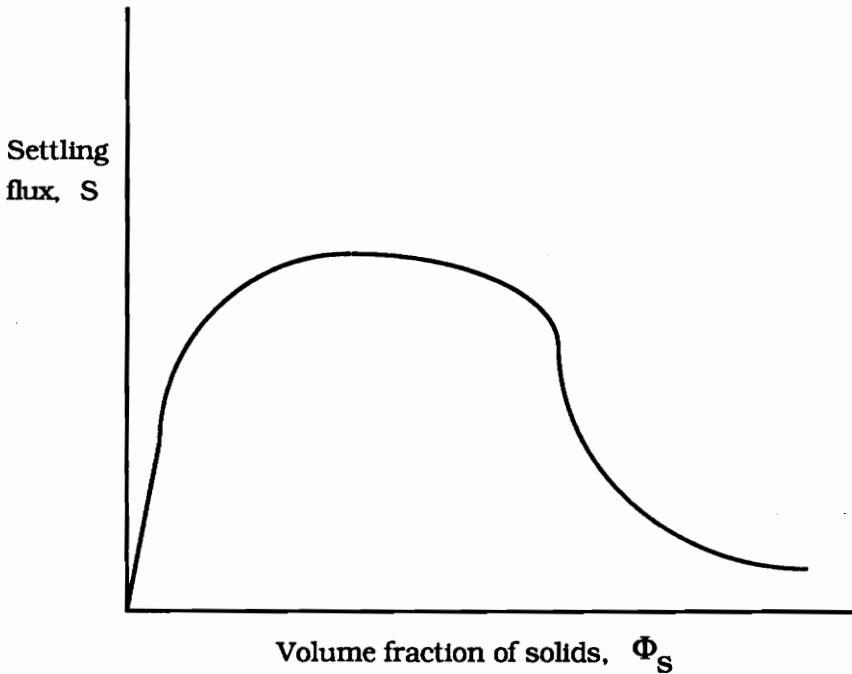


Figure 9: A typical flux curve.

In many gravity thickening models (Tarrer 1974, Chen 1986, Tiller 1981) the continuity equation is used in the form as described by equation (2.3) instead of the one in equation (2.2). Kynch's analysis postulates the existence of a family of straight lines that originate from the bottom of the cylinder (figure 10). The concentration along each of these lines remains constant and so they are called isoconcentration lines. Then along such a line,

$$\frac{d\Phi_S}{dt} = 0.$$

Therefore,
$$\frac{d\Phi_S}{dt} = \frac{\partial\Phi_S}{\partial t} + \frac{dx}{dt} \frac{\partial\Phi_S}{\partial x} = 0 \quad (2.4)$$

By comparing equations (2.3) and (2.4) we obtain:

$$\frac{dx}{dt} = - \frac{dS}{d\Phi_s} = - \frac{d(u_s\Phi_s)}{d\Phi_s} \quad (2.5).$$

By solving equation (2.5) with respect to x we can obtain the equation that represents the family of the isoconcentration lines,

$$x = - \frac{d(u_s\Phi_s)}{d\Phi_s} t + c \quad (2.6).$$

The quantity $-\frac{d(u_s\Phi_s)}{d\Phi_s}$ in equation (2.6) is defined as the slope of the isoconcentration lines. The isoconcentration lines are defined as characteristics and their slope as the characteristic velocity, v , given by,

$$v = - \frac{d(u_s\Phi_s)}{d\Phi_s} \quad (2.7).$$

Kynch ignored the rising sediment from the bottom. He argued that the constant c in equation (2.6) is equal to zero and so all the characteristics originate from the coordinates origin.

Kynch proposed a method to calculate the volume fraction of solids, Φ_s , just below the mudline interface. The initial volume of solids in a slurry is equal to the volume of solids crossing a characteristic. Thus for a characteristic that reaches the batch curve at point A during a time period t_A (figure 10) we get:

$$\Phi_{s0} H_0 = \Phi_{sA} (u_{sA} - v_A) t_A \quad \text{or,}$$

$$\Phi_{sA} = \frac{\Phi_{s0} H_0}{u_{sA} - v_A} t_A \quad (2.8),$$

where, Φ_{s0} , H_0 denote the initial volume fraction of solids and height, respectively, Φ_{sA} is the volume fraction of solids at point A, u_{sA} denotes the mudline settling velocity at point A, and v_A is the upward propagation speed of the characteristic. However, the volume of the solids that deposited at the cylinder bottom from the beginning of the test to the time of departure of the characteristic has been ignored in the derivation of equation (2.8) (Kynch 1952). Therefore, equation (2.8) is valid only in the constant rate regime of a batch settling curve, or for the first characteristic emanating from the bottom of the cylinder (figure 4). In spite of the above limitations Kynch's theoretical analysis has been the basis for subsequent developments.

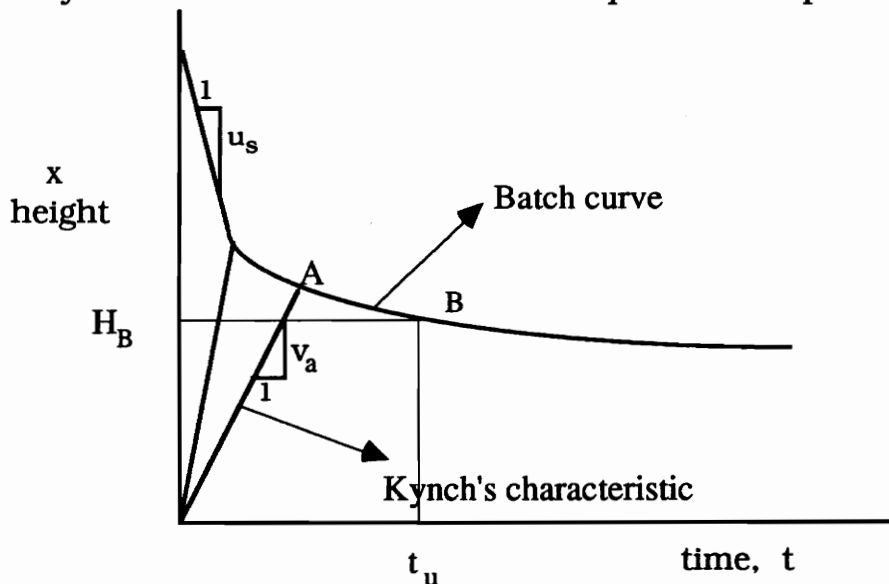


Figure 10: Kynch's characteristics (after Kynch 1952).

Talmage and Fitch's method (1955): Talmage and Fitch's work suggested a simple geometrical method to calculate the required area of a settling pond that is based on Kynch's theory of batch settling. To apply their method only one batch curve is necessary. By drawing an horizontal line from a point B with height $H_B = \frac{\Phi_{so}H_o}{\Phi_{su}}$ (Φ_{su} is the required underflow volume fraction of solids) it intersects the batch curve at some time value t_u and the required unit area is equal to $\frac{t_u}{F_{so} H_o}$. Due to its simplicity, this method is still used to estimate the area of a thickener (Diplas et al 1988). In comparison with Coe and Clevenger's method, it tends to overestimate the required thickener area and so it is used in practical applications to determine the upper limit of the surface area (Pearse 1977, Osborne 1986). The limitations of Kynch's method apply also to this method.

Tarrer's method (1974): Tarrer's analysis focused on the development of a method that predicts the variation of the mudline interface height with time. Because Kynch's continuity cannot describe truthfully the settling process in the transition and compression regimes, Tarrer suggested an empirical equation that predicts the actual solids settling velocity as a function of the solids concentration in this regime for a particular slurry (the kaolin). He used a variety of data points that relate initial settling rates to initial volume fraction of solids for different type of kaolin slurries and based on observations the following empirical equation was developed:

$$u_s = B_0 \exp.(B_1\Phi_s + B_2\Phi_s^2) + B_3 \quad (2.9)$$

where, B_0 , B_1 , B_2 , and B_3 are constant parameters with undetermined physical meaning. By combining equation (2.9) with equations (2.7) and (2.8) obtained from Kynch's method, the variation of the mudline height with time can be computed. Tarrer's analysis, however, does not consider the compression effects and so it is only efficient in the zone settling regime (Pearse 1977). Furthermore, the applicability of equation (2.9) is limited to kaolin slurries.

The above methods, known as flux theories, fully describe the suspension process in the zone settling regime of a batch settling curve. More recently, several researchers have proposed methods to modify and generalize Kynch's method so that it could be applied, in addition to zone settling, to transition, and consolidation regimes of a batch curve. Their methods are described below.

✿ Tiller's method (1981): Tiller revised Kynch's method by taking into account the rising sediment from the bottom of a graduated cylinder. The total volume of solids in the cylinder is equal to the volume of solids in the sediment (this term was ignored by Kynch) plus the volume of solids in the suspension. If ϵ_s denotes the volume fraction of solids in the sediment, Φ_s is the volume fraction of solids in the suspension, and Φ_{s0} , H_0 are the initial volume fraction of solids and height, respectively, the total volume of solids is given by,

$$\Phi_{s0} H_0 = \int_0^{L_1} \epsilon_s dx + \int_{L_1}^{H_1} \Phi_s dx.$$

In the above equation the limits L_1 , H_1 in the integrals are the sediment and mudline height, respectively, at time t_1 . Therefore, Tiller (1981) considered that the characteristics originate from the sediment - suspension interface and by using the jump boundary conditions on this interface corrected equation (2.8), which was originally proposed by Kynch, to get:

$$\Phi_{s2} = \frac{\Phi_{s0} H_0}{H_{12} - L_1} \exp\left(- \int_0^{t_1} \frac{dH_2/dt_2 - dL_1/dt_1}{H_{12} - L_1} dt_1\right) \quad (2.10).$$

The variables H_{12} , Φ_{s2} , and L_1 in equation (2.10) are defined in figure 11.

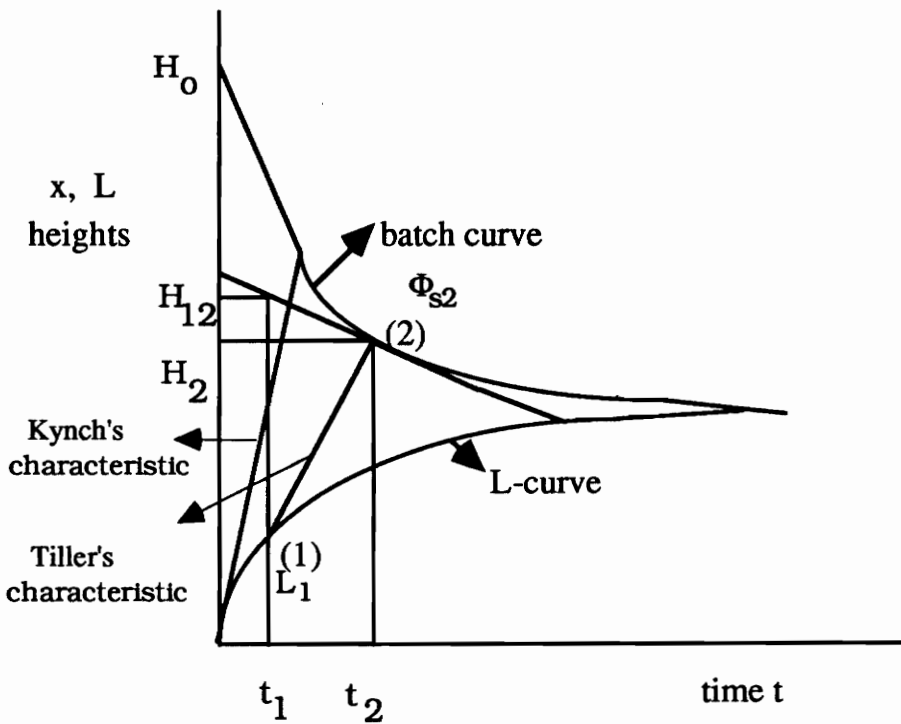


Figure 11: Tiller's characteristic line (after Tiller, 1981).

Tiller proposed a method, known as suspension-consolidation method, to describe the transition and compression regimes of a batch settling curve. However, some uncertainties regarding the physical process in the compacted sediment and the rate that the suspended material settles left this work in some way incomplete.

Fitch's Method (1983): Fitch affirmed that the characteristics originate from the top of the sediment - suspension interface, L , but he further postulated that they do so as tangents to the rising sediment curve, L .

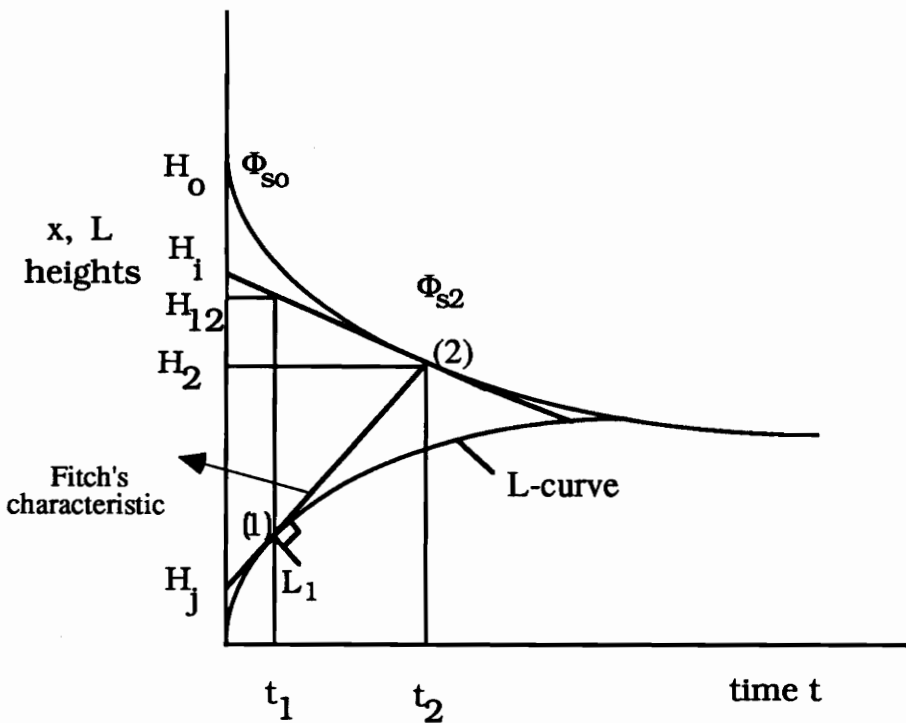


Figure 12: Generalized Kynch-type construction (after Fitch, 1983).

Based on this requirement he derived a geometrical construction (figure 12) to modify the one proposed by Kynch's equation (2.8).

From figure 12, the concentration just under the mudline interface at a point (2) is given by the following equation:

$$\Phi_{s2} = \Phi_{s0} \left[\frac{H_0 - H_i}{H_1 - H_j} \right] \quad (2.11),$$

where, H_i is the intersection point of the vertical axis and the tangent at point (2) of the batch settling curve, and H_j is the intersection point of the x-axis with the isoconcentration line reaching the point (2). Fitch (1983) highlights the need for determining the variation of the sediment-suspension interface with time, and in fact use of his method (equation (2.11)) requires prior knowledge of the L-curve. Fitch's finding that the characteristic lines are tangents on the L-curve (figure 12) is very important for any further development. However, the proposed equation is mainly obtained by using the geometry of figure 12 and is not an outcome of a theoretical process as Tiller's relation does.

Font's Method (1988): Font simplified Tiller's equation (2.10) employing the fact that the characteristics emanate tangentially from the surface cake, to obtain:

$$\Phi_{s2} = \frac{\Phi_{s0} H_0}{H_{12} - L_1} \exp\left(- \int_0^{t_1} \frac{1}{t_2 - t_1} dt_1\right) \quad (2.12).$$

In the above equation, H_{12} is the intercept height between the parallel line to the vertical axis that passes through (t_1, L_1) and the

tangent to curve $H_2 = f(t_2)$ (figure 12), L_1 is the sediment height at time t_1 . Font's experimental work does validate Fitch's postulation but a theoretical proof is not yet available. Therefore, Font (1988) by comparing his model equation with those proposed by Fitch (equation (2.11)) and Kynch (equation (2.8)) concluded that his method gives results closer to the experimental ones. Font's method also requires prior knowledge of L-curve.

CHAPTER 3

THEOREMS IN BATCH SEDIMENTATION

During a batch settling test of a slurry, sudden finite increases or decreases in the slurry's concentration are typically observed at a certain level in the batch cylinder, known as discontinuities of first kind or first order (Kynch 1952). Since the continuity equation in differential form, equation (2.3), no longer applies, it was proposed by Kynch (1952) a relation that states : " ... the flow of particles into one side of the layer equals the flow out on the other side ...". When the concentration change across a layer is infinitesimal the discontinuity is called of the second kind or of the second order (Kynch 1952). The discontinuities of first and second order as they have been defined by Kynch are known in the literature as the first and second Kynch's theorems (Fitch 1983).

(i) The first Kynch's theorem.

If there is a first order discontinuity at a certain level in a batch column it will propagate with velocity u given by (Kynch 1952),

$$u = \frac{\Delta S}{\Delta \Phi_s} \quad (3.1),$$

By applying the above equation for points (1) and (2), which are located above and below the interface of a discontinuity we obtain:

$$u = \frac{u_{s1}\Phi_{s1} - u_{s2}\Phi_{s2}}{\Phi_{s1} - \Phi_{s2}} \quad (3.2),$$

A negative sign of the propagation velocity u implies that the sediment discontinuity moves upward (figure 13) while a positive sign infers that the sediment discontinuity moves downward (figure 14). Because finite concentration discontinuities can also occur at the sediment - suspension interface the propagation velocity of the discontinuity on this interface is expressed as:

$$u = \frac{u_{s1}\Phi_{s1} - u_{s0}\epsilon_{s0}}{\Phi_{s1} - \epsilon_{s0}} \quad (3.3),$$

where, ϵ_{s0} is the volume fraction of solids at the interface, u_{s0} is the solids settling velocity at the interface, and Φ_{s1} , u_{s1} are the volume fraction of solids and solids settling velocity at point (1) just above the sediment- suspension interface.

A first order discontinuity can be defined as stable when it propagates completely unchanged through the suspension. This happens when the chord of the discontinuity lies everywhere below the flux curve (Fitch 1983). On the other hand if infinitesimal concentration steps or concentration gradients (defined as second order discontinuities) are formed within the range of a first order discontinuity the latter will not propagate unchanged with time. This type of first order of discontinuity is defined as unstable and occurs

when its chord lies everywhere above the flux curve (Fitch 1983). Both cases are illustrated in figure 15.

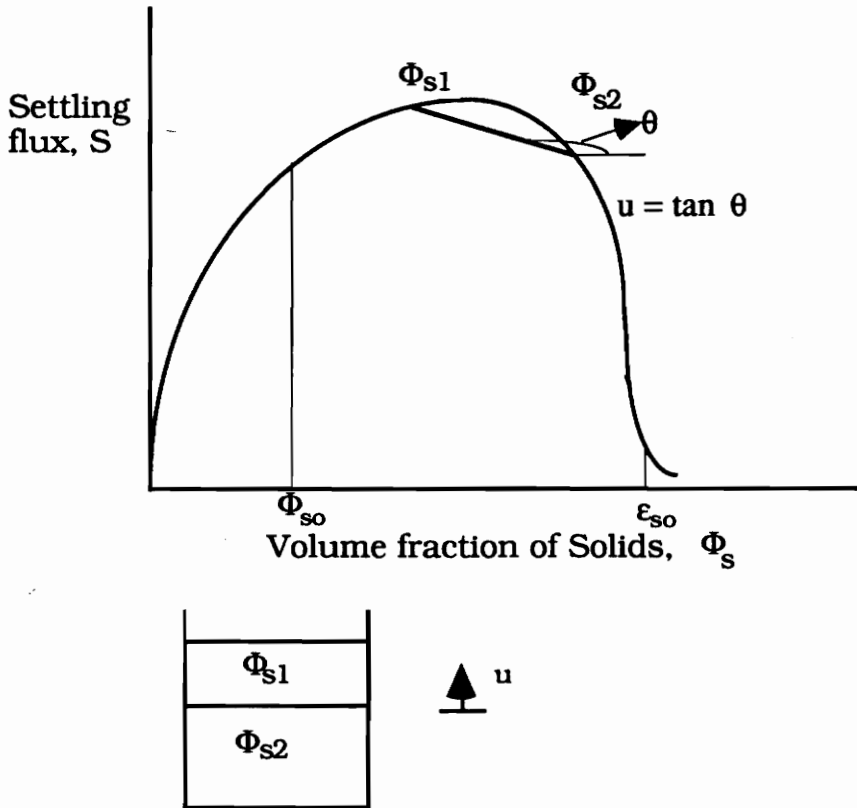


Figure 13: Upward propagation velocity of a sediment discontinuity.

(ii) The second Kynch's theorem.

Second order discontinuities are formed when small concentration changes exist across a layer. They can be constructed in the region of a finite discontinuity. When the chord of the first order of discontinuity lies everywhere below the flux curve, the discontinuity propagates faster than the existing in its region second

order of discontinuities. The second kind of discontinuities are wiped out and so the finite discontinuity propagates without perturbations. In the region of a first order of discontinuity which its chord lies everywhere above the flux curve the second order of discontinuities propagate individually. They yield to the construction of concentration gradients in region of the finite discontinuity which is now an unstable discontinuity.

Near the sediment-suspension interface infinitesimal concentration changes can be formed within the suspension which propagate upward through the suspension at the same velocity as the characteristics do. The constant rate, v , is given by,

$$v = - \frac{dS}{d\Phi_s} \quad (3.4),$$

Figure 15 illustrates second order of discontinuities.

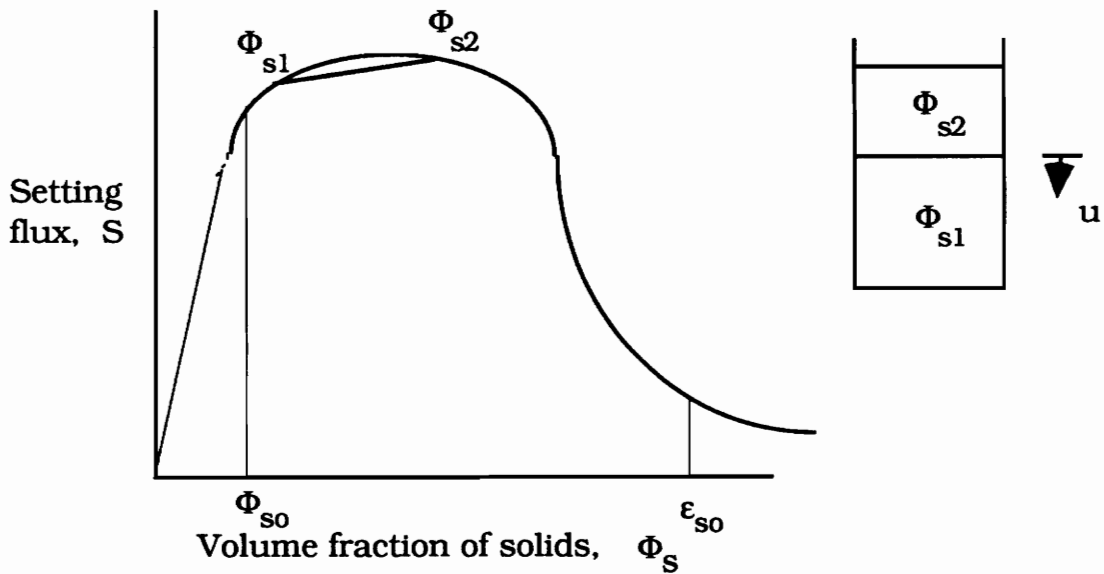


Figure 14: The downward propagation velocity of a sediment discontinuity.

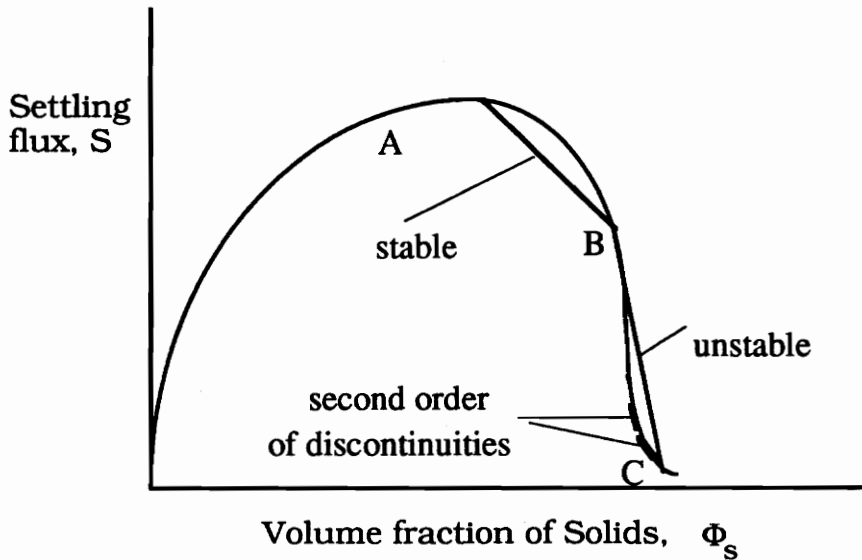


Figure 15: Stable (AB) and unstable (BC) discontinuity, and second order of discontinuities.

(iii) The modified third Kynch's theorem.

Kynch derived an expression (equation (2.8)) that computes the solids concentration just under the mudline interface without taking into consideration the rising of the sediment-suspension interface from the bottom. The relation (2.8) has been modified by Tiller (1981),

Fitch (1983), and Font (1988) to be applicable in all three regimes of a typical batch settling curve by accounting for the compression effects to the suspension process. The present work considers equation (2.12), that was proposed by Font, as the third modified Kynch's theorem and it is given as:

$$\Phi_{s2} = \frac{\Phi_{s0}H_0}{H_{12}-L_1} \exp\left(- \int_0^{t_1} \frac{1}{t_2-t_1} dt_1\right) \quad (3.5),$$

where, Φ_{s2} is the volume fraction of solids just under the mudline interface at time t_2 , Φ_{s0} is the initial volume fraction of solids, H_0 is the initial height of the slurry, L_1 is the height of the sediment layer at time t_1 , and H_{12} is defined in figure 12.

The third theorem can be used only if the location of the sediment - suspension interface is known at every time (L-curve).

CHAPTER 4

OBJECTIVES OF THE PRESENT WORK

The present work focus on batch sedimentation of slurries with intermediate up to high initial concentrations, which exhibit zone settling behavior at least at the initial stages. It is based on the principles and theory derived by Kynch (1952) and the proposed modifications of Kynch's method by Tiller (1981), Fitch (1983), and Font (1988,1991). In this work, by taking into account such factors as the upward movement of the liquid and the settling rate of the falling material, we propose a method that expands and generalizes the above analyses. The expanded model will be valid in all three settling regimes (constant, transition, and compression) and requires no prior knowledge of the L-curve, which severely limits the practical usefulness of the earlier methods. The objectives of this work are the following:

- 1) to present a theoretical model that describes the consolidation and the suspension processes that occur simultaneously during a batch thickening test,

- 2) to propose an alternative method for the representation of the consolidation process,

3) to develop a computer code that calculates the effective pressure variation within the sediment accumulated at the bottom of the cylinder. This information can be used to obtain the variations of the solids volume fraction and the intrinsic permeability with height at every time instant, the upward liquid velocity, the downward solids velocity, and the consolidating height of each sublayer in the solids bed,

4) to develop a method to obtain the height variation of the sediment layer with time,

5) to predict the height variation of the supernatant liquid-mudline interface with time.

CHAPTER 5

THEORETICAL MODEL OF BATCH THICKENING

5.1 Assumptions considered in batch sedimentation.

The assumptions considered during the suspension-consolidation processes in a batch cylinder are the following:

- 1) Three sedimentation regimes are present in slurries with intermediate initial concentrations: a) the constant regime, b) the transition regime, and c) the consolidation regime.
- 2) The cylinder wall effects are negligible.
- 3) The particles concentration is uniform along any horizontal layer.
- 4) The inertial effects in the sediment layer can be ignored since both liquid and solids velocities obtain small values.
- 5) The characteristics are straight lines.
- 6) The characteristics emanate tangentially from the L-curve.
- 7) Small discontinuities exist between zones of different solids concentration.
- 8) The null stress solidosity, ϵ_{s0} , at the consolidation - suspension interface remains constant.

9) The deformation of the solids phase in the sediment layer is due to the rearrangement of the particles in the solids structure. The particles themselves do not deform.

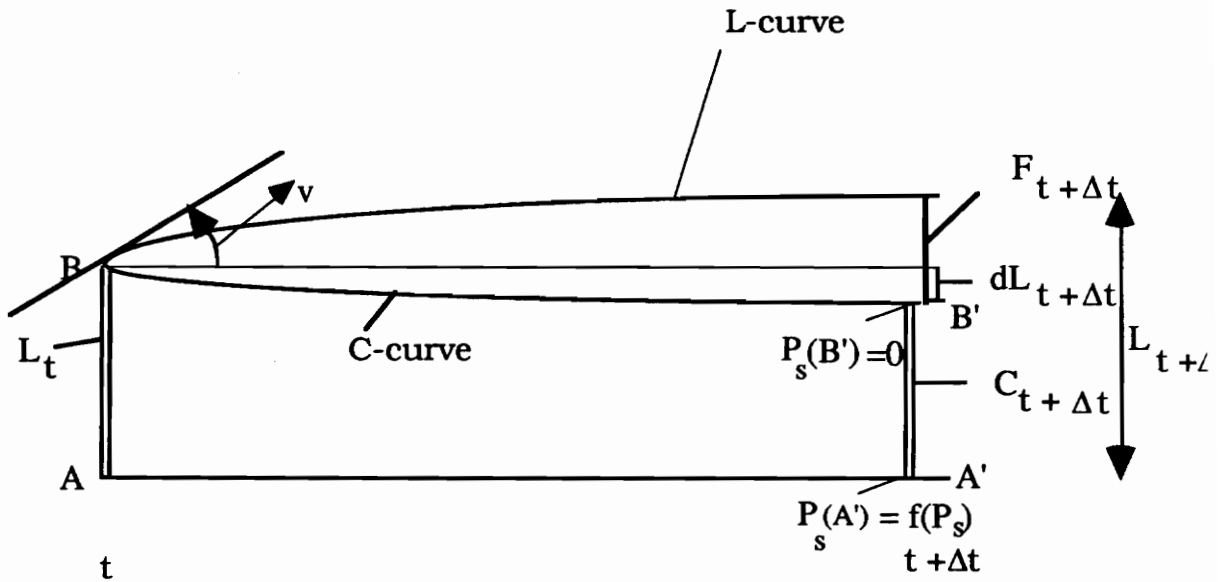


Figure 16: Consolidation - suspension problem.

5.2 The physical process in batch sedimentation.

As the particles move downwards to the bottom of a batch column, during a batch setting test, a bed of solids starts developing which is similar to a granular porous medium (Andrian and Kos 1975). During a time period Δt the height of the solids bed decreases since the particles come closer and closer due to their own weight while the water trapped in the porous structure moves upward. The decrease of

the solids bed height is illustrated by the C curve in figure 16. Simultaneously with the consolidation process deposition of the suspended solids takes place. However, the amount of the added solids on the existing bed, except for the first few time steps, is significantly smaller than the amount of solids already deposited. Therefore, from a calculation standpoint, these added solids can be considered as depositing instantly at the end of a time step Δt (Been and Sills 1981). The increment $F_{t+\Delta t}$ in figure 16 denotes the height of the added material on the top of the consolidated bed, $C_{t+\Delta t}$, over the time step Δt .

5.3 Consolidation process

5.3 1. Model for the consolidation process

To develop a theoretical model for the compacting process of the deposited solids that takes place in the area (ABB'A') (figure 16) the laws of the continuum mechanics are utilized. By considering that the solids bed constitutes a particulate system, i.e. the porous state medium is assumed to be a unique function of the effective stress, and ignoring inertial effects since the movement of the solids as well as of the liquid phase are very slow (Kos and Andrian 1975, Tiller et al 1986) we obtain the following relation from the balance of static forces in a sediment layer of thickness dx (figure 17):

$$\frac{\partial P_s}{\partial x} + \frac{\partial P_l}{\partial x} + g(\rho_e + \rho_s \epsilon_s) = 0 \quad (5.1),$$

where, P_s denotes the effective pressure of solids, P_t is the liquid pressure due to the solids, x is the vertical direction, g is the acceleration of gravity, ϵ is the porosity which is defined as:

$$\epsilon = \frac{V_e}{V_t} = \frac{V_e}{V_e + V_s},$$

where, V_e , is the volume of voids in the sediment layer, V_s , is the volume of solids in the sediment layer, and V_t is the total volume of the sediment layer.

In equation (5.1) ϵ_s is the volume fraction of solids in the sediment layer or, solidosity, which is defined as the ratio of the volume of solids to the total volume and it is given as:

$$\epsilon_s = \frac{V_s}{V_t} = \frac{V_s}{V_e + V_s},$$

ρ is the liquid density, and ρ_s is the solids density. The porosity and solidosity satisfy the following equality:

$$\epsilon + \epsilon_s = 1 \quad (5.2).$$

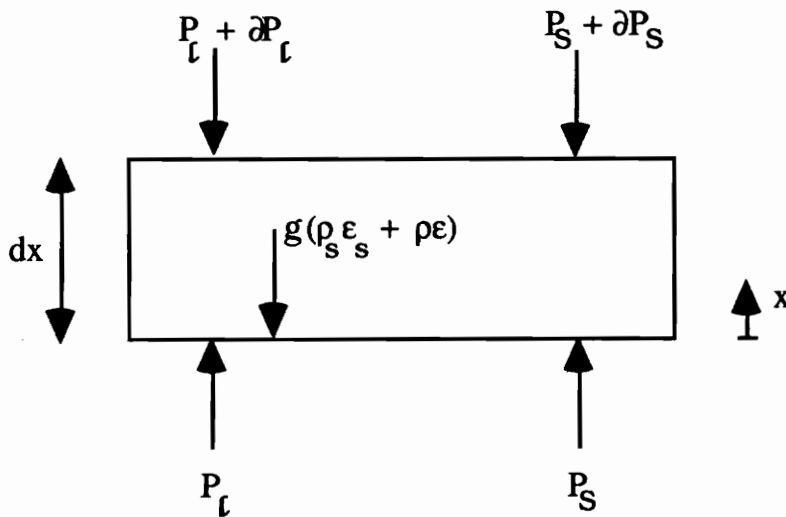


Figure 17: Stresses in a sediment layer.

By using equation (5.2), equation (5.1) becomes:

$$\frac{\partial P_l}{\partial x} + g\rho + \frac{\partial P_s}{\partial x} + g\varepsilon_s(\rho_s - \rho) = 0 \quad (5.3).$$

Shirato (1970) modified the Darcy equation by introducing the relative velocity term in its expression since in gravity sedimentation the solids velocity is not negligible. The first two terms in equation (5.3) can be expressed through the Darcy - Shirato equation as:

$$\frac{\partial P_l}{\partial x} + g\rho = \frac{(u_l - u_s)\mu(1 - \varepsilon_s)}{K} \quad (5.4),$$

where, u_l is the liquid velocity, u_s is the solids velocity, μ is the dynamic viscosity, and K is the intrinsic permeability. The reason for using the intrinsic permeability instead of the hydraulic conductivity, k , is because the latter is dependent on the temperature while the former is not. The intrinsic permeability K , is defined as:

$$K = \frac{k\mu}{\rho g} \quad (5.5).$$

By substituting equation (5.4) to (5.3) we obtain:

$$\frac{\partial P_s}{\partial x} = -g\varepsilon_s(\rho_s - \rho) - \frac{(u_l - u_s)\mu(1 - \varepsilon_s)}{K} \quad (5.6).$$

Equation (5.6) is known in the literature as the particulate structure equation and constitutes the momentum equation of the problem. The first term of the r.h.s. in equation (5.6) is the buoyant weight of particles and the second term denotes the upward friction due to Darcian flow of the liquid. From mass balance considerations, the downward particle volume flux during a batch test is equal to the displaced and upward moving fluid volume flux:

$$u_s \epsilon_s + u_f \epsilon = 0 \quad (5.7).$$

By substituting u_s from equation (5.7) into equation (5.6) and solving for u_f we get:

$$u_f = -\frac{\partial P_s}{\partial x} \frac{K(1-\epsilon)}{\mu \epsilon} - \frac{K(1-\epsilon)^2}{\mu \epsilon} g (\rho_s - \rho) \quad (5.8).$$

The next step is to utilize the continuity equation for the liquid phase in the particulate structure:

$$\frac{\partial \epsilon}{\partial t} + \left[-\frac{\partial(u_f \epsilon)}{\partial x} \right] = 0 \quad \text{or,}$$

$$\frac{\partial \epsilon}{\partial t} - \epsilon \frac{\partial u_f}{\partial x} - u_f \frac{\partial \epsilon}{\partial x} = 0 \quad (5.9).$$

Because $\epsilon = \epsilon[P_s(x,t)]$, equation (5.9) can be rewritten in the form:

$$\frac{d\varepsilon}{dP_s} \frac{\partial P_s}{\partial t} - \varepsilon \frac{\partial u}{\partial x} - u \frac{d\varepsilon}{dP_s} \frac{\partial P_s}{\partial x} = 0$$

By substituting equation (5.6) into the above equation we obtain:

$$\frac{d(1-\varepsilon_s)}{dP_s} \frac{\partial P_s}{\partial t} + \frac{K\varepsilon_s}{\mu} \frac{\partial^2 P_s}{\partial x^2} + \frac{1}{\mu} \frac{d}{dP_s} [K\varepsilon_s] \left(\frac{\partial P_s}{\partial x}\right)^2 + \frac{g\Delta\rho}{\mu} \frac{d}{dP_s} [K\varepsilon_s^2] \frac{\partial P_s}{\partial x} = 0$$

or,

$$\frac{d\varepsilon_s}{dP_s} \frac{\partial P_s}{\partial t} - \frac{K\varepsilon_s}{\mu} \frac{\partial^2 P_s}{\partial x^2} - \frac{1}{\mu} \frac{d}{dP_s} [K\varepsilon_s] \left(\frac{\partial P_s}{\partial x}\right)^2 - \frac{g\Delta\rho}{\mu} \frac{d}{dP_s} [K\varepsilon_s^2] \frac{\partial P_s}{\partial x} = 0$$

(5.10),

where, $\Delta\rho = \rho_s - \rho$.

The second term in this equation is a diffusive term and the last two terms are convective terms and so the partial differential equation is called diffusive - convective equation. Since the effective pressure P_s , the solidosity ε_s , and the intrinsic permeability K , are unknown the use of constitutive equations that relate the material properties ε_s and K with the effective pressure is necessary.

Some researchers (Schiffman 1985, Tiller 1962, and Tiller and Yeh 1987) proposed their own constitutive equations. In the present work Tiller's constitutive equations are used. Tiller (1962) proposed constitutive equations in the general form:

$$\varepsilon_s = \varepsilon_{s0} f(P_s)$$

$$K = K_0 g(P_s),$$

where, ϵ_{s0} and K_0 are the solidosity and the intrinsic permeability, respectively, at the top of the sediment - suspension interface, and $f(P_s)$ and $g(P_s)$ could be expressed in terms of power functions, polynomials or exponentials. According to Tiller (private communication) the constitutive equations which are expressed as power functions work better than the others and they are applicable for low pressures in batch thickening (Tiller and Khatib 1984). Another reason for choosing the above constitutive equations is that the necessary information to compute the parameters which is included in their expressions are available to us. Particularly, Tiller and Leu (1980) proposed the following empirical equations, with validity up to 5-10 Atm:

$$\epsilon_s = \epsilon_{s0} (1 + aP_s)^\beta \quad (5.11a)$$

$$K = K_0 (1 + aP_s)^{-\delta} \quad (5.11b).$$

Because the effective stress, P_s , is equal to zero at the top of the interface ϵ_{s0} and K_0 are called null stress solidosity and permeability, respectively (figure 16). The parameters δ and β , which are known as compressibility coefficients, indicate the degree of compactibility of the solids and vary in the interval 0.0-0.5 and 0.0-2.5 respectively. For crude approximations $\delta = 5\beta$. Based on experimental results from thirty-nine different materials, Tsai (1986) obtained best fit (least square) curves for δ and β , given by,

$$\delta = 5.19 (0.65 - \epsilon_{s0})^{2.68}$$

and

$$\beta = 3.08 (0.65 - \epsilon_{s0})^{4.0}$$

The parameter a in the constitutive equations also indicates the degree of solids compactibility. Tiller (private communication) emphasized that since a lot of empiricism is involved in obtaining the values of the coefficients in the constitutive equations, the constitutive equations just provide a reasonable basis for an approximate comparison of theory and experiment. He also referred to some of the common problems that occur during a constant - pressure sedimentation test such as " a continuous clogging of the medium" or "the solids bed collapses by sudden application of the full pressure" that cannot be adequately represented by the present constitutive relations.

Substituting equations (5.11a), (5.11b) to equation (5.10) and after manipulations we obtain:

$$\frac{\partial P_s}{\partial t} - \frac{K_0(1+aP_s)^{1-\delta}}{a\mu\beta} \frac{\partial^2 P_s}{\partial x^2} - \left(\frac{\partial P_s}{\partial x}\right) \frac{g\Delta\rho\epsilon_{s0}K_0(2\beta-\delta)(1+aP_s)^{(\beta-\delta)}}{\mu\beta} - \frac{K_0(\beta-\delta)(1+aP_s)^{-\delta}}{\mu\beta} \left(\frac{\partial P_s}{\partial x}\right)^2 = 0 \quad (5.12).$$

Equation (5.12) is a second order, non linear partial differential equation of the parabolic type and governs the consolidation process in the sediment layer (region (ABB'A') in figure 16).

5.3.2 Calculation of the height decrease in a solids bed due to consolidation process.

1) First method: During the consolidation process the particles come closer and the liquid trapped in the solids structure is squeezed out and moves upward. The height of the domain decreases and in turn the effective pressure at the bottom of the cylinder. Figure 18 illustrates the above process. The sediment layer is divided into n -sublayers, all of which have the same thickness. During a period Δt each of the individual sublayers with height $(l_i)_t$ consolidates due to the effective pressure by,

$$(dl_i)_{t+\Delta t} = (l_i m_{vi} P_{si})_t \quad (5.13),$$

where, $(P_{si})_t$ is the effective pressure value in the sublayer i at time t (figure 18) and m_{vi} is the coefficient of compressibility for the sublayer i .

The coefficient of compressibility, m_v , in soil mechanics is defined as (Smith 1990):

$$m_v = \frac{1}{1+e} \frac{de}{dP_s} \quad (5.14),$$

where, e denotes the void ratio and it is defined as:

$$e = \frac{V_e}{V_s} .$$

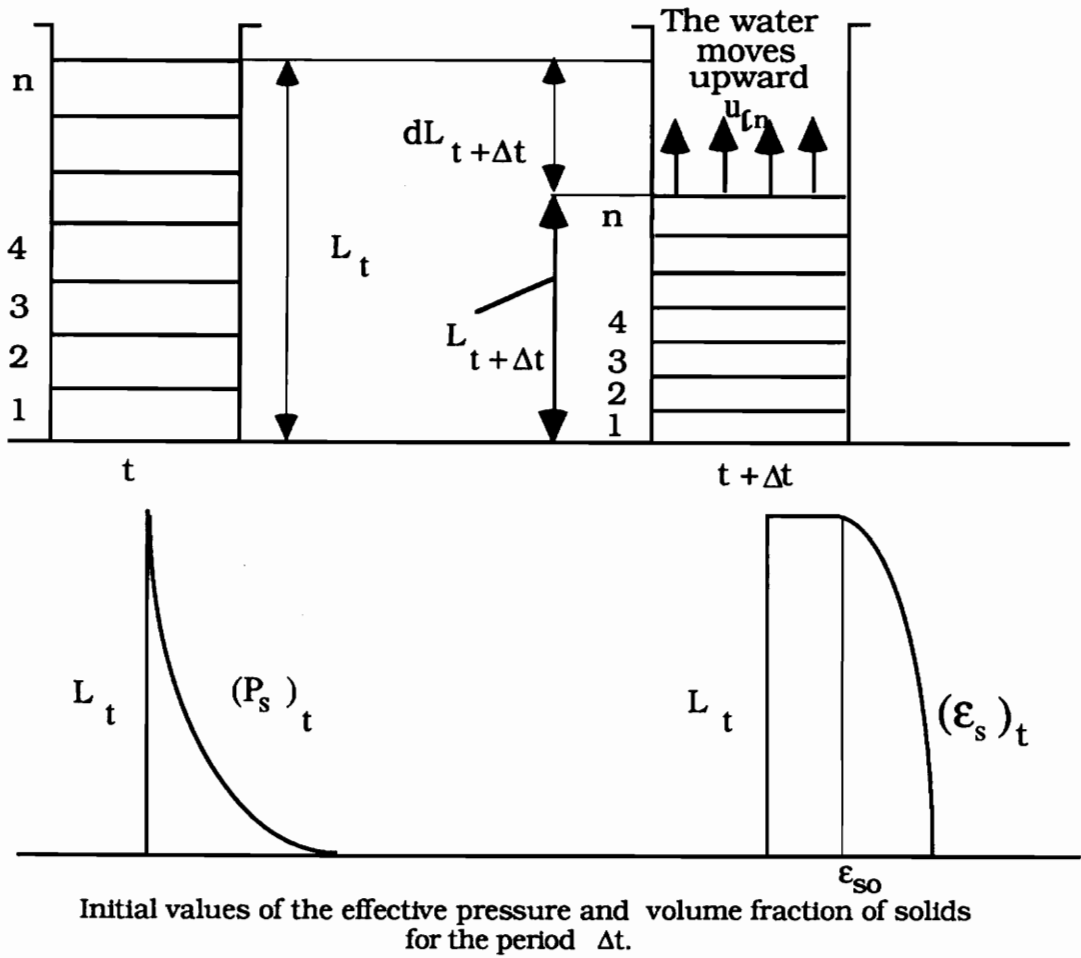


Figure 18: Consolidation of a layer at time $t + \Delta t$.

Therefore, the relation of the solidosity with the void ratio is:

$$e = \frac{1}{\epsilon_s} - 1 \quad (5.15).$$

By using the constitutive equation for the solidosity, equation (5.11a), the void ratio is expressed as a function of the effective pressure:

$$e = \frac{1}{\epsilon_{s0}(1+aP_s)^\beta} - 1 \quad (5.16).$$

With the substitution of equation (5.16) into equation (5.14) the compressibility coefficient, m_v , is obtained as function of the effective pressure P_s as:

$$m_v = - \frac{a\beta}{1+aP_s} \quad (5.17).$$

By rewriting equation (5.17) for a sublayer i and replacing it to (5.13), the decrease $(dL_i)_{t+\Delta t}$ is expressed as a function of the effective pressure with the following relation:

$$(dL_i)_{t+\Delta t} = - (L_i \frac{a\beta}{1+aP_{si}} P_{si})_t \quad (5.18).$$

The total decrease in the height of the whole sediment layer is given by:

$$dL_{t+\Delta t} = \sum_{i=1}^n (dL_i)_{t+\Delta t} \quad (5.19).$$

$$\text{and } C_{t+\Delta t} \equiv (A'B') = L_t - dL_{t+\Delta t} \quad (5.20),$$

where, all variables in equation (5.20) have been defined in figure 16.

2) Second method: An alternative way to compute the height (A'B') of the compacted layer (figure 16) is through the solidosity variation at times t and $t+\Delta t$, respectively. Thus, for an individual sublayer i in the compacted layer, its height $(L_i)_{t+\Delta t}$ is calculated with the following equality:

$$(L_i)_{t+\Delta t} = \frac{(\epsilon_{si})_t}{(\epsilon_{si})_{t+\Delta t}} (L_i)_t \quad (5.21),$$

where, $(L_i)_t$ is the height of the sublayer i at time t , $(\epsilon_{si})_t$ is the initial volume fraction of solids in the sublayer i (figure 18), and $(\epsilon_{si})_{t+\Delta t}$ is the volume fraction of solids in the sublayer i at time $t+\Delta t$. The volume fraction of solids $(\epsilon_{si})_{t+\Delta t}$ is calculated as function of the pressure variation at time t , by using the constitutive (5.11a), and it is given as:

$$(\epsilon_{si})_{t+\Delta t} = \epsilon_{so} (1 + a(P_{si})_t)^\beta.$$

Finally, the total height of the solids bed at time $t + \Delta t$ is:

$$C_{t+\Delta t} \equiv (A'B') = \sum_{i=1}^n (L_i)_{t+\Delta t} = \sum_{i=1}^n \frac{(\epsilon_{si})_t}{\epsilon_{so} (1 + a(P_{si})_t)^\beta} (L_i)_t \quad (5.22),$$

and the total decrease of the layer the same time is:

$$dL_{t+\Delta t} = L_t - C_{t+\Delta t} \quad (5.23).$$

Therefore, the ratio of the total decrease $dL_{t+\Delta t}$ that counts for the i -th sublayer can be computed as:

$$a_i = \frac{(dL_i)_{t+\Delta t}}{dL_{t+\Delta t}} \quad (5.24).$$

5.4 Alternative model for the consolidation process.

To obtain the non linear partial differential equation (5.12) we eliminated the terms of the liquid and solids velocity from the particulate equation by using equations (5.7) and (5.9). In the alternative model we will use directly the particulate structure equation by deriving expressions for the upward liquid velocity, u_l , and the downward solids velocity, u_s . To do so, the derived relations for the height decrease of a sublayer (equation (5.18) or equation (5.23)) should be utilized. At time t a sublayer i has concentration, $(\epsilon_{si})_t$, equal to:

$$(\epsilon_{si})_t = \frac{(V_{si})_t}{(L_i)_t} \quad (5.25),$$

where, $(L_i)_t$, $(V_{si})_t$ denote the height of a sublayer i and the corresponding volume of solids within it and of a unit surface area at time t .

At time $t + \Delta t$ the same sublayer has concentration, $(\epsilon_{si})_{t+\Delta t}$, equal to:

$$(\epsilon_{si})_{t+\Delta t} = \frac{(V_{si})_{t+\Delta t}}{(L_i)_{t+\Delta t}} \quad (5.26),$$

where, $(V_{si})_{t+\Delta t} = (V_{si})_t$ and $(L_i)_{t+\Delta t} = (L_i)_t - (dL_i)_{t+\Delta t}$.

By dividing equation (5.26) by equation (5.25), it results to:

$$(\epsilon_{si})_{t+\Delta t} = \frac{(L_i)_t}{(L_i)_t - (dL_i)_{t+\Delta t}} (\epsilon_{si})_t \quad (5.27).$$

The next step is to calculate the liquid and solids velocities in the sediment layer. The decrease of the layer's thickness indicates the amount of the liquid that comes out from the layer. The velocity of the liquid represents the rate at which the liquid moves upward during the consolidation period. The velocity of the liquid flowing through the i th sublayer is given by the following expression:

$$(u_{li})_{t+\Delta t} = -\frac{1}{2\Delta t} \left[(dL_i)_{t+\Delta t} + 2 \sum_{j=1}^{i-1} (dL_j)_{t+\Delta t} \right] \left[\frac{1}{1-\epsilon_{si}} \right]_{t+\Delta t} \quad (5.28).$$

The minus sign indicates the upward movement of the liquid phase in the sediment.

Similarly, the solids settling velocity through the i th sublayer can be expressed as:

$$(u_{si})_{t+\Delta t} = \frac{1}{2\Delta t} \left[(dL_i)_{t+\Delta t} + 2 \sum_{j=1}^{i-1} (dL_j)_{t+\Delta t} \right] \left[\frac{1}{\epsilon_{si}} \right]_{t+\Delta t} \quad (5.29).$$

The above definitions of the liquid and solids velocity satisfy the mass balance in the sediment layer. The intrinsic permeability can be described as function of the solidosity by combining the constitutive relations for solidosity and intrinsic permeability (equations 5.11(a) and 5.11(b)).

By solving equation 5.11(a) for P_s and substituting into the second constitutive equation, the following equality can be obtained:

$$K = K_0 \left[\frac{\epsilon_{s0}}{\epsilon_s} \right]^{\beta/\delta}$$

or for a sublayer i at time $t+\Delta t$ the above equation can be written as:

$$(K_i)_{t+\Delta t} = (K_0 \left[\frac{\epsilon_{s0}}{\epsilon_{si}} \right]^{\beta/\delta})_{t+\Delta t} \quad (5.30).$$

Equation (5.30) indicates that the intrinsic permeability obtains its maximum value at the top of the consolidation - suspension interface and it decreases gradually with depth in the sediment layer. The last step is to express the variation of the effective pressure within the particulate structure equation (5.6) in integral form for the compacting layer $C_{t+\Delta t} = (A'B')$ at time $t+\Delta t$ (figure 16):

$$dP_s = -g\epsilon_s(\rho_s - \rho)dx - \frac{(u_f - u_s)\mu(1 - \epsilon_s)}{K} dx \quad \text{or,}$$

$$P_s(x_{B'}) - P_s(x_{A'}) = - \int_{x_{A'}}^{x_{B'}} g\epsilon_s(\rho_s - \rho)dx - \int_{x_{A'}}^{x_{B'}} \frac{(u_f - u_s)\mu(1 - \epsilon_s)}{K} dx.$$

At the top of the layer $C_{t+\Delta t} \equiv (A'B')$ (figure 16) the effective pressure is equal to zero, $P_s(x_{B'}) = 0$. Thus, the above equation becomes:

$$P_s(x_{A'}) \equiv P_{s\text{bottom}} = g(\rho_s - \rho) \int_{x_{A'}}^{x_{B'}} \epsilon_s dx + \mu \int_{x_{A'}}^{x_{B'}} \frac{(u_f - u_s)(1 - \epsilon_s)}{K} dx \quad (5.31),$$

where, the variables ϵ_s , u_f , u_s , and, K are computed from equations (5.27), (5.28), (5.29), and (5.30), respectively.

5.5 Model for the suspension process.

The height of the falling material, $F_{t+\Delta t}$, on the top of the consolidated bed during a period Δt (figure 16), is equal to:

$$F_{t+\Delta t} = v \Delta t + dL_{t+\Delta t} \quad (5.32),$$

where, $dL_{t+\Delta t}$ denotes the decrease of the layer's height due to consolidation process and it is computed by using equation (5.19), and v is the upward propagation velocity of the discontinuity (figure 16) that is located just above the top of the sediment-suspension interface. According to Fitch (1983) the discontinuity propagates upwards at the same rate as the sediment layer does since the propagation velocity rises tangentially from the L-curve. Thus, equation (3.3) can be written as:

$$v = \frac{dL}{dt} = \frac{u_s \Phi_s - u_{s0} \epsilon_{s0}}{\Phi_s - \epsilon_{s0}} \quad (5.33).$$

To compute the characteristic's velocity, v , from equation (5.33) experimental data that relate the solids settling velocity, u_s , with the volume fraction of solids, Φ_s , should be available. From a curve fitting

(least square method, linear-linear) of the above data we can obtain the following relation:

$$u_s = b_0 + b_1 \Phi_s + b_2 \Phi_s^2 \quad (5.34),$$

where, the coefficients b_0 , b_1 , and b_2 are estimated from the least square method.

By multiplying both sides of equation (5.34) with Φ_s , we can relate the volumetric flux term with the volume fraction of solids as,

$$S = u_s \Phi_s = b_0 \Phi_s + b_1 \Phi_s^2 + b_2 \Phi_s^3 \quad (5.35).$$

Equation (5.35) is used to construct the flux curve. Figure 19 illustrates such a plot. At time $t = 0$ the solids have not reached the cylinder's bottom and so $\epsilon_{s0} u_{s0} = 0$. The chord (A_1B_1) constitutes an unstable first order of discontinuity. The loci of constant volume fraction of solids propagate out of the region (A_1T) with different velocities. From point B_1 , which is located just under the compression discontinuity at $t = 0$, we draw the tangent at the flux curve (the chord (B_1A_4) in figure 19). The tangents that originate from points above the A_4 have less slope than the chord (B_1A_4) and so the second order of discontinuities, which are located at these points, propagate slower than the discontinuity at point A_4 . As a result of that the discontinuities above the point A_4 are wiped out from the propagation of the chord (B_1A_4). The tangents at these points

represent a bundle of characteristics which do not originate tangentially from the L- curve.

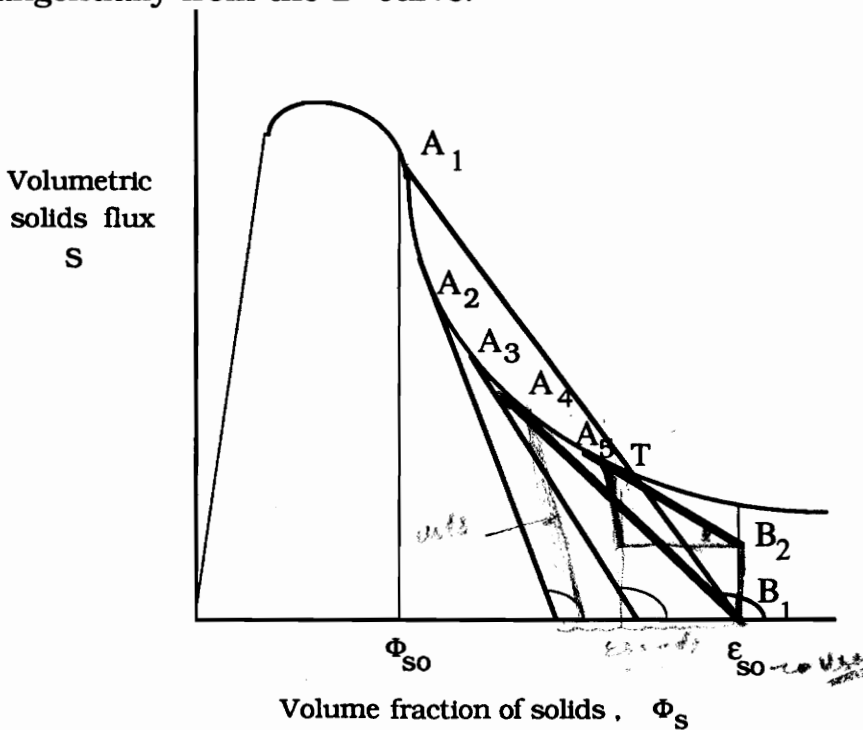


Figure 19: Use of the flux curve to compute the volume fraction of solids of the falling material at the top of the sediment-suspension interface.

Instead the chord (B₁A₄) represents a characteristic that rises tangentially from the sediment - suspension interface and according to Fitch (1983) gives the lowest volume fraction of solids that can form above the interface. An iterative technique should be employed to compute the volume fraction of solids at A₄ from the following relation:

$$\downarrow \frac{u_s \Phi_s}{\Phi_s - \epsilon_{s0}} = \frac{d(u_s \Phi_s)}{d\Phi_s} \Big|_{A_4} \text{ at point } B_1 \quad (5.36).$$

Handwritten notes:
 $\frac{u_s \Phi_s - \epsilon_{s0} u_s}{\Phi_s - \epsilon_{s0}} = \frac{d(u_s \Phi_s)}{d\Phi_s} \Big|_{A_4}$ at point B_1

Since the volume fraction of solids is known the values of v and $F_{t+\Delta t}$ can be computed by using equations (5.32) and (5.33) respectively. At later time t the flux of the subsiding solids just below the L-curve will obtain a non zero value and a characteristic will originate tangentially from that point. Point B_2 in figure 19 is the starting point for that characteristic. From this point we draw a tangent (chord (B_2A_5)) to the flux curve and the above process is repeated to compute the height of the falling material.

5.6 Methodology to obtain the variation of the consolidation - suspension interface with time.

The determination of the L-curve experimentally is troublesome. Most of the times the rising interface is not visible in a batch column during the thickening process (Font 1988, 1992) and a density scanning device is necessary to detect it (Gaudin et al 1958, Been and Sills 1981). Another way to construct the L-curve would be to run multiple batch settling tests for a given initial concentration, but at various initial column heights (figure 20). This technique (Fitch 1983) requires a lot of experimental time. In addition, it negates the main advantage of Kynch's analysis: that from a single batch test the settling process can be described adequately.

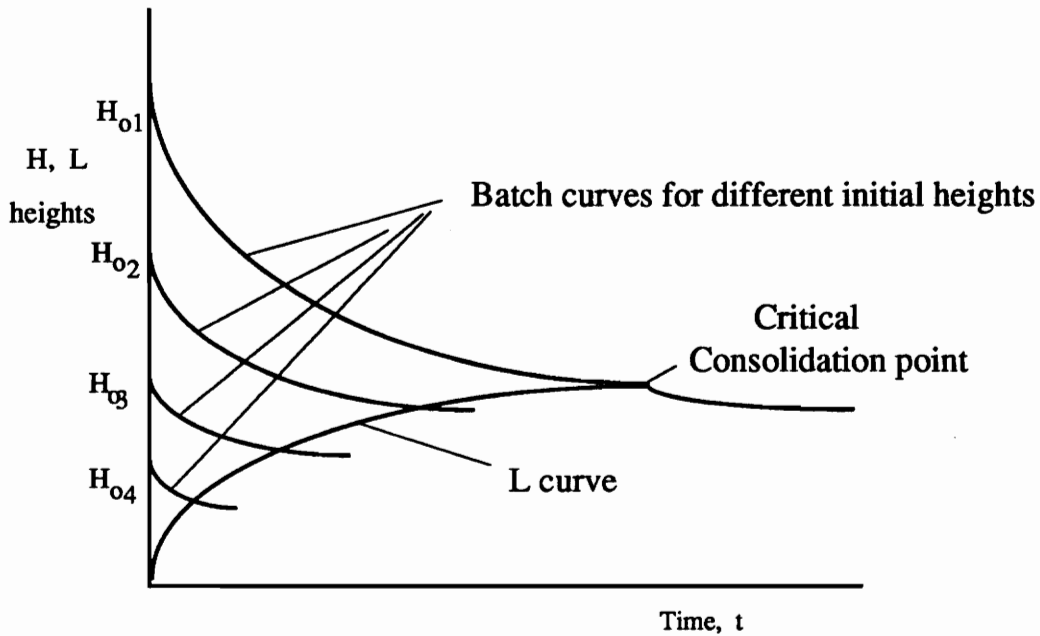


Figure 20: Multiple batch tests to construct the L- curve.

The rest of this unit illustrates the steps necessary to estimate the L- curve by using the consolidation - suspension model present here. At time $t_0 = 0$ the solids have not reach the batch cylinders bottom (figure 21(a)). During a short period of time, $\Delta t_1 = t_1 - t_0$, (figure 21) a limited number of particles deposit at the bottom of the cylinder and the height of the rising sediment is equal to L_{t_1} (figure 21). Since the above time period Δt is short it is considered that the consolidation process of the solids structure can not occur during this period. Thus, it is reasonable to assume that at the end of this period the solids bed has uniform volume fraction of solids, that is equal to the null stress

solidosity, ϵ_{s0} . Therefore, the variation of the effective pressure will be linear throughout the height L_{t1} of the solids bed and given by,

$$P_s = -g \epsilon_{s0} (\rho_s - \rho)x + g \epsilon_{s0} (\rho_s - \rho) L_{t1} \quad (5.37),$$

where, x is the vertical distance in the layer from the bottom and L_{t1} is the height of the domain at time t_1 and it is equal to:

$$L_{t1} = v_{t0} t_1 \quad (5.38).$$

In equation (5.38), v_{t0} is the slope of the characteristic that originates from point B_1 (figure 19) and it is equal to $\frac{\Phi_s u_s}{\Phi_s - \epsilon_{s0}}$ where, Φ_s is the volume fraction of the dewatering slurry and it is computed by using equation (5.36). Figures 21(d,e) illustrate the effective pressure and the volume fraction of solids variation at time t_1 . During the next period $\Delta t_2 = t_2 - t_1$ the particles start to get gradually compacted due to their own weight. Thus, the height, L_{t1} , of the layer decreases (figure 21(g)) and becomes equal to C_{t2} at the end of the period Δt_2 . The height C_{t2} can be computed by using either one of the equations (5.20) and (5.22).

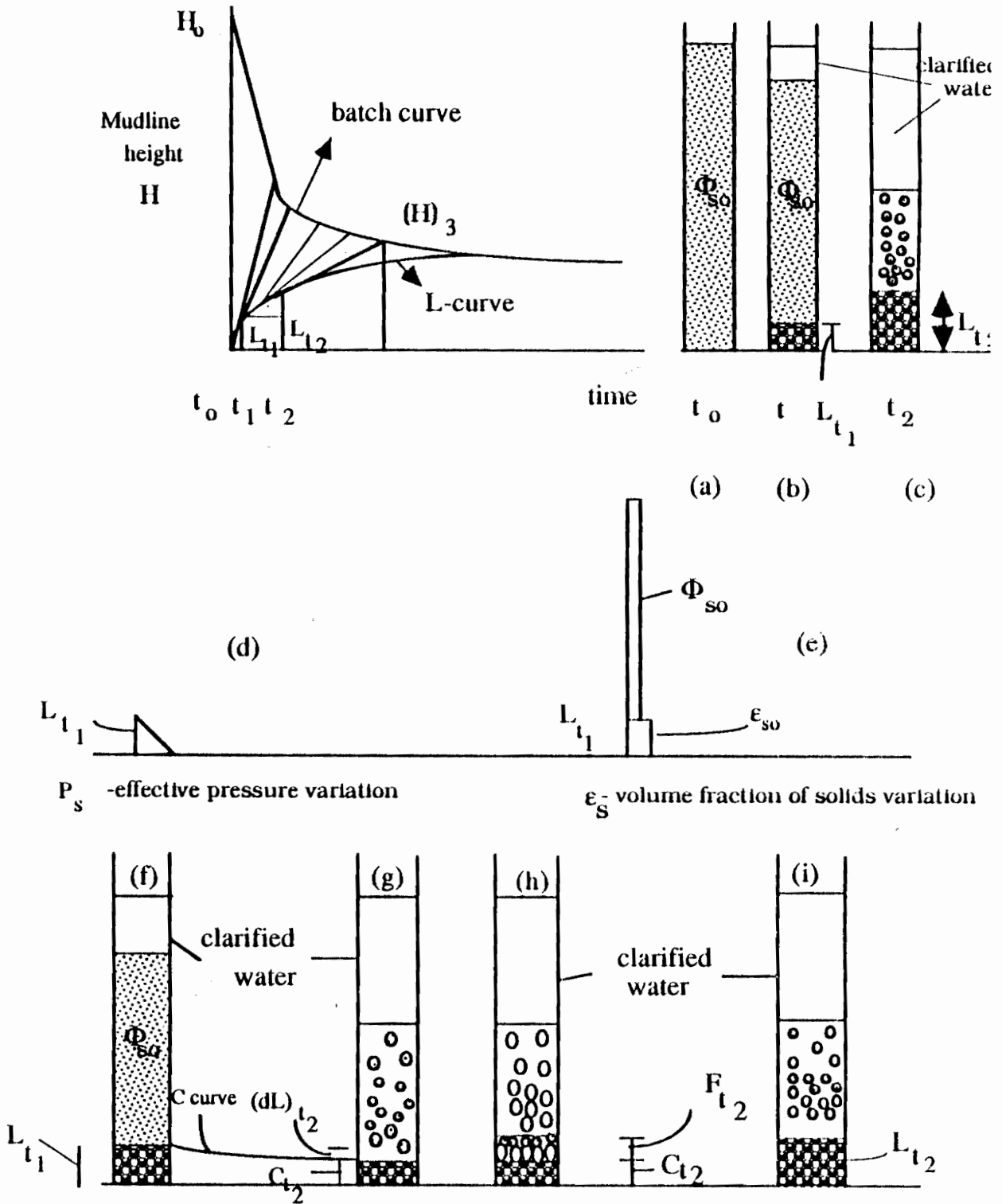


Figure 21: Steps in the consolidation- suspension processes.

the equations (5.20) and (5.22). To compute the effective pressure variation throughout the height C_{t2} (figure 21(g)) we can use either the governing relation of the consolidation process, equation (5.12), or the proposed alternative method for the consolidation process. The finite element method is used to solve numerically equation (5.12). The F.E.M. solution methodology is described in Chapter 6. Because equation (5.12) represents an initial-boundary value problem, to solve it is necessary to specify the initial and boundary conditions for the effective pressure. The initial condition, the distribution of the effective pressure at the beginning of the time step Δt_1 , is given by equation (5.37). The boundary condition at the top of the sediment layer is:

$$P_{st} = 0 \quad (5.39)$$

and is known as the essential boundary condition. At the other end of the domain, which is the bottom of the batch cylinder, the non-slip condition holds for both the fluid and the solids. As a result the particulate structure equation (5.6) at the bottom becomes:

$$\left. \begin{aligned} u_f &= u_s = 0 \\ \frac{\partial P_s}{\partial x} &= -g \varepsilon_s (\rho_s - \rho) - \frac{\mu \varepsilon}{k} (u_f - u_s) \end{aligned} \right\} \frac{\partial P_s}{\partial x} \Big|_b = -g \varepsilon_s (\rho_s - \rho)$$

By substituting the constitutive equation for the solidosity into the particulate equation we obtain the following expression:

$$\left. \frac{\partial P_s}{\partial x} \right|_b = -g \epsilon_{s0} (1 + aP_{sb})^\beta (\rho_s - \rho) \quad (5.40).$$

This is known as the natural boundary condition. Since the bottom effective pressure is unknown the natural boundary condition can not be specified and the Newton-Raphson iterative method is used to overcome this difficulty (details are given in Chapter 6). Figure 22 (b) illustrates the effective pressure variation obtained from the F.E.M. at time t_2 . At the same time a layer of new particles with height, F_{t2} , is added on the top of the consolidated bed, C_{t2} , with ϵ_{s0} (figure 22(c)). Their weight causes the increase of the existing effective pressure variation by, $g (\rho_s - \rho) \epsilon_{s0} F_{t2}$. The height, F_{t2} , (figure 22(c)) of the added layer can be calculated by using equation (5.32) and finally the height of the consolidation-suspension interface is obtained as:

$$L_{t2} = C_{t2} + F_{t2} \quad (5.41).$$

In turn, the new effective pressure variation, which is shown in figure 22 (d), will be the initial condition for the next time step. The above process will be repeated until the slope of the constructed L-curve approaches a zero value which represents the compression point. Here we try to examine the coupled components of the phenomenon. This is an approximation that is valid only when the height of the falling material, F_t , is less than the height of the consolidated bed, C_t at each time instant. In the case that the above

condition is not satisfied a smaller time step Δt should be chosen and the process should be repeated.

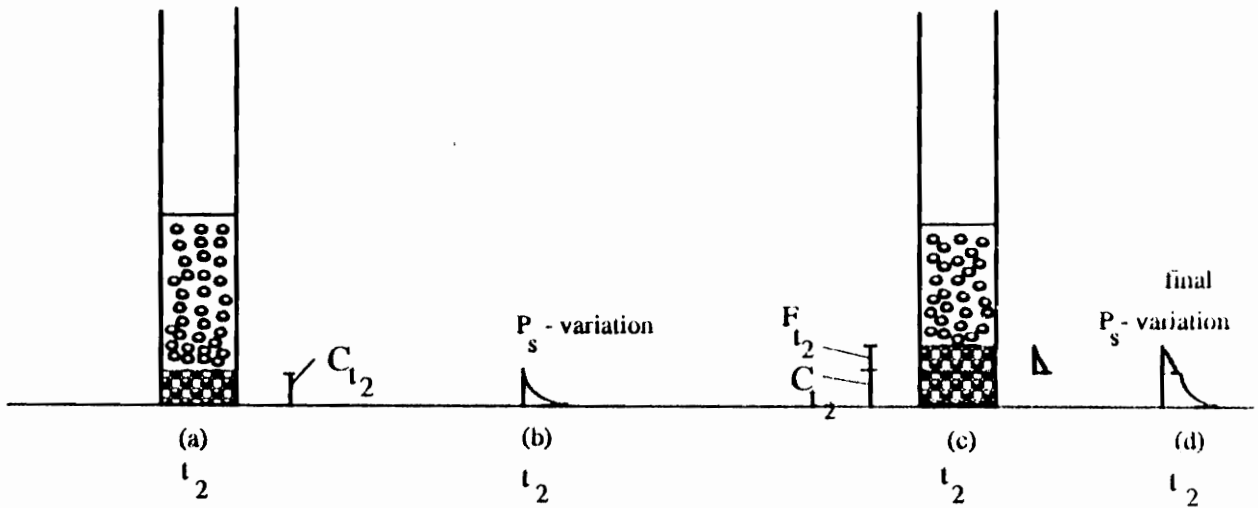


Figure 22: Steps of the consolidation - suspension process

5.7. Construction of the supernatant liquid - mudline interface.

To compute the height, H_3 , of the mudline interface at time t_3 we utilize an equality, which is deduced from the geometry of figure 23 and it is given by,

$$H_3 = v_2 \frac{\Delta t_3}{\Delta t_2} + L_{12} = v_2 (t_3 - t_2) + L_{12} \quad (5.42),$$

where, v_2 , is the characteristic velocity obtained from equation (4.33), L_{12} is computed from equation (5.41), and Δt_3 is the time

required for the characteristic that originates from point (2) to reach the mudline interface at point (3).

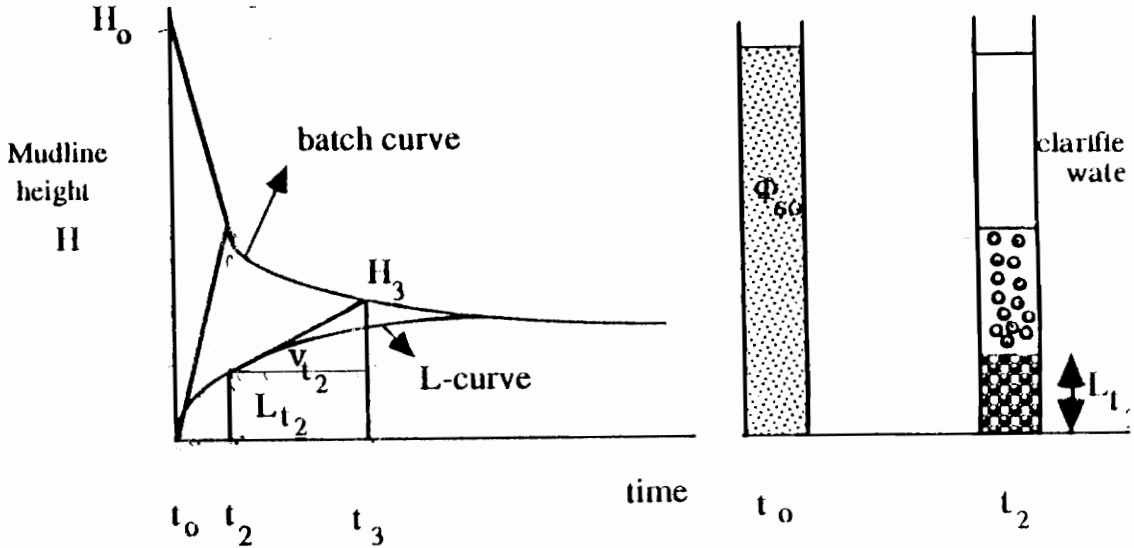


Figure 23 : Estimation of the mudline height.

The period Δt_3 can be computed by considering the total volume of solids in the graduated cylinder at time t_2 :

$$\Phi_{s0} H_0 = \int_0^{L_{t_2}} \epsilon_s dx + \int_{L_{t_2}}^{H_2} \Phi_s dx \quad (5.43).$$

The volume of solids per unit cross - sectional area that crosses the characteristic which originates from point (2) and reaches the mudline interface at point (3) is equal to:

$$\Phi_{s2} (v_{t_2} - u_{s2}) \Delta t_3 \quad \text{and}$$

by substituting the above quantity to the second term at the r.h.s. of equation (5.43) we obtain:

$$\Phi_{s0} H_0 = \int_0^{L_2} \epsilon_s dx + \Phi_{s2} (v_{t2} - u_{s2}) \Delta t_3 \quad \text{or,}$$

$$\Delta t_3 = \frac{\Phi_{s0} H_0 - \int_0^{L_2} \epsilon_s dx}{\Phi_{s2} (v_{t2} - u_{s2})} \quad (5.44).$$

5.8 Steps to construct the L and batch curves for an under investigation slurry.

To be able to use the described suspension - consolidation model the following data are necessary:

1. The initial slurry's height, H_0 , in the graduated cylinder and its initial volume fraction of solids, Φ_{s0} .
2. The experimental data that describe the variation of the solids settling velocity in the suspension with the solids volume fraction. The flux curve can be obtained from the above variation.
3. The volume fraction of solids at the sediment - suspension interface or null stress solidosity.
4. Constitutive relations that relate the solids properties (solidosity and permeability) with the effective pressure in the sediment layer.

To construct the L and batch curves the following equations should be used:

1. Based on the existing knowledge of the effective pressure variation at the beginning of the time step Δt , equations (5.18) and

(5.19) are used to compute the decrease of the sediment layer due to consolidation that occurs during a time period Δt .

2. Equation (5.12) to compute the effective pressure variation with height at the end of the period Δt . Equation (5.12) is solved by using the finite element method.

3. Equation (5.29) to compute the subsidence velocity of solids in the sediment.

4. Equation (5.32) to compute the height of the falling material at the top of the consolidated bed.

5. Equation (5.41) to compute the height of the sediment-suspension interface at the end of the period Δt .

6. Equation (5.42) to compute the height of the mudline interface.

7. By considering a linear distribution for the effective pressure within the layer of material that fell over the period Δt (equation (5.37)), and adding that to variation of the effective pressure distribution over the whole sediment layer is known at the beginning of the subsequent time step. Then the whole procedure can be repeated for the following time steps.

CHAPTER 6

NUMERICAL SOLUTION OF THE CONSOLIDATION EQUATION BY USING THE FINITE ELEMENT METHOD.

6.1 Finite element formulation.

The finite element formulation of non linear problems consists of the kinematic relations of the problems using continuum mechanics principles, the identification of the constitutive relations, and finally the discretization of the equations using finite element procedures. The first two stages have been illustrated in Chapter 5. To proceed to the third step the domain, Ω , which is the sediment layer, is initially divided into a set of line elements with equal length i.e. the finite element mesh is considered uniform (figure 24). Therefore, in later time steps as the height of the domain changes the gradual refining of the mesh is required for the convergence criterion of the finite element approximation to be satisfied. The criterion for establishing the finite element mesh for a given time instant is that the height of the element, or sublayer, should be several times greater than the diameter of the largest particle in the sublayer. If C_t denotes the height of the sediment layer at the end of the consolidation period Δt

(figure 16) and NEM is the number of elements in the layer, the following inequality has to be satisfied for a sublayer i :

$$\text{Height of a sublayer } i \equiv \frac{C_t}{\text{NEM}} \gg d_{\max} \quad (6.1).$$

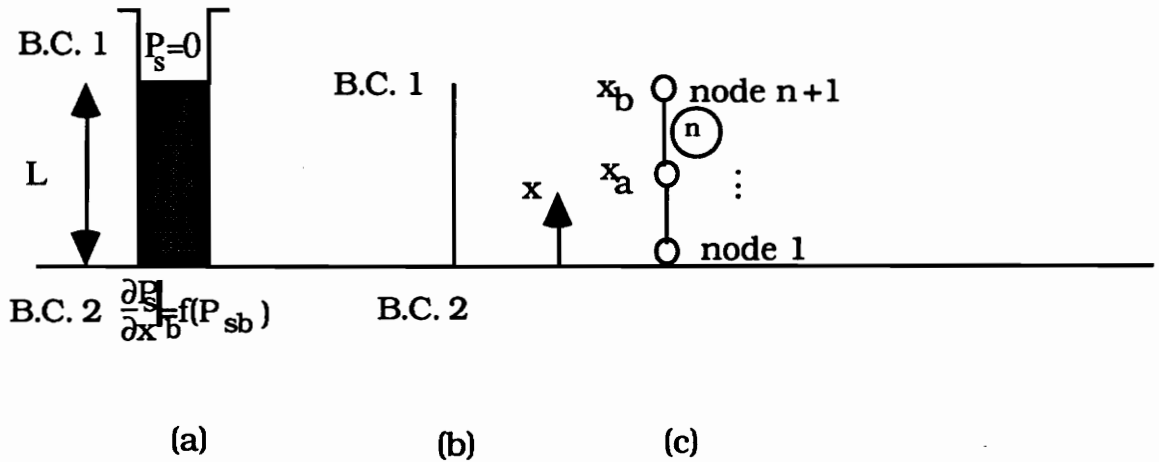


Figure 24: Finite element discretization of the domain. (a) Physical problem. (b) Mathematical idealization. (c) Finite-element discretization.

The elements chosen in this problem are non isoparametric, because the domain does not have irregular shape. The next step is to solve the governing equation over an element n (figure 24). To do so, the

variational or integral form associated with the P.D.E is written for the element n by utilizing the method of weighted residuals, which is also referred to as the Petrov-Galerkin method. The above method is preferable compared to the other variational methods (as Ritz) because the test functions can be chosen from an independent set of functions (Reddy 1984, Bathe 1982). The variational form over the element n is obtained by multiplying the integral of the governing equation (5.12) in the domain $\Omega^e = (x_a, x_b)$ (figure 24) with a test or weight function w (which is an arbitrary continuous function):

$$\int_{x_a}^{x_b} w \left[\frac{\partial P_s}{\partial t} + \frac{K_0(1+aP_s)^{1-\delta}}{a\mu\beta} \frac{\partial}{\partial x} \left(\frac{\partial P_s}{\partial x} \right) + \left(\frac{\partial P_s}{\partial x} \right) \frac{g\Delta\rho\epsilon_{s0}K_0(2\beta-\delta)(1+aP_s)^{(\beta-\delta)}}{\mu\beta} + \frac{K_0(\beta-\delta)(1+aP_s)^{-\delta}}{\mu\beta} \left(\frac{\partial P_s}{\partial x} \right)^2 \right] dx = 0$$

By using the technique of integration by parts, we obtain:

$$\int_{x_a}^{x_b} \left[w \frac{\partial P_s}{\partial t} - \frac{\partial}{\partial x} \left\{ w \frac{K_0(1+aP_s)^{1-\delta}}{a\mu\beta} \right\} \frac{\partial P_s}{\partial x} + w \left(\frac{\partial P_s}{\partial x} \right) \frac{g\Delta\rho\epsilon_{s0}K_0(2\beta-\delta)(1+aP_s)^{(\beta-\delta)}}{\mu\beta} + w \frac{K_0(\beta-\delta)(1+aP_s)^{-\delta}}{\mu\beta} \left(\frac{\partial P_s}{\partial x} \right)^2 \right] dx + \left[w \frac{K_0(1+aP_s)^{1-\delta} \partial P_s}{a\mu\beta} \right] \Big|_{x_a}^{x_b} = 0$$

or,

PS includes as boundary

$$\begin{aligned}
 & \int_{x_a}^{x_b} \left[w \frac{\partial P_s}{\partial x} - \left(\frac{K_0(1+aP_s)^{1-\delta}}{a\mu\beta} \frac{\partial w}{\partial x} \right) \frac{\partial P_s}{\partial x} + w \left(\frac{\partial P_s}{\partial x} \right) \frac{g\Delta\rho\varepsilon_{s0}K_0(2\beta-\delta)(1+aP_s)^{(\beta-\delta)}}{\mu\beta} + \right. \\
 & \left. w \frac{K_0(\beta-1)(1+aP_s)^{-\delta}}{\mu\beta} \left(\frac{\partial P_s}{\partial x} \right)^2 \right] dx + \left[w \frac{K_0(1+aP_s)^{1-\delta}}{a\mu\beta} \frac{\partial P_s}{\partial x} \right]_{x_b} - \\
 & \left[w \frac{K_0(1+aP_s)^{1-\delta}}{a\mu\beta} \frac{\partial P_s}{\partial x} \right]_{x_a} = 0 \quad (6.3).
 \end{aligned}$$

The obtained variational form (equation (6.3)) is non symmetric, because the governing equation, (5.12), includes highly non linear terms (Reddy 1984, Herting 1984). Therefore, the relation (6.3) is known as the weak form of the governing equation and the described process consistutes the first step in the finite element formulation. The last two terms of the l.h.s. in equation (6.3) have to satisfy in combination with the contribution of the adjacent elements at these nodes, the equilibrium conditions for the "internal forces". Since no external forces are applied in the internal nodes of the mesh these terms cancel each other and so they do not contribute to the global force vector. However, the above statement does not apply for the first global node of the finite element mesh (at the bottom of the column, figure 24). Thus, when the weak form is written over the first element the term that includes the secondary variable evaluated at $x = x_a$ (position of the first global node) should not be eliminated

from its expression. Subsequently, the weak form of the governing equation, equation (6.3), is used to obtain a system of n-algebraic equations for the n-elements in the mesh by using the obtained weak form. To do so, the definition of the weighted residuals is utilized for the dependent variable, $P_s = P_s(x,t)$ and its first derivative. In particular, the spatial approximation method is used since the solving problem is time dependent problem. Thus,

$$P_s^{(e)} = \sum_{j=1}^n P_{sj}^{(e)}(t_n) \Psi_j^{(e)}(x) \quad (6.4a),$$

$$\frac{\partial P_s^{(e)}}{\partial x} = \sum_{j=1}^n P_{sj}^{(e)}(t_n) \frac{d\Psi_j^{(e)}}{dx}$$

where, $\Psi_j^{(e)}$ denotes the shape function of an element (e) and $P_{sj}(t_n)$ is the value of the effective pressure at node j the time $t = t_n$ for the same element. Also the non linear term $(\frac{\partial P_s}{\partial x})^2$ is introduced in the

formulation as:

$$\left(\frac{\partial P_s}{\partial x}\right)^2 = \sum_{j=1}^n P_{sj}(t) \frac{d\Psi_j}{dx} \left(\frac{\partial P_s}{\partial x}\right) \quad (6.4b).$$

Equations (6.4a) (spatial approximation method) allow the finite element model of the obtained weak form to be developed by utilizing the static or steady-state problems analyses, while carrying all time-dependent terms in the formulation. Therefore, it implies that the finite element solution that we obtain at the end of the analysis is

continuous in space but not continuous in time. Substituting equations (6.4a), (6.4b), and $w = \psi_i$ into weak form, we obtain:

$$\sum_{j=1}^n \left(\int_{x_a}^{x_b} \left[\psi_i \frac{dP_j}{dt} \psi_j - \left(\frac{K_0(1+aP_s)^{1-\delta}}{a\mu\beta} \frac{d\psi_i}{dx} \right) \left(P_j \frac{d\psi_j}{dx} \right) + \right. \right. \\ \left. \left. \psi_i \frac{g\Delta\rho\epsilon_{so}K_0(2\beta-\delta)(1+aP_s)^{(\beta-\delta)}}{\mu\beta} \left(P_j \frac{d\psi_j}{dx} \right) + \right. \right. \\ \left. \left. \psi_i \frac{K_0(\beta-1)(1+aP_s)^{-\delta}}{\mu\beta} \left(\frac{\partial P_s}{\partial x} \right) \left(P_j \frac{d\psi_j}{dx} \right) \right] dx - \left[\psi_i \frac{K_0(1+aP_s)^{1-\delta}}{a\mu\beta} \frac{\partial P_s}{\partial x} \right]_{x_a} = 0$$

or,

$$\sum_{j=1}^n [M_{ij}^{(e)} P_{sij}^{(e)} + K_{ij}^{(e)} P_{sij}^{(e)}] - F_i^{(e)} = 0 \quad \text{when } i = 1, j = 1, \text{ and } (e) = 1$$

and

(6.5),

$$\sum_{j=1}^n [M_{ij}^{(e)} P_{sij}^{(e)} + K_{ij}^{(e)} P_{sij}^{(e)}] = 0 \quad \text{when } i \neq 1 \text{ and } (e) \neq 1$$

where, P_s' denotes the derivative of the dependent variable with time, (e) implies the element number and the matrices $K_{ij}^{(e)}$, $M_{ij}^{(e)}$, and $F_i^{(e)}$ are equal to:

$$K_{ij}^{(e)} = \int_{x_a}^{x_b} \left[- \frac{K_0(1+aP_s)^{1-\delta}}{a\mu\beta} \frac{d\psi_i}{dx} \left(\frac{d\psi_j}{dx} \right) + \right. \\ \left. + \psi_i \frac{g\Delta\rho\epsilon_{so}K_0(2\beta-\delta)(1+aP_s)^{(\beta-\delta)}}{\mu\beta} \left(\frac{d\psi_j}{dx} \right) + \right. \\ \left. \psi_i \frac{K_0(\beta-1)(1+aP_s)^{-\delta}}{\mu\beta} \left(\frac{\partial P_s}{\partial x} \right) \left(\frac{d\psi_j}{dx} \right) \right] dx \quad (6.6a),$$

$$M_{ij}^{(e)} = \int_{x_a}^{x_b} \psi_i \psi_j dx \quad (6.6b),$$

and

$$F_i^{(e)} = \left[\psi_i \frac{K_0(1+aP_s)^{1-\delta}}{a\mu\beta} \frac{\partial P_s}{\partial x} \right]_{x_a} \quad \text{when } i = 1, j = 1, \text{ and } (e) = 1.$$

By substituting equation (5.38) to the last equality for $F_i^{(e)}$, we obtain:

$$F_i^{(e)} = \left[\psi_i \frac{K_0(1+aP_s)^{1-\delta}}{a\mu\beta} (-g \epsilon_{so} (1 + aP_{sb})^\beta (\rho_s - \rho)) \right]_{x_a} \quad \text{or,}$$

$$F_i^{(e)} = \left[\psi_i \frac{K_0(1+aP_s)^{1-\delta+\beta}}{a\mu\beta} (-g \epsilon_{so} (\rho_s - \rho)) \right]_{x_a} \quad (6.6c).$$

In matrix form equation (6.5) can be written as:

$$\boxed{[M] \{P'\} + [K] \{P\} - \{F\} = 0} \quad (6.7).$$

The above relation is known as the semidiscrete finite element equation and constitutes the third step of the F.E. analysis. The fourth step is to use the α -family of approximation for solving equation (6.7).

In this technique a weighted average of the time derivative of the dependent variable is approximated at two consecutive time steps by linear interpolation of the values of the variable at the two time steps:

$$(1-\alpha)\{P'\}_n + \alpha\{P'\}_{n+1} = \frac{\{P\}_{n+1} - \{P\}_n}{\Delta t_{n+1}} = \{P'\}_{n+\alpha} \quad (6.8).$$

From equation (6.8) we can obtain a number of well known different schemes by choosing the values of α :

when, $\alpha = \frac{1}{2}$ Crank-Nicolson scheme,

when, $\alpha = \frac{2}{3}$ Galerkin method,

when, $\alpha = 1$ backward-difference scheme.

For linear type of problems the above schemes are unconditionally stable i.e. their stability is independent of the time step chosen in the problem. However, for non linear problems the above schemes are conditionally stable (Reddy, private communication) and the critical time step that leads to a stable numerical scheme should be defined by doing an eigenvalue analysis.

By using equation (6.8), we convert the ordinary differential equation (6.7) to a system of algebraic equations among P_{sj} at time t_{n+1} , and so we obtain:

$$[K^{Hat}]_{n+1} \{P_s\}_{n+1} = \{F^{Hat}\}_{n,n+1} \quad (6.9),$$

where,

$$[K^{Hat}]_{n+1} = [M] + \alpha \Delta t [K]_{n+1}, \quad (6.9a)$$

$$\{F^{Hat}\}_{n,n+1} = ([M] - \Delta t(1-\alpha)[K]_n) + \Delta t(\alpha\{F\}_{n+1} + (1-\alpha)\{F\}_n) \quad (6.9b)$$

The fifth and last step of this analysis involves the use of an iterative technique to take care of the non linearity. The Newton - Raphson

iterative technique, which is utilized here, consists of the following stages (Reddy 1984):

1) Computation of the residual matrix $\{R\}$ at time t_{n+1} and for an iteration step r :

$$\{R\}_{n+1}^r = ([K^{Hat}]_{n+1}^r \{P_s\}_{n+1}^r - \{F^{Hat}\}_{n,n+1}^r) \quad (6.10).$$

2) Computation of the tangent stiffness matrix $[K]^T$ at time t_{n+1} and for an iteration step r , by using the following definition (Reddy, in press)

$$[K]^T \Big|_{n+1}^r = \frac{\partial \{R\}_{n+1}^r}{\partial \{P_s\}_{n+1}^r}$$

By substituting equation (6.10) to the above definition we are led to:

$$[K]^T \Big|_{n+1}^r = \frac{\partial ([K^{Hat}]_{n+1}^r \{P_s\}_{n+1}^r - \{F^{Hat}\}_{n,n+1}^r)}{\partial \{P_s\}_{n+1}^r}$$

In addition, by elaborating equations (6.9a) and (6.9b) the previous relation becomes:

$$[K]^T \Big|_{n+1}^r = \frac{\partial ([K^{Hat}]_{n+1}^r \{P_s\}_{n+1}^r)}{\partial \{P_s\}_{n+1}^r} - \frac{([M] - \Delta t(1-\alpha)[K]_n) + \Delta t(\alpha\{F\}_{n+1} + (1-\alpha)\{F\}_n)}{\partial \{P_s\}_{n+1}^r}$$

Since we take the derivatives of the above matrices with respect the dependent variable at time $n+1$, the terms which are evaluated at the previous time n are constants and so their derivatives are zero. Thus, we obtain:

$$[K]^T \Big|_{n+1}^r = \frac{\partial([K^{Hat}]_{n+1}^r \{P_s\}_{n+1}^r)}{\partial \{P_s\}_{n+1}^r} - \frac{\Delta t \alpha \{F\}_{n+1}}{\partial \{P_s\}_{n+1}^r}$$

The above equation is further simplified by using the definition of $[K^{Hat}]_{n+1}$, equation (6.9a) as it follows:

$$[K]^T \Big|_{n+1}^r = \frac{\partial([M]\{P_s\}_{n+1}^r + \alpha \Delta t [K]_{n+1} \{P_s\}_{n+1}^r)}{\partial \{P_s\}_{n+1}^r} - \frac{\Delta t \alpha \partial \{F\}_{n+1}}{\partial \{P_s\}_{n+1}^r} \quad \text{or,}$$

$$[K]^T \Big|_{n+1}^r = [K^{Hat}]_{n+1} + a \Delta t \frac{\partial [K]_{n+1}}{\partial \{P_s\}_{n+1}^r} \{P_s\}_{n+1}^r - \frac{\Delta t \alpha \partial \{F\}_{n+1}}{\partial \{P_s\}_{n+1}^r} \quad (6.11).$$

The second term of the r.h.s. can be expanded by using equation (6.6a) and writing all the expressions in index form as follows:

$$a \Delta t \frac{K_{ip}}{\partial P_{sj}} P_p = a \Delta t \frac{1}{\partial P_{sj}} \int_{x_a}^{x_b} \left[-\frac{K_0 (1+aP_s)^{1-\delta}}{a\mu\beta} \frac{d\psi_1}{dx} \left(\frac{d\psi_p}{dx} \right)_+ \right]$$

$$\begin{aligned}
& + \psi_i \frac{g\Delta\rho\varepsilon_{so}K_o(2\beta-\delta)(1+aP_s)^{(\beta-\delta)}}{\mu\beta} \left(\frac{d\psi_p}{dx} \right) + \\
& \left. \psi_i \frac{K_o(\beta-1)(1+aP_s)^{-\delta}}{\mu\beta} \left(\frac{\partial P_s}{\partial x} \right) \left(\frac{d\psi_p}{dx} \right) \right] P_{sp} = \\
& = a \Delta t \int_{x_a}^{x_b} \left[-\frac{K_o(1+aP_s)^{-\delta}}{a\mu\beta} (1-\delta) \frac{d\psi_i}{dx} \frac{d\psi_p}{dx} \frac{\partial(1+aP_{sl}\psi_l)}{\partial P_{sj}} + \right. \\
& \quad \left. + \psi_i (-\delta) \frac{K_o(\beta-1)(1+aP_s)^{-1-\delta}}{\mu\beta} \left(\frac{\partial P_s}{\partial x} \right) \left(\frac{d\psi_p}{dx} \right) \frac{\partial(1+aP_{sl}\psi_l)}{\partial P_{sj}} + \right. \\
& \quad \left. \psi_i \frac{K_o(\beta-1)(1+aP_s)^{-\delta}}{\mu\beta} \left(\frac{\partial}{\partial P_{sj}} \left(\frac{\partial P_s}{\partial x} \right) \right) \left(\frac{d\psi_p}{dx} \right) + \right. \\
& \quad \left. + \psi_i \frac{g\Delta\rho\varepsilon_{so}K_o(2\beta-\delta)(1+aP_s)^{(\beta-\delta+1)}}{\mu\beta} (\beta-\delta) \left(\frac{d\psi_p}{dx} \right) \frac{\partial(1+aP_{sl}\psi_l)}{\partial P_{sj}} \right] P_p = \\
& = a \Delta t \int_{x_a}^{x_b} \left[-\frac{K_o(1+aP_s)^{-\delta}}{a\mu\beta} (1-\delta) a \psi_j \frac{d\psi_i}{dx} \frac{d\psi_p}{dx} \frac{\partial(1+aP_{sl}\psi_l)}{\partial P_{sj}} + \right. \\
& \quad \left. \psi_i (-\delta) \frac{K_o(\beta-1)(1+aP_s)^{-1-\delta}}{\mu\beta} \left(\frac{\partial P_s}{\partial x} \right) \left(\frac{d\psi_p}{dx} \right) \psi_j + \right. \\
& \quad \left. \psi_i \frac{K_o(\beta-1)(1+aP_s)^{-\delta}}{\mu\beta} \frac{d\psi_i}{dx} \left(\frac{d\psi_p}{dx} \right) + \right. \\
& \quad \left. \psi_i \frac{g\Delta\rho\varepsilon_{so}K_o(2\beta-\delta)(1+aP_s)^{(\beta-\delta+1)}}{\mu\beta} (\beta-\delta) \left(\frac{d\psi_p}{dx} \right) \psi_j \right] P_p =
\end{aligned}$$

$$\begin{aligned}
&= a \Delta t \int_{x_a}^{x_b} \left[-\frac{K_o(1+aP_s)^{-\delta}}{\mu\beta} (1-\delta) \psi_j \frac{d\psi_i}{dx} \frac{\partial P_s}{\partial x} + \right. \\
&\quad \left. + \psi_i (-\delta) \frac{K_o (\beta-1)(1+aP_s)^{-1-\delta}}{\mu\beta} \left(\frac{\partial P_s}{\partial x} \right)^2 \psi_j + \right. \\
&\quad \left. + \psi_i \frac{K_o (\beta-1)(1+aP_s)^{-\delta}}{\mu\beta} \frac{d\psi_i}{dx} \frac{\partial P_s}{\partial x} + \right. \\
&\quad \left. + \psi_i \frac{g\Delta\rho\varepsilon_{so}K_o(2\beta-\delta)(1+aP_s)^{(\beta-\delta+1)}}{\mu\beta} (\beta-\delta) \frac{\partial P_s}{\partial x} \psi_j \right] P_p .
\end{aligned}$$

Similarly, the third term of the r.h.s. in equation (6.11) can be expanded in index form as:

$$-a \Delta t \frac{\partial F_i}{\partial P_{sj}} = + a \Delta t \psi_i \frac{K_o(\beta+\delta-1)(1+aP_s)^{-\delta+\beta}}{\mu\beta} g \varepsilon_{so} (\rho_s-\rho) \psi_j.$$

The above term is evaluated only at the first global node of the finite element mesh.

3) Calculation of the linear solution increment, δP_s , in between of two consecutive iteration steps as:

$$\{\delta P_s\} = - [K^T] \{R\}$$

4) Computation of the solution, at the iteration step r+1 by using stage 3:

$$\{P_s\}^{r+1} = \{P_s\}^r + \{\delta P_s\}$$

5) Check for the convergence. The convergence criterion is:

$$\sqrt{\frac{(\{P_s\}^{r+1} - \{P_s\}^r)^2}{(\{P_s\}^r)^2}} < \varepsilon$$

If the convergence criterion is not satisfied and the maximum number of the iterations is not exceeded the described process (stage 1 through stage 5) should be repeated. If the convergence criterion is satisfied then the values of the $\{P_s\}^{r+1}$ consist the solution at time $n+1$. Therefore, as we have already noticed in Chapter 5, the added material causes the equal increase of the existing effective pressure variation $\{P_s\}^{r+1}$ in the compacted bed by:

$$P_s = g \varepsilon_{s0} (\rho_s - \rho) F_{t+\Delta t},$$

and thus the final effective pressure value for a node (i) is:

$$P_{s \text{ final at node (i)}} = \{P_s\}_i^{r+1} + g \varepsilon_{s0} (\rho_s - \rho) F_{t+\Delta t}$$

6.2. Description of the computer code.

A computer code is in FORTRAN language and has been written with the aim to obtain the variation of the effective pressure in the compacted sediment. The code consists of three parts: 1) the first

part involves the relations necessary to compute the decrease of a layer during a time period Δt , 2) the second part includes calculation of the effective stress by using the particulate structure equation and the derived expressions for the liquid and solids velocity, and 3) the third part includes the deduced finite element formulation for equation (5.12). The third part composed from the following subroutines: a) Subroutine MESH1D: It is applicable only for 1-D problems and it is constructed to discretize the domain for a given length and number of elements.

b) Subroutine COEFNT: In COEFNT are evaluated the stiffness matrix, the mass matrix and the source vector over an element in the finite element mesh.

c) Subroutine ASSMBL: It assembles the obtained from the COEFNT element matrices in a banded storage.

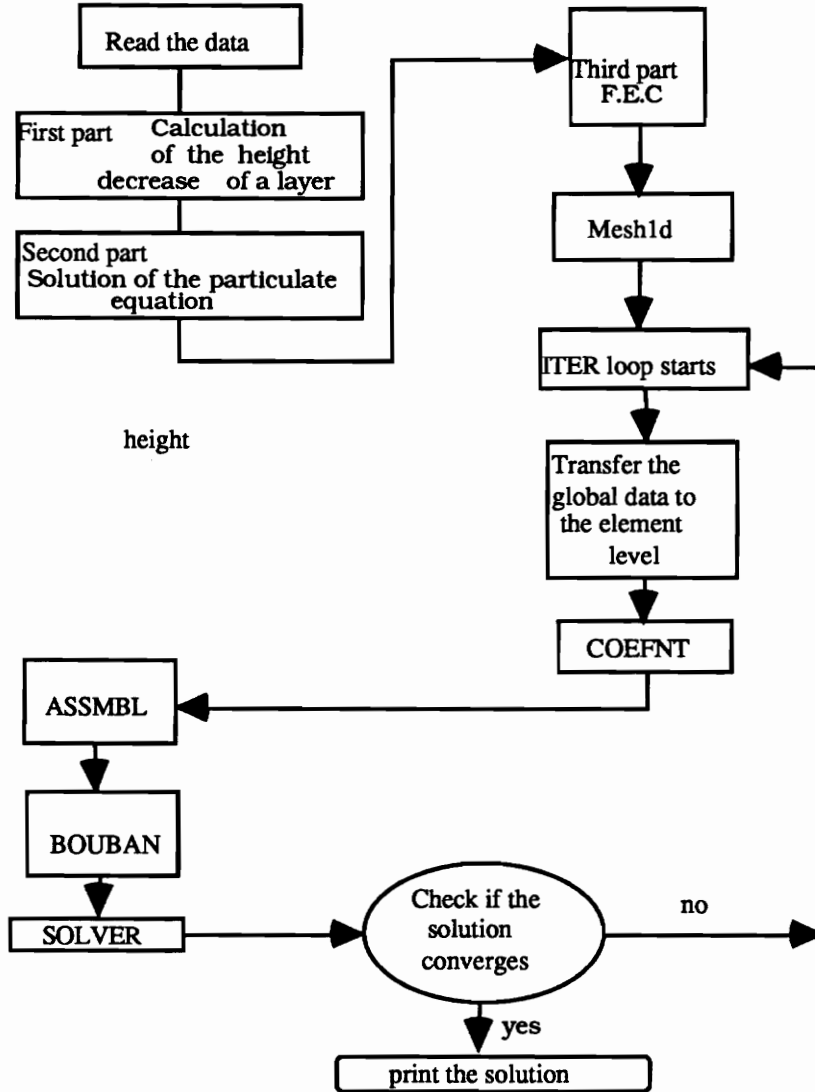
d) Subroutine BOUBAN: In this subroutine takes place the imposition of the essential boundary condition of the problem.

e) Subroutine SOLVER: The SOLVER is an interface subroutine and it is written in that way such as the source vector to become the solution vector of the algebraic system of equations. It contains the subroutine BNDSOL which is the actual solver for banded unsymmetric system of equations.

f) Subroutine INTRPL: In this subroutine are given the interpolation functions for linear and quadratic elements.

g) Subroutine PSTPRC: It is the post processor part of the code.

The following flow chart illustrates the different parts in the computer code.



Flow chart of the computer code.

A printout of the computer code is listed in the appendix.

CHAPTER 7

REQUIRED EXPERIMENTAL DATA FOR THE NUMERICAL SCHEME

7.1 Experimental data.

To be able to utilize the derived model we need to know in advance the values of the empirical constants that are involved in the constitutive equations. This is not an easy task since in most of the cases a lot of experimental difficulties (for example during measurements to obtain the solidosity and permeability) should be overcome to obtain the necessary information. The majority of the available tests describe the variation of the mudline height with time without giving any information for the variation of solids concentration with time. The only complete, in some degree, set of information is available from Tiller's (1981) experimental work. A mineral clay, the attapulgite with density $\rho_s = 2.3 \text{ gr/cm}^3$, is subjected to a sedimentation test in a batch cylinder. The initial volume fraction of solids, Φ_{s0} , in the slurry is 3% (69 gr/lit) and the initial height, H_0 , is 0.4m. The batch curve is shown in figure 25. The constant rate ends at (0.34m,2000sec) and the initial solids settling velocity is $u_{s0} = 3 \times 10^{-5} \text{ m/s}$. The figure also illustrates the variation of the sediment-suspension interface, L , with time. Information as to how this curve is obtained experimentally is not available. The coordinates

of the intersection point of the (H vs. t) and (L vs. t) curves are (0.125m,11800sec).

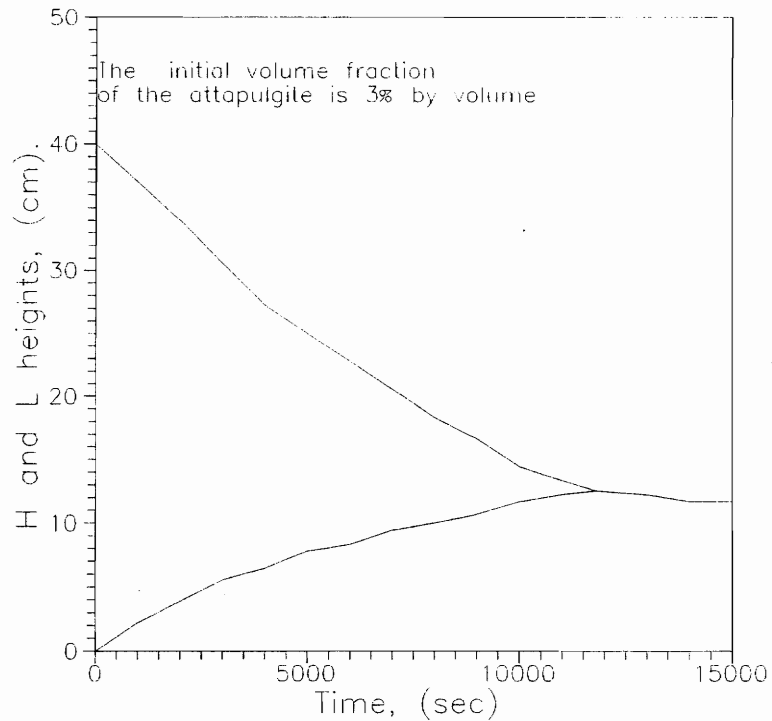


Figure 25: The (H vs. t) and (L vs. t) curves for attapulgite.

Furthermore, the plot (u_s vs. Φ_s) is shown in figure 26 and thus the flux curve (S vs. Φ_s) can be obtained and it is illustrated in figure 27. The relation of the solids velocity with the volume fraction of solids is given as:

$$u_s = 0.000119711 - 0.00428381 \Phi_s + 0.0418934 \Phi_s^2$$

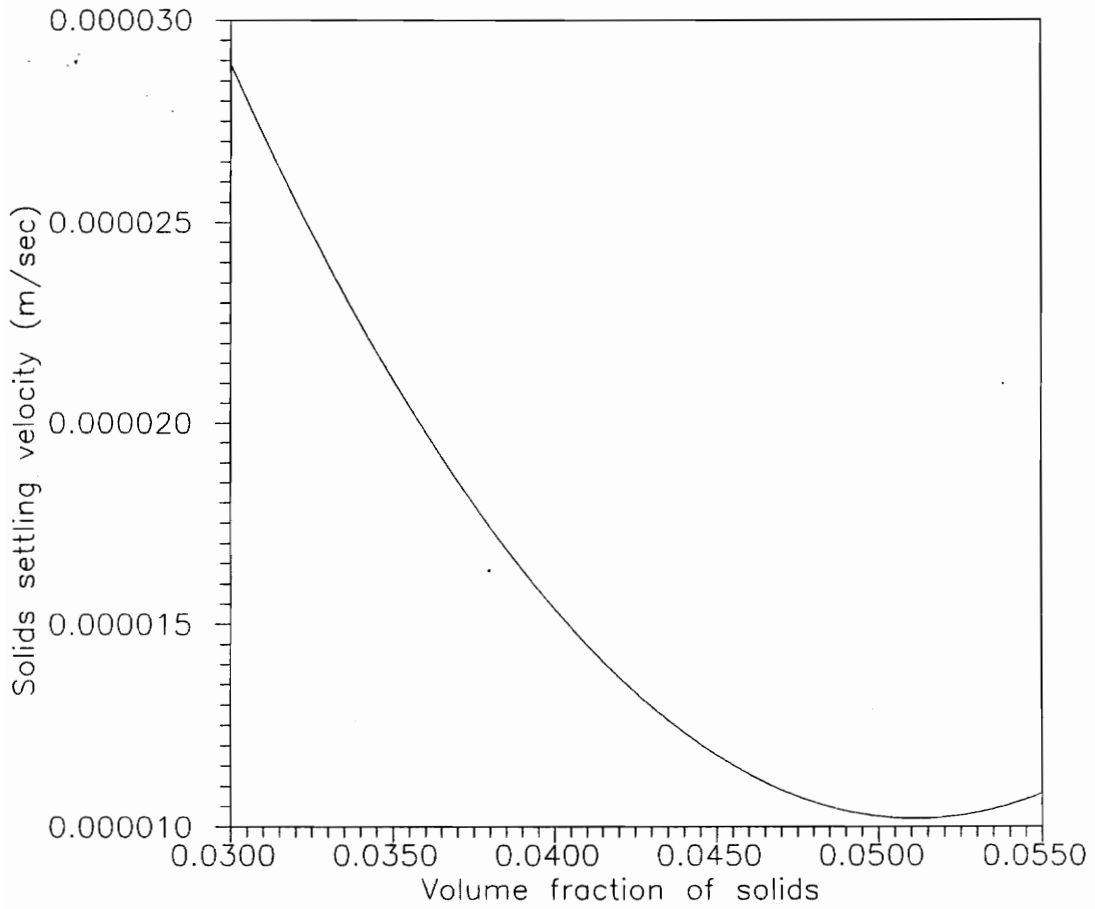


Figure 26: Solids settling velocity, u_s , vs. volume fraction of solids.

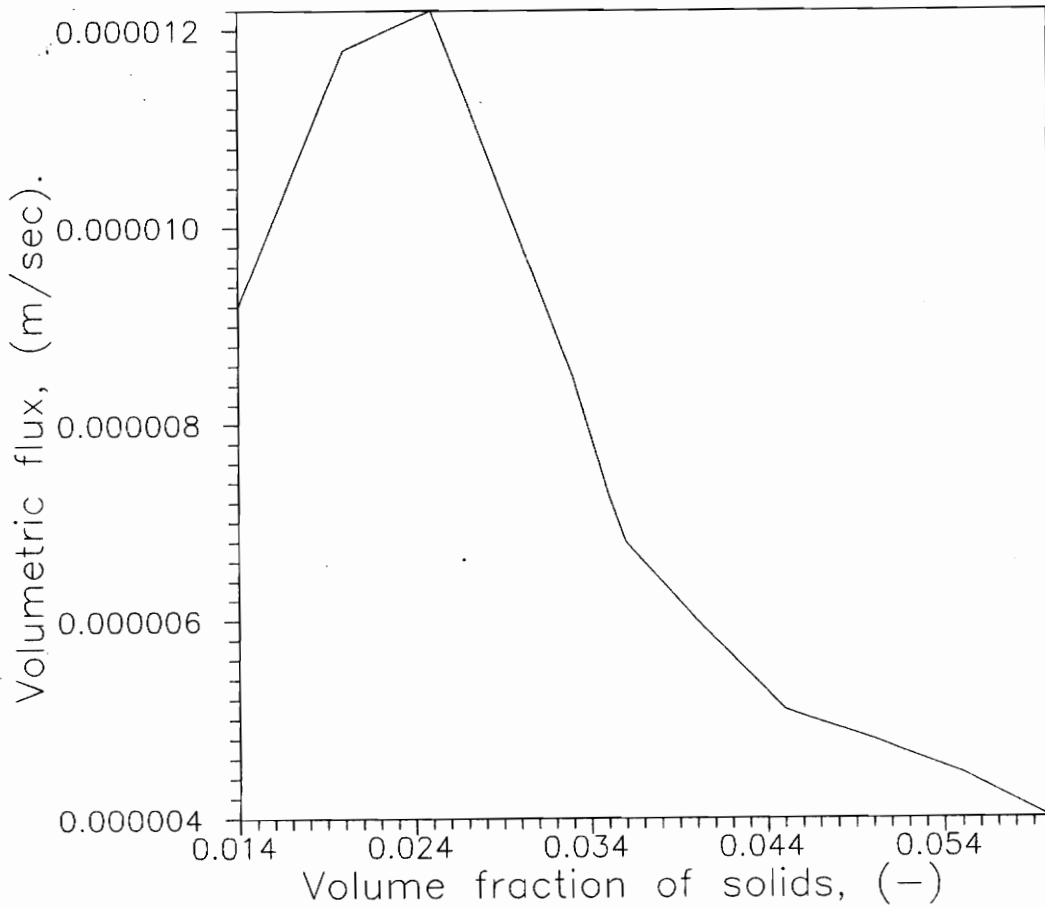


Figure 27: Flux curve for the attapulgite.

7.2 Calculation of the parameters included in the constitutive equations.

Tiller and Khatib (1984) proposed a method to compute the volume fraction of solids at the top of the sediment-suspension

interface, ϵ_{s0} . By taking material balance at time $t_0 = 0$, the rate of deposition of solids at the bottom of the batch cylinder is equal to the solids flux at the mudline interface,

$$\Phi_{s0} \left(\frac{-dH_0}{dt_0} \right) = \epsilon_{s0} \frac{dL_0}{dt_0} \quad \text{and}$$

rearranging the above equation we get:

$$\epsilon_{s0} = \Phi_{s0} \left(- \frac{dH_0}{dL_0} \right) \quad (7.1)$$

By applying this equation they computed the value of ϵ_{s0} to be equal to 6.5% for the attapulgate. However, Tiller (private communication) noticed that this method does not take into consideration the characteristics that emanate tangentially from the L- curve and so the delay that the upward liquid causes to the settling process of solids. Hence, it overestimates the value of the null stress solidosity, ϵ_{s0} . By utilizing this observation and applying equation (3.3) we obtain:

$$\frac{dL_0}{dt_0} = \frac{u_{s1}\Phi_{s1} - u_{s0}\epsilon_{s0}}{\Phi_{s1} - \epsilon_{s0}},$$

where, u_{s1} , Φ_{s1} are, respectively, the solids settling velocity and volume fraction of solids at point (1), which is the intersection point of the first tangent characteristic to the L- curve.

At time t_0 equal to zero the solids velocity at the sediment interface, u_{s0} , is zero since the solids bed has not started to build up at the bottom of the cylinder. Thus, the above relation can be simplified as:

$$\frac{dL_0}{dt_0} = \frac{u_{s1}\Phi_{s1}}{\Phi_{s1}-\epsilon_{s0}} \quad \text{or,}$$

$$\epsilon_{s0} = -\Phi_{s1} \frac{\frac{dH_1}{dt_1}}{\frac{dL_0}{dt_0}} + \Phi_{s1} \quad (7.2).$$

The value of Φ_{s1} is computed by using the geometry in figure 19 and the described methodology in unit 5.5. The parameter a indicates the bottom effective pressure in the sediment at time infinity ($t > 14000$ sec for the under study attapulgite) and it can be calculated by using equation (5.31). Therefore, at time infinity there is no movement of solids and fluid and thus without taking the Darcian term into consideration equation (5.31) yields (Font 1991):

$$a = (\rho_s - \rho) g \epsilon_{s \text{ average}} L_{\infty} \quad (7.3)$$

where: L_{∞} is the height of the sediment layer at time infinity and $\epsilon_{s \text{ average}}$ is defined as the ratio $\frac{(\Phi_{s0} H_0)}{L_{\infty}}$.

For the present batch test the value of a is: $(2300-1000) \times 9.81 \times 0.03 \times 4 = 153.04$ Pascal.

If α_0 denotes the local specific flow resistance on the top of the sediment, K_0 is the permeability of the unstressed bed, and ϵ_{s0} is the unstressed value of the solidosity they are related with the following equality (Tiller 1989) :

$$\alpha_0 K_0 \epsilon_{s0} = 1.$$

For the attapulgate the value of a_0 (which is estimated based upon the hydraulic gradient obtained at $t = 0$) is: $8.23 \times 10^{11} \text{ m}^{-2}$.

7.3 Measurement of the solidosity in the compression zone.

Equation (7.3) gives information for the surface volume fraction of solids, ϵ_{s0} . However, knowledge of the solidosity variation throughout the cake structure can be obtained from the method proposed in Chapter 5 or experimentally by means of x - rays absorption or gamma radiation. The type of radiation to be used will depend on the material properties. The difference of radiation attenuation between solids and liquid must be large enough to be distinguished by the detector or the measurement will fail. Thus, if λ_s , λ_l are the linear attenuation coefficients for solids and liquid respectively, I_l is the liquid intensity, ϵ_s is the solidosity and I the intensity of the radiation they relate each other with the following equality (Chen 1986):

$$\ln \frac{I}{I_l} = - (\lambda_s - \lambda_l) \epsilon_s \quad (7.4).$$

The above equation shows that the intensity of the radiation decreases as a negative exponential of the volume fraction of solids.

CHAPTER 8

CONCLUSIONS

The flux theories (Coe and Clevenger 1916, Kynch 1952, Talmage and Fitch 1955) are valid only in the zone settling regime. Recent methods proposed by Tiller (1981), Fitch (1983), and Font (1988) modified the third Kynch's theorem by taking into consideration the sediment rising from the bottom of a graduated cylinder. Their methods are applicable if the variation of the sediment- suspension interface, known as L-curve is known beforehand.

The present study provides a method to obtain the L-curve. Two coupled processes lead to the formation of the L-curve: (i) the consolidation of the solids bed at the bottom of a graduated cylinder and (ii) the deposition of new solid particles on the top of the existing sediment. The height of the L-curve is computed by adding to the height of the compacting bed the height of the material falling on the top of the sediment at the end of a time period. The major thrust of this work was on the development of a computer code for a F.E.M. model that simulates the consolidation process of the sediment layer and provides the distribution of the effective pressure within it. The computer program is written in Fortran language and consists of three main parts: 1) the first part describes the consolidation process that occurs in the solids bed, 2) the second subprogram has been written to obtain the effective stress variation by using the particulate

structure equation, and 3) the third part includes the finite element formulation that is elaborated to solve the governing equation of the consolidation process. The code is capable to eliminate the enormous task of conducting batch settling tests for a slurry when it is tested for different initial heights. Based on the calculated L-curve, the mudline variation with time, as well as the solids settling concentration throughout the batch column can be calculated, at any time instant.

References

Andrian D. and Kos P. 1975, Transport Phenomena Applied to Sludge Dewatering. Journal of the Environmental Engineering division ASCE 101(EE6), 947-965.

Bathe K.J. 1982, Finite Elements in Engineering Analysis, Prentice Hall, Englewood Cliffs, N.J.

Been K. and Sills G.C. 1981, Self-weight consolidation of soft soils: an experimental and theoretical study. Geotechnique 31(4), 519-535.

Bhargava D.S and Rajagopal K. 1990, Modeling in Zone settling for different Types of suspended Materials. Wat. Res. 24(6), 675-683.

Chen W. 1986, Sedimentation and Thickening. Ph.D Dissertation at University of Houston Texas.

Concha F. and Bustos M.C. 1991, Settling velocities of particulate systems, 6.Kynch sedimentation processes: batch settling. International Processing 32, 193-212.

Cullum R. 1988, Sedimentation Phenomena in Swine Waste Slurries: Model Development. Transactions of the ASAE 31(6), 1760-1766.

Dick R. and Ewing B. 1967, Evaluation of Activated Sludge Thickening Theories. Journal of the Sanitary Eng. Division 93(SA4), 9-29.

Elder D. and Sills G. 1985, Thickening and Consolidation of Sediment due to Self Weight. Engineering Foundation conference. "Flocculation, Sedimentation and Consolidation". Sea Island, GA.

Diplas P., Kennedy J.F., and Jain S. 1988, Features of Flow in Slurry-Thickening Ponds. ASCE'88 Conference on Hydraulic Eng., Colorado Springs, Colorado.

Fitch B. 1979, Sedimentation of Flocculent Suspensions: State of Art. *AIChE Journal* 25(6), 913-930.

Fitch B. 1983, Kynch Theory and Compression Zones. *AIChE Journal* 29(6), 940-947.

Font R. 1988, Compression Zone Effect in Batch Sedimentation. *AIChE* 34(2), 229-238.

Font R. 1990, Calculation of the Compression Zone Height in Continuous Thickeners. *AIChE* 36(1), 3-12.

Font R. 1991, Analysis of the Batch Sedimentation Test. *Chemical Engineering Science* 46(10) , 2473-2482.

Gaudin A.M., Fuerstenau M.C., and Mitchel S.R. 1959, Effect of Pulp Depth and Initial Pulp Density in Batch Thickening. *AIME Trans.* 214, 613-616.

Herting D.N. 1984, A general Purpose Nonlinear Transient Integration System. *Proceedings of the International Conference on Innovative Methods for Nonlinear problems.*

Javaheri, A.R. 1971, Continuous Thickening of Non-Ideal Suspensions. Ph.D Dissertation at University of Illinois at Urbana.

Kearsey H.A. 1963, A Study of the Sedimentation of Flocculated Thoria Slurries Using a Gamma-Ray Technique. *Trans. Instn. Chem. Engrs* 41, 297-306.

Kos P. 1977, Fundamentals of Gravity Thickening. Chem. Eng. Prog. 11, 99-105.

Kos P. 1985, Sedimentation and Thickening. Eng. Foundation conference. "Flocculation, Sedimentation and Consolidation " . Sea Island, GA.

Kynch G.T. 1952, A Theory of Sedimentation. Trans. Faraday Soc. 48, 166-176.

Lambe T.W. 1969, Soil Mechanics, SI version, John Wiley and Sons, Inc., New York, New York.

Mitchel J.K. 1976, Fundamentals of Soil Behavior, John Wiley and Sons, Inc., New York, New York.

Osborne D.G. 1986, Gravity Thickening. Design and Installation of Concentration and Dewatering Circuits, Chapt.5, Soc. Mining Engineers, SME AIME, 133-201.

Pearse, M.J. 1977, Gravity Thickening Theories: a Review. Warren Spring Laboratory, Hertfordshire, England.

Reddy J.N. 1984, An Introduction to the Finite Element Method, Mc Graw-Hill Publishing Company, New York.

Reddy J.N. 1992, Private Communication.

Reddy J.N. (in press) , An Introduction to the Finite Element Method, (Second Edition) Mc Graw-Hill Publishing Company, New York.

Schiffman R.L., Pane V., and Sunara V. 1985, Sedimentation and Consolidation. Engineering Foundation conference."Flocculation, Sedimentation and Consolidation". Sea Island, GA.

Smith G.N. 1989, Elements of Soil Mechanics (sixth edition), BSP Professional Books.

Talmage W.P. and Fitch E.B. 1955, Dewatering Thickener Unit Areas. I. and E.C. 47, 38.

Tarrer A. 1974, Continuous Thickening. Ind. Eng. Chem. 13(4), 341-346.

Terzaghi K. 1942, Theoretical Soil Mechanics, John Wiley and Sons, Inc., New York, New York.

Tiller F.M. 1981, Revision of Kynch Sedimentation Theory. AIChE Journal 27(5), 823-829.

Tiller F.M. and Khatib Z. 1984, Journal of Colloid and Interface Science 100(1), 55-67.

Tiller F.M., Yeh C.S., Chen Wu, Tsai C.D. 1985, Compression of particulate structures in Relation to Sediment and Cakes. Engineering Foundation conference. "Flocculation, Sedimentation and Consolidation". Sea Island, GA.

Tiller F.M. and Yeh C.S. 1987, The Role of Porosity in Filtration. AIChE Journal 33(8), 1241-1255.

Tiller F.M., Yeh C.S., Tsai C.D., and Chen W 1987, Generalised Approach to Thickening, Filtration, Centrifugation. Filtration and Separation, proceedings of the filtration Society, 121-126.

Tiller F.M. 1989, Unifying the Theory of Thickening. Filtration and Centrifugation, Proceedings of the Eng. Foundation Conference. Palm Coast Florida, 89-141.

Tiller F.M. 1992, Private Communication.

APPENDIX
COMPUTER CODE

P R O G R A M W I T H F . E . A N A L Y S I S

```

C *****
C
C |-----|
C | This is a finite element computer program for the FE |
C | ANALYSIS OF FOLLOWING EQUATIONS IN ONE DIMENSION (GOVERNING |
C | heat transfer, fluid mechanics, bars, and cables): |
C | |
C | (P)~ - (AX.P')' + CX.P = FX |
C | |
C | In the above equation (') denotes differentiation with |
C | respect to space x, and AX, CX, and FX are functions of |
C | P(X,T): |
C | |
C | AX = AX0 + AX1.P |
C | BX = BX0 + BX1.P |
C | CX = CX0 + CX1.P |
C | FX = FX0 + FX1.P |
C | THE SYMBOL ( )~ DENOTES DIFFERENTIATION WITH RESPECT TO TIME |
C | T. |
C |-----|
C
C ***** Methodology *****
C .
C . THE MODEL EQUATION FOR THIS PROBLEM IS PARABOLIC AND THE INDICATED
C . METHODOLOGY IS SIMILAR TO THAT USED FOR THE CLASSICAL HEAT TRANSFER
C . PROBLEMS. THE MODEL EQUATION HAS NON LINEAR TERMS SO THE .

```

C . METHODOLOGY FOR NON LINEAR ANALYSIS SHOULD BE UTILIZED HERE. THE .
C . TRANSIENT ANALYSIS IS ALSO INVOLVED. THE FOLLOWING STEPS SHOULD .
C . BE FOLLOWED: .
C . 1) THE FIRST LOOP SHOULD BE THE LOAD LOOP. .
C . 2) THE SECOND LOOP SHOULD BE WITH THE TIME. THE A-FAMILY OF .
C . APPROXIMATION IS USED FOR PARABOLIC EQUATIONS. .
C . 3) THE THIRD LOOP SHOULD BE RELATED WITH THE NUMBER OF ITERATIONS. .
C . 4) IN THE PROCESSOR UNIT: .
C . - INITIALIZE THE MATRICES: .
C . GLOBAL COEFFICIENT MATRIX GLK .
C . GLOBAL MASS MATRIX GLM .
C . GLOBAL FORCE VECTOR GLF .
C . - DO LOOP FOR ELEMENT CALCULATIONS AND ASSEMBLY .
C . - CALL THE SUBROUTINE COEFNT(OR STIFF) FOR CALCULATION OF ELK, .
C . ELK(HAT) FROM TRANSIENT ANALYSIS, AND ELK (TANGIENT) USING .
C . THE NEWTON-RAMPHSON ITERATION SCHEME. .
C . - CALL BOUBAN TO IMPOSE BOUNDARY CONDITIONS ON *BANDED* .
C . EQUATIONS FOR TRANSIENT ANALYSIS. .
C . - CALL SOLVER TO SOLVE THE FINITE - ELEMENT EQUATIONS. .
C . - UPDATE THE SOLUTION AND CHECK FOR CONVERGENCE. IF THE .
C . ITERATION SCHEME COVERGENCES WE CONTINUE WITH THE POST .
C . PROCESSOR UNIT. .
C .
C . - CALL PSTPRC .

C . _____ .

C

C

C . DEFINITIONS OF THE VARIABLES .

C

C _____

C

C . KEY VARIABLES USED IN THE PROGRAM .

C

C . NDF..... NUMBER OF DEGREES OF FREEDOM PER NODE .

C . NEQ..... NUMBER OF EQUATIONS IN THE MODEL (BEFORE B. C.) .

C . NGP..... NUMBER OF GAUSS POINTS USED IN THE EVALUATION OF .

C . THE ELEMENT COEFFICIENTS, [ELK], {ELF}, [ELM] .

C . NHBW..... Half bandwidth of global coefficient matrix [GLK] .

C . NPE..... Number of nodes per element (NODPELM) .

C . NGP..... Number of Gauss points used in the integration .

C . NNM..... Number of nodes in the finite element mesh (NODFELEM) .

C . NPRNT..... Indicator to print element matrices (PRINT) .

C . (NO PRINT:0, PRINT:1) .

C . IELEM..... INDICATES THE TYPE OF THE INTERPOLATION FUNCTION (INTERPOL) .

C . IELEM = 1 : LINEAR INTRPL FUNCTION .

C . IELEM > 1 : QUADRATIC INTPL FUNCTION .

C _____

C

C . DIMENSIONS OF VARIOUS ARRAYS IN THE PROGRAM .

C

C . Values of MXELM, MXNOD, etc. in the PARAMETER statement should .

C . be changed to meet the requirements of problem: .

C

C . MXELM..... Maximum number of elements in the mesh: .

C . MXEBC..... Maximum number of speci. primary deg. of freedom .

C . MXNBC..... Maximum number of speci. secondary deg. of freedom .
 C . MXNEQ..... Maximum number of equations in the FE model .
 C . MXNOD..... Maximum number of nodes in the mesh .

C
 C ELX(I).....GLOBAL COORDINATES OF AN ELEMENT
 C ELK(I,J)...ELEMENT COEFFICIENT MATRIX
 C ELM(I,J)...ELEMENT MASS MATRIX
 C ELF(I).....ELEMENT FORCE VECTOR
 C GLF(I).....COLUMN VECTOR OF GLOBAL FORCES BEFORE GOING INTO THE
 C SUBROUTINE SOLVER. AFTER COMING OUT OF THE SUBROUT.
 C SOLVER IT CONTAINS THE INCREMENT OF THE SOLUTION OF EACH
 C ITERATION.

C GLX(I).....GLOBAL COORDINATES OF AN ELEMENT
 C ***** PARAMETERS FOR THE NON LINEAR ANALYSIS *****

C *GFPR* GFPR(I)....COLUMN VECTOR WITH THE TOTAL SOLUTION UP TO THE
 C CURRENT ITERATION AND LOAD STEP.

C ITLIM.....MAXIMUM ALLOWABLE NUMBER OF ITERATIONS WITHIN
 C EACH LOAD STEP

C *EPSLN* EPSLN.....CONVERGENCE COEFFICIENT

C ITER.....ITERATION COUNTER

C *ISTEP* ISTEP.....LOAD STEP COUNTER

C NLDST.....TOTAL NUMBER OF STEPS IN WHICH LOAD IS APPLIED

C ***** PARAMETERS FOR THE TRANSIENT ANALYSIS*****

c Alpha |

c A1,A2 | Parameters used in the time Approximations Schemes

PVARIN c Gwo(i)...Vector of initial values of the primary variables

TS c DT.....TIME STEP

c NTS.....INDICATION OF THE CURRENT NO. OF TIME STEP

c TMAX.....MAX.VALUE OF TIME THAT WE CAN REACH IN THE TIME LOOP

c TIME.....INDICATION OF THE CURRENT TIME VALUE

C INTVL.....THE INTERVAL AMONG THE NTS VALUES

C

C

C PARAMETER (MAXELM= 20, MXNEQ = (MAXELM +1)*3, MXNBC = 20)

C

IMPLICIT REAL*8(A-H,O-Z)

REAL MV,NES,K,NESS

PARAMETER (MXELM=50, MXNEQ=153, MXEBC=50, MXNBC=50, MXNOD=55)

C PARAMETER (NCMAX = 55, NRMAX = 153)

DIMENSION GLK(MXNEQ,MXNEQ),GLF(MXNEQ),GLX(MXNOD),DX2(MXNOD),

* GLM(MXNEQ,MXNEQ),DH1(MXNOD)

DIMENSION GFPR(MXNEQ),ELU(6),GWO(MXNEQ),EWO(6)

DIMENSION NOD(MXELM,3),ISPV(MXEBC,2),ISSV(MXNBC,2)

DIMENSION VSPV(MXEBC),VSSV(MXNBC)

DIMENSION ES(MXNEQ),MV(MXNOD),GWO(MXNEQ),DDH1(MXNOD),A(MXNOD)

DIMENSION DDX2(MXNOD),NES(MXNEQ),UL(MXNOD),US(MXNOD)

DIMENSION K(MXNOD),EWP(MXNOD),WS(MXNOD),NESS(MXNEQ)

C

COMMON/STR1/ELK(6,6),ELM(6,6),ELF(6),ELX(3),ELKI(6,6),ELFI(6)

COMMON/STR2/A1,A2

COMMON/STR3/PA,R,D,EK,EM,DR,E

COMMON/IO/IN,IT

C-----C

C

C

C

C

P R E P R O C E S S O R U N I T

IN=5

IT=6

OPEN(UNIT=5,FILE='TEST DATA')

OPEN(UNIT=6,FILE='TEST OUT')

C * ONE DEGREE OF FREEDOM PROBLEM*

NDF=1

C

C READ(IN,300) TITLE

READ(IN,*) NPE,NEM,NPRNT,IELEM

READ(IN,*) ITLIM,EPSLN

C

NHBW = 0.0

NHBW = NPE*NDF

NNM NNM = NEM*(NPE-1)+1

NN = NPE*NDF

NEM1=NEM + 1

C

C

NEQ=NNM*NDF

C

C | READ DATA ON BOUNDARY CONDITIONS OF TWO KINDS: THE DIRICHLET (PV) |

C | AND THE NEUMANN (SV) TYPE. |

C |

READ(IN,*) ALPHA,DT,TMAX

A1 = ALPHA*DT

A2 = (1.0-ALPHA)*DT

C

C | NSPV: NUMBER OF SPECIFIED PRIMARY VARIABLES |

C |

C

READ(IN,*) NSPV

IF(NSPV.NE.0)THEN

DO 40 IB=1,NSPV

READ(IN,*) (ISPV(IB,J),J =1,2),VSPV(IB)

40 CONTINUE

ENDIF

C

C | NSSV:NUMBER OF SPECIFIED SECONDARY VARIABLES |

C |

C

READ(IN,*) NSSV

WRITE(6,*) NSSV

IF(NSSV.NE.0)THEN

DO 50 IB=1,NSSV

C 50 READ(IN,*) (ISSV(IB,J),J=1,2),VSSV(IB)

50 READ(IN,*) (ISSV(IB,J),J=1,2)

C WRITE(6,*) ISSV(IB,1),ISSV(IB,2)

ENDIF

C ENDIF

READ(IN,*) (GWO(I),I=1,NEQ)

READ(IN,*) (ES(I),I=1,NEQ)

C-----C

C SET THE THICKNESS HEIGHT X OF THE CONSOLIDATED SOLIDS AT TIME T C

C-----C

READ(IN,*) X0

WRITE(6,*) 'THE HEIGHT OF THE BED AT TIME T0 IS:',X0

READ(IN,*) X1

WRITE(6,*) 'THE HEIGHT OF THE BED AT TIME T1 IS:',X1

C READ(IN,*) TDDX2 at Time T2

C READ(IN,*) FALX

C

C

C E N D O F T H E I N P U T D A T A

C-----C

C

C
C
C
C
C
C
C

P R I N T T H E I N P U T D A T A

WRITE(IT,530)

WRITE(IT,310)

WRITE(IT,530)

C WRITE(IT,300) TITLE

WRITE(IT,350) NPE,NDF,NEM,NEQ,NSPV,NSSV

C
C

IF(NSPV.NE.0)THEN

WRITE(IT,480)

DO 100 IB=1,NSPV

WRITE(IT,490)(ISPV(IB,J),J=1,2),VSPV(IB)

100 CONTINUE

ENDIF

C

C IF(NSSV.NE.0)THEN

WRITE(IT,500)

DO 110 IB=1,NSSV

110 WRITE(IT,490) (ISSV(IB,J),J=1,2)

C 110 WRITE(IT,490) (ISSV(IB,J),J=1,2),VSSV(IB)

C ENDIF

C

IF(NSSV.EQ.0) THEN

WRITE(IT,620)

END IF

DO 115 I = 1,NEQ

OFF-POSSIBLE

10 CONTINUE

DO 9 I = 1,NNM-1

C

DDH1(I) = DH1(I)*MV(I)*GWO0(I)

C

WRITE(6,*) 'DDH1(I):SUBL.DECREASE OF THE HEIGHT AT THE INITIAL T'

WRITE(6,*) DDH1(I)

C

TDDH1 =TDDH1 + DDH1(I)

C

9 CONTINUE

WRITE(6,*) '*****'

WRITE(6,*) 'TDDH1,TOTAL DECREASE OF THE HEIGHT OF THE SEDIMENT'

WRITE(6,*) 'DUE TO CONSOLIDATION AT TIME, T'

WRITE(6,*) '*****'

WRITE(6,*) TDDH1

DO 8 I = 1,NNM-1

C

A(I) = DDH1(I)/TDDH1

C

8 CONTINUE

C

C

C*****

C END OF STEP 1

*

C*****

C

C

C

C * * * * *

C STEP 2. CALCULATION OF THE FOLLOWING VARIABLES AT THE END OF THE
C CONSOLIDATION PERIOD $DT = T2 - T1$;

C

C BY USING THE ASSUMED TOTAL DECREASE AT TIME T2 WE CALCULATE:

C $DDX2$ = THE DECREASE FOR EACH SUBLAYER.

C $TDDX2$ = THE ASSUMED TOTAL DECREASE.

C $NESS(I)$ = THE AVERAGE INITIAL CONCENTRATION OF EACH LAYER.

C $NES(I)$ = THE NEW (T2) AVERAGE CONCENTRATION OF EACH LAYER.

C DT = THE CONSOLIDATION PERIOD.

C $UL(I)$ = THE WATER THAT MOVES UP FROM EACH SUBLAYER AT T2. *plus included*

C $US(I)$ = THE SOLIDS VELOCITY AT TIME T2. *")*

C $K(I)$ = THE PERMEABILITY AT EACH SUBLAYER AT TIME T2.

C $EWP(I)$ = EXCESS WATER PRESSURE

C $WS(I)$ = WEIGHT OF SOLIDS THAT COUNTS FOR EACH SUBLAYER AT T2.

C FPB = THE BOTTOM EFFECTIVE PRESSURE AT TIME T2.

C * * * * *

C-----C

C WRITE THE TOTAL DECREASE, $TDDX2$, OF THE LAYER AT TIME (T + DT)

C-----C

WRITE(6,*) 'THE ASSUMED TOTAL DECREASE AT T+DT IS:', $TDDX2$

DO 12 I = 1, NNM-1

C

$DDX2(I) = A(I) * TDDX2$

C

WRITE(6,*) ' A(I)', 'DDX2(I)'

WRITE(6,*) A(I), DDX2(I)

$NESS(I) = (ES(I+1) + ES(I)) / 2.$

C

WRITE(6,*) 'NESS'

```

C   WRITE(6,*)  NNESS(I)
C
C   IF (I .EQ. NNM-1) GOTO 14
C
C   NES(I) =((DH1(I))/(DH1(I)-DDX2(I)))*NESS(I)
C
14  NES(NNM-1) = 0.065
C   WRITE(6,*) 'THE SOLIDS CONCENTRATION FOR EACH SUBLAYER IS:'
C   WRITE(6,*) NES(I)
12  CONTINUE
C   DO 13 I = 1,NNM-1
C
C   K(I) = EK*(E/NES(I))**(R/D)
C
C   WRITE(6,*) 'K INTRINSIC PERMEABILITY FOR EACH SUBLAYER IS:'
C   WRITE(6,*) K(I)
13  CONTINUE
C   UL(1) = 0.5*(DDX2(1)/DT)*(1/(1-NES(1)))
C   US(1) = 0.5*(DDX2(1)/DT)*(1/NES(1))
C   SUMM = 0.0
C   DO 20 I = 2,NNM-1
C
C   SUMM = SUMM + A(I-1)
C   WRITE(6,*) 'SUMM',SUMM
C   UL(I) = 0.5*(1/DT)*TDDX2*(A(I)+2*SUMM)*(1/(1-NES(I)))
C
C   WRITE(6,*) 'UL THE LIQUID VELOCITY FOR EACH SUBLAYER IS:'
C   WRITE(6,*) UL(I)
C
C   US(I) = 0.5*(1/DT)*TDDX2*(A(I)+2*SUMM)*(1/NES(I))
C

```

```
WRITE(6,*) 'US THE SOLIDS VELOCITY FOR EACH SUBLAYER IS:'
```

```
WRITE(6,*) US(I)
```

```
20 CONTINUE
```

```
AA = UL(NNM-1)
```

```
BB = US(NNM-1)
```

```
C
```

```
TEWP = 0.0
```

```
TWS = 0.0
```

```
DO 30 I =1,NNM-1
```

```
C
```

```
EWP(I)=(((UL(I)-US(I))*EM*(1-NES(I)))/K(I))*
```

```
+ (DH1(I)-DDX2(I))
```

```
C
```

```
TEWP = TEWP + EWP(I)
```

```
C
```

```
C
```

```
WS(I)= DR*9.81*NES(I)*(DH1(I)-DDX2(I))
```

```
C
```

```
TWS = TWS + WS(I)
```

```
30 CONTINUE
```

```
C
```

```
C
```

```
C
```

```
WRITE(6,*) 'TEWP, TOTAL EXCESS WATER PRESSURE'
```

```
WRITE(6,*) TEWP
```

```
WRITE(6,*) 'TWS, TOTAL WEIGHT OF SOLIDS'
```

```
WRITE(6,*) TWS
```

```
C*****
```

```
C
```

```
FPB = TWS + TEWP
```

```
C
```

C

WRITE(6,*) '-----'

WRITE(6,*) 'EXTERNALS LOOP BOTTOM EFFECTIVE PRESSURE FPB0'

WRITE(6,*) FPB

WRITE(6,*) '-----'

DFPB = -DR*9.81*E*(1+(1/PA)*FPB)**(R-D+1)*EK*(PA/(EM*R))

C WRITE(6,*) '*****'

C WRITE(6,*) 'DFPB, THE SECONDARY VARIABLE AT THE BOTTOM OF '

C WRITE(6,*) 'THE SEDIMENT'

C WRITE(6,*) '*****'

C WRITE(6,*) DFPB

C

C

C * * * * *

C END OF STEP 2.

C * * * * *

C

C

C END OF THE FIRST METHOD

C

C

C

C

C

C

C

C

C

C

C

C

C

C 2 ND M E T H O D: U S E O F T H E F. E. C.

C

C

C

C

C * * * * *

C CALCULATE THE HEIGHT OF THE CONSOLIDATED BED AT TIME T2 C *

C *

C USE THE F.E.C. TO FIND THE BOTTOM PRESSURE. *

C *

C *

C COMPARE THE BOTTOM PRESSURE THAT YOU OBTAIN FROM THE CODE *

C WITH THE PRESSURE OBTAINED AT STEP 2. *

C IF THEY ARE DIFFERENT ASSUME ANOTHER DECREASE AT TIME T2. *

C IF THEY ARE NOT DIFFERENT THEN CALCULATE THE FOLLOWING:

C PROPV = THE PROPAGATION VELOCITY OF A CHARACTERISTIC LINE.

C SLIPC = THE MUDLINE HEIGHT (MUDLINE)

C SUS = THE VELOCITY OF THE SUSPENDED SOLIDS VSS

C SC = THE CONCENTRATION OF THE SUSPENDED SOLIDS CS

C FALX = THE HEIGHT OF THE FALLING MATERIAL

C TOTALX = THE TOTAL HEIGHT OF SOLIDS AFTER THE CONSOLIDATION AND

C THE FALL OF NEW PARTICLES HAVE ALREADY OCCURED.

C * * * * *

C

C THE HEIGHT OF THE SOLIDS AT THE END OF THE CONSOLIDATION PERIOD

$$X2 = X1 - TDDH1 - TDDX2$$

WRITE(6,*) 'THE HEIGHT AT TIME T+DT:', X2

C

C

C

C

DO 15 I=1,NEM1

IF (I.EQ.1) THEN

DX2(I) = 0.0 *any?*

ELSE

DX2(I) = X2/NEM

ENDIF

15 CONTINUE

C-----

CALL MESH1D (NEM,NPE,NOD,MXELM,MXNOD,DX2,GLX)

C-----

WRITE(IT,410)

WRITE(IT,540) (GLX(I),I=1,NNM)

C

C

C

C=====

C JUST FOR THE FIRST ITERATION SET THE CURRENT SOLUTION VECTOR

C GFPR EQUAL TO THE VECTOR OF THE INITIAL CONDITIONS GWO.

C=====

DO 40000 I = 1,NEQ

40000 GFPR(I) = GWO(I)

C-----

C |

C |

ITERATION LOOP |

C |

Initialize the iteration parameters |

C-----

C

C

C


```
DO 200 N = 1, NEM
```

C

```
C WRITE(6,*) 'THIS IS THE ELEMENT', N
```

```
L = 0.0
```

```
DO 180 I=1,NPE
```

```
NI=NOD(N,I)
```

C

C

C

C

C

```
C | Transfer the global data to the element data |
```

C

C

```
ELX(I)=GLX(NI)
```

C

C

C

C

C

C

C

```
C | NDF IS ONE (FOR THE X-DIRECTION) |
```

C

```
C | LI = (NI-1)*NDF |
```

C

C

```
LI= NI-1
```

```
DO 170 J = 1,NDF
```

```
LI = LI + 1
```

```
L = L + 1
```

C

```
EW(L) = GW(LI)
```

```
170
```

```
170
```

1
 2
 3
 4
 5
 6
 7
 8
 9
 10
 11
 12
 13
 14
 15
 16
 17
 18
 19
 20
 21
 22
 23
 24
 25
 26
 27
 28
 29
 30
 31
 32
 33
 34
 35
 36
 37
 38
 39
 40
 41
 42
 43
 44
 45
 46
 47
 48
 49
 50
 51
 52
 53
 54
 55
 56
 57
 58
 59
 60
 61
 62
 63
 64
 65
 66
 67
 68
 69
 70
 71
 72
 73
 74
 75
 76
 77
 78
 79
 80
 81
 82
 83
 84
 85
 86
 87
 88
 89
 90
 91
 92
 93
 94
 95
 96
 97
 98
 99
 100
 101
 102
 103
 104
 105
 106
 107
 108
 109
 110
 111
 112
 113
 114
 115
 116
 117
 118
 119
 120
 121
 122
 123
 124
 125
 126
 127
 128
 129
 130
 131
 132
 133
 134
 135
 136
 137
 138
 139
 140
 141
 142
 143
 144
 145
 146
 147
 148
 149
 150
 151
 152
 153
 154
 155
 156
 157
 158
 159
 160
 161
 162
 163
 164
 165
 166
 167
 168
 169
 170
 171
 172
 173
 174
 175
 176
 177
 178
 179
 180
 181
 182
 183
 184
 185
 186
 187
 188
 189
 190
 191
 192
 193
 194
 195
 196
 197
 198
 199
 200
 201
 202
 203
 204
 205
 206
 207
 208
 209
 210
 211
 212
 213
 214
 215
 216
 217
 218
 219
 220
 221
 222
 223
 224
 225
 226
 227
 228
 229
 230
 231
 232
 233
 234
 235
 236
 237
 238
 239
 240
 241
 242
 243
 244
 245
 246
 247
 248
 249
 250
 251
 252
 253
 254
 255
 256
 257
 258
 259
 260
 261
 262
 263
 264
 265
 266
 267
 268
 269
 270
 271
 272
 273
 274
 275
 276
 277
 278
 279
 280
 281
 282
 283
 284
 285
 286
 287
 288
 289
 290
 291
 292
 293
 294
 295
 296
 297
 298
 299
 300
 301
 302
 303
 304
 305
 306
 307
 308
 309
 310
 311
 312
 313
 314
 315
 316
 317
 318
 319
 320
 321
 322
 323
 324
 325
 326
 327
 328
 329
 330
 331
 332
 333
 334
 335
 336
 337
 338
 339
 340
 341
 342
 343
 344
 345
 346
 347
 348
 349
 350
 351
 352
 353
 354
 355
 356
 357
 358
 359
 360
 361
 362
 363
 364
 365
 366
 367
 368
 369
 370
 371
 372
 373
 374
 375
 376
 377
 378
 379
 380
 381
 382
 383
 384
 385
 386
 387
 388
 389
 390
 391
 392
 393
 394
 395
 396
 397
 398
 399
 400
 401
 402
 403
 404
 405
 406
 407
 408
 409
 410
 411
 412
 413
 414
 415
 416
 417
 418
 419
 420
 421
 422
 423
 424
 425
 426
 427
 428
 429
 430
 431
 432
 433
 434
 435
 436
 437
 438
 439
 440
 441
 442
 443
 444
 445
 446
 447
 448
 449
 450
 451
 452
 453
 454
 455
 456
 457
 458
 459
 460
 461
 462
 463
 464
 465
 466
 467
 468
 469
 470
 471
 472
 473
 474
 475
 476
 477
 478
 479
 480
 481
 482
 483
 484
 485
 486
 487
 488
 489
 490
 491
 492
 493
 494
 495
 496
 497
 498
 499
 500
 501
 502
 503
 504
 505
 506
 507
 508
 509
 510
 511
 512
 513
 514
 515
 516
 517
 518
 519
 520
 521
 522
 523
 524
 525
 526
 527
 528
 529
 530
 531
 532
 533
 534
 535
 536
 537
 538
 539
 540
 541
 542
 543
 544
 545
 546
 547
 548
 549
 550
 551
 552
 553
 554
 555
 556
 557
 558
 559
 560
 561
 562
 563
 564
 565
 566
 567
 568
 569
 570
 571
 572
 573
 574
 575
 576
 577
 578
 579
 580
 581
 582
 583
 584
 585
 586
 587
 588
 589
 590
 591
 592
 593
 594
 595
 596
 597
 598
 599
 600
 601
 602
 603
 604
 605
 606
 607
 608
 609
 610
 611
 612
 613
 614
 615
 616
 617
 618
 619
 620
 621
 622
 623
 624
 625
 626
 627
 628
 629
 630
 631
 632
 633
 634
 635
 636
 637
 638
 639
 640
 641
 642
 643
 644
 645
 646
 647
 648
 649
 650
 651
 652
 653
 654
 655
 656
 657
 658
 659
 660
 661
 662
 663
 664
 665
 666
 667
 668
 669
 670
 671
 672
 673
 674
 675
 676
 677
 678
 679
 680
 681
 682
 683
 684
 685
 686
 687
 688
 689
 690
 691
 692
 693
 694
 695
 696
 697
 698
 699
 700
 701
 702
 703
 704
 705
 706
 707
 708
 709
 710
 711
 712
 713
 714
 715
 716
 717
 718
 719
 720
 721
 722
 723
 724
 725
 726
 727
 728
 729
 730
 731
 732
 733
 734
 735
 736
 737
 738
 739
 740
 741
 742
 743
 744
 745
 746
 747
 748
 749
 750
 751
 752
 753
 754
 755
 756
 757
 758
 759
 760
 761
 762
 763
 764
 765
 766
 767
 768
 769
 770
 771
 772
 773
 774
 775
 776
 777
 778
 779
 780
 781
 782
 783
 784
 785
 786
 787
 788
 789
 790
 791
 792
 793
 794
 795
 796
 797
 798
 799
 800
 801
 802
 803
 804
 805
 806
 807
 808
 809
 810
 811
 812
 813
 814
 815
 816
 817
 818
 819
 820
 821
 822
 823
 824
 825
 826
 827
 828
 829
 830
 831
 832
 833
 834
 835
 836
 837
 838
 839
 840
 841
 842
 843
 844
 845
 846
 847
 848
 849
 850
 851
 852
 853
 854
 855
 856
 857
 858
 859
 860
 861
 862
 863
 864
 865
 866
 867
 868
 869
 870
 871
 872
 873
 874
 875
 876
 877
 878
 879
 880
 881
 882
 883
 884
 885
 886
 887
 888
 889
 890
 891
 892
 893
 894
 895
 896
 897
 898
 899
 900
 901
 902
 903
 904
 905
 906
 907
 908
 909
 910
 911
 912
 913
 914
 915
 916
 917
 918
 919
 920
 921
 922
 923
 924
 925
 926
 927
 928
 929
 930
 931
 932
 933
 934
 935
 936
 937
 938
 939
 940
 941
 942
 943
 944
 945
 946
 947
 948
 949
 950
 951
 952
 953
 954
 955
 956
 957
 958
 959
 960
 961
 962
 963
 964
 965
 966
 967
 968
 969
 970
 971
 972
 973
 974
 975
 976
 977
 978
 979
 980
 981
 982
 983
 984
 985
 986
 987
 988
 989
 990
 991
 992
 993
 994
 995
 996
 997
 998
 999
 1000
 1001
 1002
 1003
 1004
 1005
 1006
 1007
 1008
 1009
 1010
 1011
 1012
 1013
 1014
 1015
 1016
 1017
 1018
 1019
 1020
 1021
 1022
 1023
 1024
 1025
 1026
 1027
 1028
 1029
 1030
 1031
 1032
 1033
 1034
 1035
 1036
 1037
 1038
 1039
 1040
 1041
 1042
 1043
 1044
 1045
 1046
 1047
 1048
 1049
 1050
 1051
 1052
 1053
 1054
 1055
 1056
 1057
 1058
 1059
 1060
 1061
 1062
 1063
 1064
 1065
 1066
 1067
 1068
 1069
 1070
 1071
 1072
 1073
 1074
 1075
 1076
 1077
 1078
 1079
 1080
 1081
 1082
 1083
 1084
 1085
 1086
 1087
 1088
 1089
 1090
 1091
 1092
 1093
 1094
 1095
 1096
 1097
 1098
 1099
 1100
 1101
 1102
 1103
 1104
 1105
 1106
 1107
 1108
 1109
 1110
 1111
 1112
 1113
 1114
 1115
 1116
 1117
 1118
 1119
 1120
 1121
 1122
 1123
 1124
 1125
 1126
 1127
 1128
 1129
 1130
 1131
 1132
 1133
 1134
 1135
 1136
 1137
 1138
 1139
 1140
 1141
 1142
 1143
 1144
 1145
 1146
 1147
 1148
 1149
 1150
 1151
 1152
 1153
 1154
 1155
 1156
 1157
 1158
 1159
 1160
 1161
 1162
 1163
 1164
 1165
 1166
 1167
 1168
 1169
 1170
 1171
 1172
 1173
 1174
 1175
 1176
 1177
 1178
 1179
 1180
 1181
 1182
 1183
 1184
 1185
 1186
 1187
 1188
 1189
 1190
 1191
 1192
 1193
 1194
 1195
 1196
 1197
 1198
 1199
 1200
 1201
 1202
 1203
 1204
 1205
 1206
 1207
 1208
 1209
 1210
 1211
 1212
 1213
 1214
 1215
 1216
 1217
 1218
 1219
 1220
 1221
 1222
 1223
 1224
 1225
 1226
 1227
 1228
 1229
 1230
 1231
 1232
 1233
 1234
 1235
 1236
 1237
 1238
 1239
 1240
 1241
 1242
 1243
 1244
 1245
 1246
 1247
 1248
 1249
 1250
 1251
 1252
 1253
 1254
 1255
 1256
 1257
 1258
 1259
 1260
 1261
 1262
 1263
 1264
 1265
 1266
 1267
 1268
 1269
 1270
 1271
 1272
 1273
 1274
 1275
 1276
 1277
 1278
 1279
 1280
 1281
 1282
 1283
 1284
 1285
 1286
 1287
 1288
 1289
 1290
 1291
 1292
 1293
 1294
 1295
 1296
 1297
 1298
 1299
 1300
 1301
 1302
 1303
 1304
 1305
 1306
 1307
 1308
 1309
 1310
 1311
 1312
 1313
 1314
 1315
 1316
 1317
 1318
 1319
 1320
 1321
 1322
 1323
 1324
 1325
 1326
 1327
 1328
 1329
 1330
 1331
 1332
 1333
 1334
 1335
 1336
 1337
 1338
 1339
 1340
 1341
 1342
 1343
 1344
 1345
 1346
 1347
 1348
 1349

```

C      0.95 0.95
      ELU(L) = GFPR(LI)
C      WRITE(6,*) 'ELU='
C      WRITE(6,*) ELU(L)
170 CONTINUE
180 CONTINUE

C
C
C
C
C-----
C
C
C
C-----
      CALL COEFNT (NDF,NPE,N,NI,ELU,EWO,IELEM,NEM,NNM,AA,BB)
C-----
      IF(NPRNT .NE.0)THEN
          IF(NPRNT .LE.2)THEN
              IF(ITER.NE.1) GO TO 195
C              IF(N.EQ.1)THEN
C                  WRITE(IT,550)
C                  DO 190 I=1,NN
C 190              WRITE(IT,540) (ELK(I,J),J=1,NN)
C                  WRITE(IT,560)
C                  WRITE(IT,540) (ELF(I),I=1,NN)
C                  WRITE(IT,565)
C                  DO 193 I =1,NN
C 193              WRITE(IT,540) (ELM(I,J),J=1,NN)
C                  ENDIF
      ENDIF
      ENDIF

```

ENDIF

C

C

C

C

C

C | -----
C | Assemble element matrices into banded global matrix |

C | (for transient analysis) |

C | -----

195 CALL ASSMBL (NOD,MXELM,MXNEQ,NDF,NPE,N,GLK,GLF,NHBW)

C | -----

C

C

200 CONTINUE

C

C | -----

C | -----

C

C

C

C

IF (ITER .EQ. 1) THEN

IF(NPRNT.EQ.2)THEN

C

C | -----

C | Print assembled coefficient matrices if required |

C | That depends on the value of NPRNT |

C | -----

WRITE(IT,570)

DO 210 I=1,NEQ

210 WRITE(IT,540) (GLK(I,J),J=1,NEQ)

```

C      WRITE(IT,575)
C      DO 212 I = 1,NEQ
C 212  WRITE(IT,540) (GLM(I,J),J=1,NEQ)
C      WRITE(IT,580)
C      WRITE(IT,540) (GLF(I),I=1,NEQ)
      ENDIF
      ENDIF

C
C
C-----C
C
C
C
C
C -----
C | Call subroutine BOUBAN to impose essential and natural type |
C | BOUNDARY CONDITIONS ON THE PRIMARY VARIABLES.                |
C |                                                                |
C -----
      CALL BOUBAN (MXNEQ,NCMAX,NEQ,NHBW,GLK,GLF,NSPV,ISPV,VSPV,MXEBC,
*              NDF)
C
C
C
C
C
C -----
C | AFTER COMPLETING THE FIRST ITERATION
C | SET THE SPECIFIED PRIMARY VARIABLES TO ZERO
C -----

```



```
C
C
C
C
C -----
C | UPDATE THE SOLUTION AND CHECK FOR CONVERGENCE |
C -----
C
C   DIFF = 0.0
C   SOLN = 0.0
C   DO 215 I =1,NEQ
C     DIFF = DIFF + GLF(I)*GLF(I)
C
C   GFPR(I) = GFPR(I) + GLF(I)
C
C   WRITE(6,*) 'GFPR'
C   WRITE(6,*) GFPR(I)
C 215 SOLN = SOLN + GFPR(I)*GFPR(I)
C     ERR = DSQRT(DIFF/SOLN)
C     IF (ERR .GT. EPSLN) THEN
C       IF (ITER .EQ. ITLIM) THEN
C         WRITE(IT,610)
C         STOP
C       ENDIF
C
C -----
C | THE ITERATION LOOP RETURNS WHERE IT STARTS |
C -----
C
C   GO TO 222
C
C   ENDIF
C
C
```



```
WRITE(6,*) 'DIF BETWEEN FPB0 AND GLF(1)'
```

```
WRITE(6,*) DIF
```

```
20000 CONTINUE
```

```
C
```

```
IF (DABS(DIF) .LE. 0.001) GOTO 272
```

```
WRITE(6,*) 'IT STOPS AT THE EXTERNAL LOOP-MUST GUESS ANOTHER TDDX2'
```

```
STOP
```

```
C
```

```
C CALCULATE THE FOLLOWING VARIABLES
```

```
C
```

```
C
```

```
C
```

```
272 PROPV = (X1-X0)/DT
```

```
C
```

```
SLIFC = PROPV*DT + X1
```

```
C WRITE(6,*) '*****'
```

```
C WRITE(6,*) 'THE HEIGHT OF THE MUDLINE INTERFACE AT TIME T+DT'
```

```
C WRITE(6,*) 'SLIFC'
```

```

C      WRITE(6,*) '*****'
      P1 = -0.0129
      P2 = (-LOG(PROPV))/202.5109
      SC = P1+P2
C      WRITE(6,*) 'SC IS THE SOLIDS CONCENTRATION AT TIME T+DT'
C      WRITE(6,*) SC
C
C      SC0 = 0.03
      SUS0 = 0.00003
      IF (SC .LT. SC0) THEN
      SC = SC0
      SUS = SUS0
      ELSE
C
      SUS = 0.0000946754-0.0026552*SC + 0.018926*SC*SC
C
C      WRITE(6,*) 'THE SOLIDS SETTLING VELOCITY AT TIME T+DT'
C      WRITE(6,*) SUS
      ENDIF
C
C
      FALX = SUS * SC * DT * (1/E)
C
C      WRITE(6,*) '-----'
C      WRITE(6,*) 'THE HEIGHT OF THE FALLING SOLIDS ON THE TOP OF THE BED'
C      WRITE(6,*) 'FALX'
C      WRITE(6,*) FALX
C      WRITE(6,*) '-----'
C
C

```


C

```
CALL PSTPRC (GLF, GLX, NOD, NPE, MXELM, MXNEQ, MXNOD, NEM, ELU, N, NDF, FALX)
```

C

C

```
-----  
F O R M A T S  
-----
```

C

C

```
C 300 FORMAT(20A4)
310 FORMAT(4X, 'OUTPUT FROM THE THESIS COMPUTER CODE T.PAPANICO.')
```

```
350 FORMAT(/,5X, 'No. of nodes per element.....=',I4,/,
*       5X, 'No. of deg. of freedom per node, NDF....=',I4,/,
*       5X, 'No. of elements in the mesh, NEM.....=',I4,/,
*       5X, 'No. of total DOF in the model, NEQ.....=',I4,/,
*       5X, 'No. of specified primary DOF, NSPV.....=',I4,/,
*       5X, 'No. of specified secondary DOF, NSSV....=',I4)
410 FORMAT(/,3X, 'Global coordinates of the nodes, {GLX}:',/)
480 FORMAT(/,3X, 'Boundary information on primary variables:',/)
490 FORMAT(5X,2I5,2E13.5)
500 FORMAT(/,3X, 'Boundary information on secondary variables:',/)
530 FORMAT(56('_'),/)
540 FORMAT(5X,5E13.5/)
550 FORMAT(/,3X, 'Element coefficient matrix, [ELK]:',/)
560 FORMAT(/,3X, 'Element source vector, {ELF}:',/)
565 FORMAT(/,3X, 'Element mass matrix, [ELM]:',/)
570 FORMAT(/,3X, 'Global coefficient matrix, [GLK]:',/)
575 FORMAT(/,3X, 'GLOBAL MASS MATRIX, [GLM]:',/)
580 FORMAT(/,3X, 'Global source vector, {GLF}:',/)
590 FORMAT(/,1X, 'Solution (values of PVs) at the nodes: ',/)
610 FORMAT(/,3X, '**THE SCHEME DID NOT CONVERGE**',/)
620 FORMAT(/,3X, 'INITIAL VALUES OF THE PRIMARY VARIABLES, [GFPR]:',/)
630 FORMAT(5X,4E13.5)
640 FORMAT(5X, 'ALPHA=',E11.4,5X, 'DT=',E12.4,5X, 'TMAX=',E12.4,/,)
```

650 FORMAT(/,5X,'TIME=',E12.4,/)

660 FORMAT(/,3X,'VALUES OF PRIM.VARIABLES,GLF:',/)

670 FORMAT(5X,3E13.5/)

STOP

END

C

SUBROUTINE ASSMBL(NOD,MXELM,MXNEQ,NDF,NPE,N,GLK,GLF,NHBW)

C

C

C THE SUBROUTINE CALLS SUBROUTINES TO COMPUTE ELEMENT C
MATRICES

C AND ASSEMBLES THEM IN A FULL MATRIX FORM

C

C MXELM.... Maximum number of elements in the mesh:

C MXNEQ.... Maximum number of equations in the FE model

C NDF Number of degrees of freedom per node

C N ELEMENT NUMBER

C NPE Nodes per element

C {ELF}.... Element source vector, {F}

C {ELK}.... Element coefficient matrix, [K]

C {GLF}.... Global source vector

C {GLK}.... Global coefficient matrix

C {GLM}.... Global mass matrix

C [NOD].... Connectivity matrix

C

C

IMPLICIT REAL*8 (A-H,O-Z)

DIMENSION GLK(MXNEQ,MXNEQ),GLF(MXNEQ),NOD(MXELM,3)

COMMON/STR1/ELK(6,6),ELM(6,6),ELF(6),ELX(3),ELKI(6,6),ELFI(6) ?

C

C Assemble element coefficient matrix ELK and source vector ELF

C

DO 30 I = 1, NPE

NR = (NOD(N,I) - 1)*NDF

C WRITE(6,*) 'NOD(N,I)'

C WRITE(6,*) NOD(N,I)

DO 30 II = 1, NDF

NR = NR + 1

L = (I-1)*NDF + II

GLF(NR) = GLF(NR) + ELF(L)

DO 30 J = 1, NPE

NCL = (NOD(N,J)-1)*NDF

DO 30 JJ = 1, NDF

M = (J-1)*NDF + JJ

NC = NCL+JJ-NR+NHBW

IF (NC) 30,30,20

20 GLK(NR,NC) = GLK(NR,NC) + ELK(L,M)

30 CONTINUE

RETURN

END

C SUBROUTINE BOUBAN(MXNEQ,NCMAX,NEQ,NHBW,S,SL,NBDY,ISPV,VBDY,MJ,NDF)

C

C

C The subroutine is used to implement specified boundary conditions

C on the assembled system of finite element equations

C

C MXEBC.... Maximum number of speci. primary deg. of freedom

C MXNBC.... Maximum number of speci. secondary deg. of freedom

C

C

```
IMPLICIT REAL*8 (A-H,O-Z)
```

```
DIMENSION S(MXNEQ,MXNEQ),SL(MXNEQ)
```

```
DIMENSION IBDY(50),VBDY(NBDY),ISPV(MJ,2)
```

C

```
C Include specified PRIMARY degrees of freedom
```

C

```
NBWM1 = 2.0*NHBW - 1
```

```
DO 300 NB = 1,NBDY
```

```
IBDY(NB) = (ISPV(NB,1)-1)*NDF + ISPV(NB,2)
```

```
IE = IBDY(NB)
```

```
SVAL = VBDY(NB)
```

```
DO 60 J = 1,NBWM1
```

```
60 S(IE,J) = 0.0
```

```
S(IE,NHBW) = 1.0
```

```
300 SL(IE) = SVAL
```

```
C WRITE(6,*) 'IE', IE, 'SVAL', SVAL
```

```
RETURN
```

```
END
```

```
SUBROUTINE MESH1D(NEM,NPE,NOD,MXELM,MXNOD,DX2,GLX)
```

C

C

C

```
    The subroutine computes the arrays {GLX} and [NOD]
```

C

C

```
{GLX}.... Vector of global coordinates
```

C

```
{DX2}..... VECTOR OF ELEMENT LENGTHS [DX(1) = NODE 1 COORD.]
```

C

```
[NOD].... Connectivity matrix
```

C

C

```
IMPLICIT REAL*8 (A-H,O-Z)
```

```
DIMENSION GLX(MXNOD),DX2(MXNOD),NOD(MXELEM,3)
```

```
C
```

```
C Generate the elements of the connectivity matrix
```

```
C
```

```
DO 10 I=1,NPE node for element
```

```
10 NOD(1,I)=I
```

```
DO 20 N=2,NEM node for element
```

```
DO 20 I=1,NPE
```

```
20 NOD(N,I) = NOD(N-1,I)+NPE-1
```

```
C 20 WRITE(6,*) 'NOD(N,I)',NOD(N,I)
```

```
C
```

```
C Generate global coordinates of the global nodes
```

```
C
```

```
GLX(1)=DX2(1)
```

```
IF(NPE.EQ.2)THEN
```

```
DO 30 I=1,NEM
```

```
30 GLX(I+1) = GLX(I) + DX2(I+1)
```

```
ELSE
```

```
DO 40 I=1,NEM
```

```
II=2*I
```

```
GLX(II) = GLX(II-1) + 0.5*DX2(I+1)
```

```
40 GLX(II+1)=GLX(II-1) + DX2(I+1)
```

```
ENDIF
```

```
RETURN
```

```
END
```

C-----

C AN INTERFACE SOLVER

SUBROUTINE SOLVER(MXNEQ,NEQ,GLK,GLF,NHBW,NPE,NDF)

IMPLICIT REAL*8 (A-H,O-Z)

DIMENSION GLK(MXNEQ,MXNEQ),GLF(MXNEQ)

C-----

NBW = 2*NHBW?

DO 5 I = 1,NEQ

5 GLK(I,NBW) = GLF(I)

NHBW = NPE * NDF

ITERM = NHBW

CALL BNDSOL(GLK,MXNEQ,NEQ,ITERM)

DO 6 I = 1,NEQ

6 GLF(I) = GLK(I,NBW)

RETURN

END

C

C

C

SUBROUTINE BNDSOL(A,MXNEQ,N,ITERM)

C

C THE ACTUAL SOLVER

C

C

C

C EQUATION SOLVER FOR BANDED UNSYMMETRIC EQUATIONS

C

IMPLICIT REAL*8(A-H,O-Z)

DIMENSION A(MXNEQ,MXNEQ)

C WRITE(6,*) 'MXNEQ',MXNEQ, 'N',N, 'ITERM',ITERM

CERO = 1.D-8

1.0-8

C

PARE = CERO**2

NBND = 2*ITERM

NBM = NBND - 1

C BEGINS ELIMINATION OF THE LOWER LEFT

DO 1000 I = 1,N

C WRITE(6,*) 'A', A(I,ITERM)

IF (DABS(A(I,ITERM)) .LT. CERO) GO TO 410

GO TO 430

410 IF (DABS(A(I,ITERM)) .LT. PARE) GO TO 1600

C WRITE(6,*) 'N',N

C WRITE(6,*) 'ITERM',ITERM

430 JLAST = MINO(I+ITERM-1,N)

L = ITERM + 1

DO 500 J =I, JLAST

L =L-1

IF (DABS(A(J,L)) .LT. PARE) GO TO 500

B= A(J,L)

DO 450 K = L,NBND

450 A(J,K) = A(J,K)/B

IF (I .EQ. N) GO TO 1200

500 CONTINUE

L = 0

JFIRST = I + 1

IF (JLAST .LE. I) GO TO 1000

DO 900 J = JFIRST,JLAST

L= L+1

IF (DABS(A(J,ITERM-L)) .LT. PARE) GO TO 900

DO 600 K = ITERM,NBM

600 A(J,K-L) = A(J-L,K) -A(J,K-L)

A(J,NBND) = A(J-L,NBND)-A(J,NBND)

```

      IF (I .GE. N-ITERM+1) GO TO 900
      DO 800 K =1,L
      800 A(J,NBND-K) = -A(J,NBND-K)
      900 CONTINUE
      1000 CONTINUE
      1200 L = ITERM - 1
      DO 1500 I = 2,N
      DO 1500 J = 1,L
      IF (N+1-I+J .GT. N) GO TO 1500
      A(N+1-I,NBND) = A(N+1-I,NBND) - A(N+1-I+J,NBND)*A(N+1-I,ITERM+J)
C      WRITE(6,*) A(N+1-I,NBND) , N+1-I
      1500 CONTINUE
      RETURN
      1600 WRITE(6,1601)
      1601 FORMAT(/,2X,'COMPUTATION STOPPED IN BNDSOL BECAUSE ZERO APPEARED
      *ON THE MAIN DIAGONAL. THE MATRIC FOLLOWS:',/)
C      WRITE(6,1602)I,A(I,ITERM)
C      WRITE(6,*)I,A(I,ITERM)
C1602 FORMAT(10X,I5,E12.4)
      STOP
      END

```

```

SUBROUTINE COEFNT(NDF,NPE,N,NI,ELU,EWO,IELEM,NEM,NNM,AA,BB)

```

C

C

C The subroutine computes the coefficient matrices and source vector
C for the model problem (see the MAIN program)

C

C X..... Global (i.e., problem) coordinate

C XI Local normalized coordinate

C H..... Element length


```
* 0.55555555D0,2*0.0D0,.34785485D0,2*.65214515D0,.34785485D0,0.0D0,
* 0.236927D0,.478629D0,.568889D0,.478629D0,.236927D0/
```

C

```
IT = 6
```

C

```
C TABLE OF THE EMPIRICAL PARAMETERS C
```

C

```
PA =30.
```

```
E = 0.065
```

```
R = 3.08*(0.65-E)**4.
```

```
D = 5.19*(0.65-E)**2.68
```

```
EK = 1.869*10**(-11.)
```

```
DR = 1300.
```

```
EM = 0.001
```

C

C

```
C WRITE(6,*) 'AA',AA,'BB',BB
```

```
NN =NPE*NDF
```

```
NGP=NPE
```

```
H=ELX(NPE)-ELX(1)
```

C

```
C | INITIALIZE ALL ARRAYS |
```

C

```
DO 10 I=1,NN
```

```
ELFI(I)=0.0
```

```
ELF(I)=0.0
```

```
DO 10 J=1,NN
```

C

```
ELA(I,J) = 0.0
```

```
ELKI(I,J) = 0.0
```

```
ELK(I,J) = 0.0
```

```
10 ELM(I,J) = 0.0
```

```
C
```

```
C      CALCULATION OF THE ELEMENT FORCE VECTOR
```

```
C-----
```

```
C
```

```
C
```

```
C
```

```
      IF (N .GT. 1) GO TO 350
```

```
C
```

```
C      FOR THE FIRST ELEMENT(FROM THE BOTTOM)
```

```
C
```

```
      DO 380 I = 1,NPE
```

```
      IF (I .EQ. 1) THEN
```

```
C
```

```
C      ELFI IS THE FORCE VECTOR ESTIMATED AT TIME N
```

```
C
```

```
      ELFI(I) = EK*PA*DR*9.81*E*((1+EWO(1)/PA)**(R-D+1))/(EM*R)
```

```
C
```

```
C      ELF IS THE FORCE VECTOR ESTIMATED AT TIME N+1
```

```
C
```

```
      ELF(I) = EK*PA*DR*9.81*E*((1+ELU(1)/PA)**(R-D+1))/(EM*R)
```

```
      ELSE
```

```
      ELF(I) = 0.0
```

```
      ELF(I) = 0.0
```

```
      ENDIF
```

```
C      WRITE(6,*) 'ELF(I)',ELF(I)
```

```
380 CONTINUE
```

```
C
```

```
      GO TO 1000
```

```
C
```

```
350 IF (N .LT. NEM) GO TO 500
```

```

C
C   FOR THE LAST ELEMENT (AT THE TOP)
C
      DO 600 I = 1,NPE
      IF (I .LT. NPE) THEN
        ELFI(I) = 0.0
        ELF(I) = 0.0
      ELSE
        ELFI(I) = ((EK*PA)/(EM*R))*(EWO(NPE)*(1/H)+EWO(NPE-1)*(-1/H))
        ELF(I) = ((EK*PA)/(EM*R))*(ELU(NPE)*(1/H)+ELU(NPE-1)*(-1/H))
      ENDIF
C   WRITE(6,*) 'ELF(I)',ELF(I)
600 CONTINUE
C
      GO TO 1000
C
C   FOR THE INTERMEDIATE ELEMENTS
C
500 DO 370 I = 1,NPE
      ELFI(I) = 0.0
      ELF(I) = 0.0
370 CONTINUE
C -----
C | DO-LOOP ON NUMBER OF GAUSS POINTS STARTS HERE |
C -----
1000 DO 20 NI=1,NGP
      XI = GAUSPT(NI,NGP)
C   WRITE(6,*) 'XI',XI
C -----
C | CALL SUBROUTINE 'INTRPL' TO EVALUATE THE INTERPOLATION FUNCTIONS |
C | AND THEIR DERIVATIVES AT THE GAUSS POINTS |

```

possibly the no of particles

gauss point

```

C -----
      CALL INTRPL (H,NPE,XI,IELEM)
C -----C
      CONST = GJ*GAUSWT(NI,NGP)
      X = ELX(1)+0.5*H*(1.0+XI)
C -----C
      FOR ISOPARAMETRIC ELEMENTS
      X = ELX(1)+0.5*H*(1-XI*XI)+H*0.5*XI*(1+XI)
C -----C
      PSS = 0.0
      DPSSDX = 0.0
      PS = 0.0
      DPSDX = 0.0
C -----
      DO 21 I = 1,NPE
C
C   FOR THE TIME N
C
      PSS = EWO(I)*SF(I)+PSS
      DPSSDX = EWO(I)*GDSF(I)+DPSSDX
C
C   FOR THE TIME N+1
C
      PS = ELU(I)*SF(I) + PS
      DPSDX = ELU(I)*GDSF(I) + DPSDX
C -----
      21 CONTINUE
C   WRITE(6,*) 'PS'
C   WRITE(6,*)   PS
C   WRITE(6,*) 'DPSDX'
C   WRITE(6,*)  DPSDX

```

```

C
C
C
C-----C
C 1ST STEP : DIRECT MATRICES
C | EVALUATE THE MATRICES {ELF}, [ELK] AND [ELM] BEFORE USING THE |
C | NEWMARK'S TEMPORAL APPROXIMATION SCHEME. |
C -----
C -----
      DO 40 I = 1,NN
      DO 40 J = 1,NN
C
C CALCULATION OF THE K MATRIX AT TIME N
C
      ELKI(I,J)=ELKI(I,J)+CONST*(GDSF(I)*GDSF(J)*EK*PA*(1/EM*R)*
+      (1+PSS*(1/PA))**(1-D)-
+      SF(I)*GDSF(J)*((9.81*DR*E*EK*(2*R-D))/(EM*R))*
+      (1+PSS*(1/PA))**(R-D)+
+      SF(I)*GDSF(J)*(DPSSDX)*EK*(1-R)*(1/EM*R)*
+      (1+PSS*(1/PA))**(-D))
C-----C
C
C CALCULATION OF THE K MATRIX AT TIME N+1
C
      ELK(I,J)=ELK(I,J)+CONST*(GDSF(I)*GDSF(J)*EK*PA*(1/EM*R)*
+      (1+PS*(1/PA))**(1-D)-
+      SF(I)*GDSF(J)*((9.81*DR*E*EK*(2*R-D))/(EM*R))*
+      (1+PS*(1/PA))**(R-D)+
+      SF(I)*GDSF(J)*(DPSSDX)*EK*(1-R)*(1/EM*R)*
+      (1+PS*(1/PA))**(-D))
C-----C

```

```

C -----
      ELM(I,J) = ELM(I,J) + SF(I)*SF(J)*CONST
C -----
C
C CALCULATION OF THE EXTRA TERM IN ELK TANGENT
C THE ELA(I,J) DENOTES THE EXTRA TERM OF THE K TANGENT.
C IT IS CALCULATED AT TIME N+1.
C
40 ELA(I,J)=ELA(I,J)+(A1*(EK/EM*R)*GDSF(I)*SF(J)*(1-D)*DPSDX*
+      (1+PS*(1/PA))**(-D)-A1*SF(I)*SF(J)*(R-D)*DPSDX*(2*R-D)*
+      ((9.81*DR*E*EK)/(EM*R*PA))*(1+PS*(1/PA))**(R-D-1)+
+      A1*SF(I)*GDSF(J)*DPSDX*(EK*(1-R)/EM*R)*
+      (1+PS*(1/PA))**(-D) +
+      A1*SF(I)*SF(J)*((EK*(1-R))/EM*R)*(-D)*(1/PA)*DPSDX*DPSDX*
+      (1+PS*(1/PA))**(-D-1))*CONST
20 CONTINUE
C
C
C -----
C 2ND STEP:  N E W M A R K ' S      A P P R O X I M A T I O N
C | EVALUATE THE MATRICES [ELK hat] and {ELF hat} USING THE NEWMARK'S |
C | APPROXIMATION |

```

C -----
 C -----

DO 50 I = 1, NN

C

C TO SIMPLIFY THE EQUATIONS WE INTRODUCE THE PARAMETER: (SUM)

C

SUM = 0.0

DO 60 J = 1, NN

C

C THE TERM SUM IS COMPUTED AT TIME N

C

SUM = SUM + (ELM(I, J) - A2*ELKI(I, J))*EWO(J)

C

C CALCULATE [ELK,hat] using the equation:[ELK hat] = [ELM] + A1*[ELK]

C

C

60 ELK(I, J) = ELM(I, J) + A1*ELK(I, J)

C

C

C CALCULATE {ELF,hat} using the parameter SUM

C

C

50 ELF(I) = SUM + A1*ELF(I) + A2*ELFI(I)

C

C

C

C

C 3RD STEP: NEWTON'S METHOD

C | COMPUTE THE RESIDUAL IN MATRIX FORM {R} OF THE SOLUTION |

C | FROM DEFINITION THE RESIDUAL IS:{R} = [ELK,HAT] {P} - {ELF,HAT} |

C | THEN WE CAN CONSTRUCT THE EQUATION WITH THE FOLLOWING FORM: |

C | [ELK,tan]{dP} = -{R} for an iteration r |

C -----

DO 70 I = 1,NN

C THE L.H.S OF THE FOLLOWING STATEMENT IS THE -{R}

DO 80 J = 1,NN

ELF(I) = ELF(I) - ELK(I,J)*ELU(J)

80 CONTINUE

70 CONTINUE

C

C

C

C -----

C | EVALUATE THE TANGENT MATRIX [ELK,tan] USING THE PREVIOUS STEPS |

C |

C -----

C

C -----

IF (N.GT.1) GOTO 200

C

DO 90 I = 1,NN

DO 90 J = 1,NN

IF (I.EQ.1 .AND.J.EQ.1) THEN

C

C -----

C HERE IS CALCULATED THE GLOBAL ELK(1,1)TANGENT

C -----

ELK(I,J)=ELK(I,J)+ ELA(I,J)-A1*(EK/(EM*R))*(R-D+1)*

+ (1+ELU(1)*(1/PA))*(R-D)*DR*9.81*E

ELSE

ELK(I,J)=ELK(I,J)+ELA(I,J)

ENDIF

```

C      WRITE(6,*) 'ELU(1)',ELU(1)
      90 CONTINUE
C
      GO TO 110
C
C-----
      200 IF (N . EQ. NEM) GO TO 5000
C
C      HERE IS CALCULATED FOR THE INTERMEDIATE ELEMENTS
C
      DO 100 I = 1,NN
      DO 100 J = 1,NN
      100 ELK(I,J)=ELK(I,J)+ELA(I,J)
C
      GO TO 110
C
C-----
C      HERE IS CALCULATED THE GLOBAL ELK(NNM,NNM)TANGENT
C-----
      5000 DO 6000 I = 1,NN
      DO 6000 J = 1,NN
      IF (I .EQ. 2 .AND. J .EQ. 2) THEN
      ELK(I,J) =ELK(I,J)+ELA(I,J)-A1*((EK*PA)/(EM*R))*
+           (1/H)
      ELSE
      ELK(I,J) =ELK(I,J)+ELA(I,J)
      ENDIF
C      WRITE(6,*) 'ELU(1)',ELU(1)
      6000 CONTINUE
      110 RETURN
      END

```

C

SUBROUTINE INTRPL (H,NPE,XI,IELEM)

C

C

The subroutine computes shape functions and their derivatives for
 Hermite cubic and Lagrange linear and quadratic elements.

IN THIS PARTICULAR PROBLEM LAGRANGE LINEAR AND QUADRATIC ELEMENTS
 WILL BE USED.

C

X..... Global (i.e., problem) coordinate

XI Local (i.e., element) coordinate

H..... Element length

{SF}..... Lagrange interpolation (or shape) functions

{DSF}..... First derivative of SFL w.r.t. XI

{GDSF}.... First derivative of SFL w.r.t. X

GJ..... Jacobian of the transformation

C

IMPLICIT REAL*8 (A-H,O-Z)

COMMON/SHP/SF(4),GDSF(4),GJ

DIMENSION DSF(4)

C*****

C LAGRANGE interpolation functions used for linear and quadratic

C approximation of second-order equations

C*****

C

IF (IELEM-2) 10,20,20

C

C LINEAR interpolation functions (NPE = 2)

C

10 SF(1) = 0.5*(1.0-XI)

SF(2) = 0.5*(1.0+XI)

DSF(1) = -0.5

DSF(2) = 0.5

GO TO 30

C-----
C QUADRATIC INTERPOLATION FUNCTIONS (NPE = 3)

20 SF(1) = -.5*XI*(1.0-XI)

SF(2) = 1.0-XI*XI

SF(3) = .5*XI*(1.0+XI)

DSF(1) = -.5*(1.0-2.0*XI)

DSF(2) = -2.0*XI

DSF(3) = 0.5*(1.0+2.0*XI)

GO TO 30

C-----
C COMPUTE DERIVATIVES OF THE INTERPOLATION FUNCTIONS W.R.T. X

30 GJ = H*0.5

DO 40 I = 1,NPE

40 GDSF(I) =DSF(I)/GJ

C
RETURN

END

C
SUBROUTINE PSTPRC(GLF, GLX, NOD, NPE, MXELM, MXNEQ, MXNOD, NEM, ELU,
+ N, NDF, FALX)

C-----
C
C The subroutine computes the solution and its derivatives at five
C points, including the nodes of the element.
C

C X..... Global (i.e., problem) coordinate
 C XI Local (i.e., element) coordinate
 C SF..... Element interpolation (or shape) functions
 C GDSF..... First derivative of SF w.r.t. global coordinate

C

IMPLICIT REAL*8 (A-H,O-Z)

DIMENSION GLF(MXNEQ),GLX(MXNOD),NOD(MXELM,3),XP(9)

C DIMENSION ELU(6),DX2(16)

DIMENSION ELU(6)

COMMON/STR1/ELK(6,6),ELM(6,6),ELF(6),ELX(3),ELKI(6,6),ELFI(6)

COMMON/STR2/A1,A2

COMMON/STR3/PA,R,D,EK,EM,DR,E

COMMON/SHP/SF(4),GDSF(4),GJ

COMMON/IO/IN,IT

DATA XP/-1.0D0,-0.75,-0.5,-0.25,-0.0,0.25,0.5,0.75,1.0/

C DATA XP/-1.0D0,-0.5,0.0,0.5,1.0/

NDF = 1

C WRITE(IT,75)

C 75 FORMAT(/,69('_'),/,5X,'X',6X,'P-EFF.PRESSURE',9X,'DP',12X,'U',

C + 16X,'US',/,69('_'),/)

C 75 FORMAT(/,69('_'),/,5X,'X',6X,'P-EFF.PRESSURE',9X,'UL',

C + 16X,'ES',/,69('_'),/)

C TOTALX = 0.00271461538

C X1 = TOTALX

C WRITE(6,*) 'X1'

C WRITE(6,*) X1

C NEM = 15

C NNM = NEM*(NPE-1) + 1

C DO 15 I = 1,NEM+1

C IF (I .EQ. 1) THEN

*How about
 2nd derivative*

GDSF

*total of bed at 1000
 no of element 2 m
 1000 / 2 = 500*

```

C      DX1(I) = 0
C      ELSE
C      DX1(I) = X1/NEM
C      ENDIF
C 15 CONTINUE
C      CALL MESH1D (NEM,NPE,NOD,MXELM,MXNOD,DX1,GLX) ✓
C      WRITE(6,*) 'GLX'
C      WRITE(6,*) (GLX(I), I = 1,NNM)
C      DO 100 N= 1,NEM
C      WRITE(6,89) N
89  FORMAT(//,5X,'ELEMENT =',I4,/)
      L=0
      DO 90 I = 1,NPE
      NI=NOD(N,I)
      ELX(I)=GLX(NI)
      LI= NI-1
      DO 90 J = 1,NDF
      LI=LI+1
      L=L+1
90  ELU(L)=GLF(LI)
      NET = NPE
      H = ELX(NPE)-ELX(1)
      DO 40 NI=1,9
      XI = XP(NI)
C-----
      CALL INTRPL(H,NPE,XI,IELEM)
C-----
      X = 0.5*H*(1.0+XI)+ELX(1) ✓
C-----C
C TABLE OF THE VALUES OF THE EMPIRICAL PARAMETERS C
C-----C

```

C EM = THE DYNAMIC VISCOCITY OF WATER IN 20 DEGREES C

EM = 0.001

E=0.065 *CO*

C EK IS THE KO:INTRINSIC PERMEABILITY WHEN PS = 0 *also PM*

EK = 6.669*10**(-11.)

C R IS THE COMPRESSIBILITY COEFFICIENT B

R=3.08*(0.65-E)**4.

C D IS THE COMPRESSIBILITY COEFFICIENT D

D = 5.19*(0.65-E)**2.68

DR = 1300.

PA = 30.

C-----C

C

PS= DR*9.81*E*FALX

C

C

C WRITE(6,*) 'PS-LINEAR DISTRIBUTION OF THE FALLING MATERIAL'

C WRITE(6,*) PS

UL = 0.0

US = 0.0

DPSDX = 0.0

ES = 0.0 *CO (low) and earlier*

C PM DENOTES THE INTRINSIC PERMEABILITY

PM= 0.0

DH = 0.0

DO 30 I=1,NET *NDDPSELN*

PS= PS + SF(I)*ELU(I)

DPSDX = DPSDX + GDSF(I)*ELU(I) ✓

C

C-----C
C CALCULATE THE CONCENTRATION IN THE RISING SEDIMENT,ES

C-----C

$$ES = E * (1+PS*(1/PA))**R$$

$$PM = EK*(1+(1/PA)*PS)**(-D)$$

C-----C

C CALCULATE THE SOLID AND LIQUID VELOCITY

C-----C

$$UL = -DPSDX * EK*(1+(1/PA)*PS)**(-D)*ES*(1/(EM*(1-ES)))-$$

$$+ EK*(1+(1/PA)*PS)**(-D)*ES**(2.0)*(1/(EM*(1-ES)))*9.81*DR$$

$$US = UL*(ES-1)*(1/ES)$$

C-----C

C CALCULATE THE PRESSURE DIFFERENCE CAUSED BY THE UPWARD

C MOVEMENT OF C

C THE TRAPPED WATER IN THE PARTICLES

C

C-----C

$$C DH = DH + (EM*(1-ES)/K)*(UL-US) ✓$$

30 CONTINUE

C

C WRITE(IT,35) X,P,DP,U,US

C WRITE(IT,35) X,PS,UL,ES

40 CONTINUE

100 CONTINUE

35 FORMAT (E9.3,5X,E12.5,5X,E12.5,5X,E10.5)

RETURN

END

VITA

The author was born on December 10, 1966 in Greece. He enrolled at Aristotle University of Thessaloniki (A.U.T.) in 1984 and he got his bachelor degree in Civil Engineering in 1989. During his studies he received scholarship from the Greek Government, and awards from the Technical Chamber of Greece and the Greek Math Association. He began work on a Masters of Science degree at Virginia Tech in 1990 and he is currently enrolled for the Ph.D. program at the same University.

A. Papadimitriou